THE IDEAL FREE DISTRIBUTION: THEORY AND ENGINEERING APPLICATION

DISSERTATION

Presented in Partial Fulfillment of the Requirements for

the Degree Doctor of Philosophy in the

Graduate School of The Ohio State University

By

Nicanor Quijano, M.S.

* * * * *

The Ohio State University

2006

Ph.D. Examination Committee:

Doctor Kevin M. Passino, Adviser

Doctor Andrea Serrani

Doctor José B. Cruz Jr.

Approved by

Adviser

Graduate Program in
Electrical and Computer
Engineering

ABSTRACT

An important concept from theoretical ecology is the "ideal free distribution" (IFD). This dissertation analyzes the IFD idea from three different perspectives. First, we start by defining a general class of "suitability" functions, and show that the IFD is an evolutionarily stable strategy (ESS), and a global optimum point. We introduce the "replicator dynamics" for the IFD and show that they provide an allocation strategy that is guaranteed to achieve the IFD. We show how this allocation strategy can achieve an IFD for a multizone temperature control problem that corresponds to achieving the maximum uniform temperature on a grid under a multivariable saturation constraint. Then, using a bioinspired methodology, we view an animal as a software agent, the foraging landscape as a spatial layout of temperature zones, and nutrients as errors between the desired and actual temperatures in the zones. Using foraging theory, we define a decision strategy for the agent that has an objective of reducing the temperature errors in order to track a desired temperature. We show that the use of multiple agents defines a distributed controller that can equilibrate the temperatures in the zones in spite of interzone, ambient, and network effects. Finally, a model of honey bee social foraging is introduced to create an algorithm that solves a class of optimal resource allocation problems. We prove that if several such algorithms compete in the same problem domain, the strategy they use is an

ESS but for finite populations. Moreover, for a single or multiple hives we prove that the allocation strategy is globally optimal.

Para el núcleo familiar, Carlos, Lilia, y Catalina...

ACKNOWLEDGMENTS

I would like to extend my sincere thanks to my advisor Professor Kevin M. Passino for his guidance and support throughout my research. This dissertation would not be possible without his experience, time, encouragement, knowledge, and support especially during the difficult moments of my studies. In my life I have had strongly believed when Albert Camus said *"Tout ce que je sais de plus sûr à propos de la moralité et des obligations des hommes, c'est au football que je le dois."* Now, after working with Professor Passino, I am sure that the 1957 Nobel Prize winner was not 100% correct.

I would also like to extend my sincere thanks to Professor Andrea Serrani for helping me during my studies, and teaching me that the answer to one of Camus's questions in "*Le mythe de Sysiphe*," "*Je veux savoir si je puis vivre avec ce que je sais et avec cela seulement*," is no.

I would also like to offer my appreciation to Professor José B. Cruz Jr. for being on my examination committee, and to Professor Thomas A. Waite for his help and being on my candidacy exam committee.

I am grateful to the National Institute of Standards and Technology (NIST) and my parents for giving me the financial support and opportunity to study in the United States during my first years. Also, I am grateful to the OSU office of Research for partial financial support via an interdisciplinary research grant during the last two

years, and to the Electrical and Computer Engineering Department for giving me the opportunity of being a teaching assistant during the past four years.

I would like to thank my parents (Carlos and Lilia), my sister (Catalina), my family, and Blanca for always being there for me when I needed them, and always encouraging and supporting me in my studies.

Also I would like to thank Jorge Finke, Alvaro Gil, Burt Andrews, Brandon Moore, José López, Miguel González, Blanca Bernal, Victor Argueta, Julio Chanamé, María González, Hiram Irizarry, Roberto Solano, Felipe Guerrero, Veronica Melián, Veysel Gazi, Sriram Ganapathy, Élie Abi-Akel, Garo Zarikian, Ernesto Machado, Alfonso León, Edgar Bernal, Samuel Duque, Francisco Forero, Jairo Gordillo, Cesar Bautista, Adolfo Recio, Juan Pablo González, Jesús López, and also other friends and colleagues for their help during my studies, and their inputs in some of the chapters of this document.

VITA

May 7, 1974	Born - Bogotá, Colombia
July 1997 - January 1998	Electrical Engineering Intern, British Petroleum Exploration Instrumentation Dept., Bogotá/Cusiana, Colombia
January 1996 - July 1999	Teaching Assistant, Pontificia Universidad Javeriana, Bogotá, Colombia
October 1999	B.S. Electrical Engineering, Pontificia Universidad Javeriana, Bogotá, Colombia
August 1999 - December 2000	Instructor, Pontificia Universidad Javeriana, Bogotá, Colombia
August 2000 - December 2000	Traffic Engineer, Capitel-Telecom, Traffic Dept., Bogotá, Colombia
July 2001 - December 2002	Graduate Teaching and Research Associate, The Ohio State University, Columbus, Ohio
December, 2002	M.S. in Electrical Engineering The Ohio State University, Columbus, Ohio
January 2003 - December 2006	Graduate Teaching and Research Associate, The Ohio State University, Columbus, Ohio

PUBLICATIONS

Research Publications

Nicanor Quijano and Kevin M. Passino, "Resource Allocation Strategies for Multizone Temperature Control," *Proc. of 2nd IFAC Symposium on System, Structure and Control, Oaxaca, México, December 2004.*

Nicanor Quijano, Alvaro E. Gil, and Kevin M. Passino, "Experiments for Dynamic Resource Allocation, Scheduling, and Control," *IEEE Control Systems Magazine, Vol. 25, No. 1, pp. 63-79, Feb. 2005.*

Nicanor Quijano and Kevin M. Passino, "Optimality and Stability of the Ideal Free Distribution with Application to Temperature Control," *Proceedings of the 2006 American Control Conference, pp. 4836-4841, June 14-16 Minneapolis, Minnesota, 2006.*

Nicanor Quijano and Kevin M. Passino, "The Ideal Free Distribution: Theory and Engineering Application," *To appear, IEEE Transactions on Systems, Man, and Cybernetics Part B, 2006.*

Nicanor Quijano, Burton W. Andrews, and Kevin M. Passino, "Foraging Theory for Multizone Temperature Control," *To appear, IEEE Computational Intelligence Magazine, 2006.*

Nicanor Quijano and Kevin M. Passino, "Honey Bee Social Foraging Algorithms for Resource Allocation: Theory and Application," *Submitted for journal publication, IEEE Transactions on Evolutionary Computation, 2006.*

Nicanor Quijano and Kevin M. Passino, "Honey Bee Social Foraging Algorithms for Resource Allocation, Part I: Algorithm and Theory," *Submitted, American Control Conference, 2007.*

Nicanor Quijano and Kevin M. Passino, "Honey Bee Social Foraging Algorithms for Resource Allocation, Part II: Application," *Submitted, American Control Conference, 2007.*

Instructional Publications

Nicanor Quijano and Kevin M. Passino "Pre-lab and post-lab notes for ECE 758", Online: http://www.ece.osu.edu/~passino/ee758.html

FIELDS OF STUDY

Major Field: Electrical and Computer Engineering

TABLE OF CONTENTS

Page

Abstract ii

Dedication iv

Acknowledgments v

Vita vii

List of Figures xiii

Chapters:

1. Introduction 1

    1.1 Problem Statement 1
    1.2 Thesis Summary 2

2. Optimality, Stability, and Allocation Strategies for the Ideal Free Distribution 4

    2.1 Introduction 4
    2.2 The Ideal Free Distribution 8
        2.2.1 A General Class of Suitability Functions 8
        2.2.2 Habitat and Input Matching Rules 10
        2.2.3 Ideal Free and Dominance Distributions 13
        2.2.4 Individual Animal Fitness Equalization 15
    2.3 Game-Theoretic and Optimality Properties of the IFD 18
        2.3.1 Nash Equilibria and Evolutionarily Stable Strategies 18
        2.3.2 Game-Theoretic Characteristics of the IFD 19
        2.3.3 Optimality of the IFD 21

2.4 Evolutionary Allocation Dynamics for IFD Achievement 23
2.4.1 The Replicator Dynamics Model 23
2.4.2 Constraint Set Invariance for the Replicator Dynamics . . . 25
2.4.3 Stability Analysis of the IFD 26
2.4.4 Allocation Dynamics: Gradient Optimization Perspective . 28
2.5 Multizone Temperature Control Application 30
2.6 Conclusions 33

3. Foraging Theory for Multizone Temperature Control 34

3.1 Introduction 34
3.2 Foraging Model 37
3.3 Temperature System and Application of the Prey Model 41
3.4 Experiments and Results 46
3.4.1 Tracking 46
3.4.2 Disturbance Effects 48
3.4.3 Search Limitations 50
3.4.4 Discussion 51
3.5 Conclusions 54

4. Honey Bee Social Foraging Algorithms for
Resource Allocation: Theory and Application 56

4.1 Introduction 56
4.2 Honey Bee Social Foraging Algorithm 60
4.2.1 Foraging Profitability Landscape 60
4.2.2 Bee Roles and Expeditions 61
4.2.3 Dance Strength Determination 63
4.2.4 Explorer Allocation and Forager Recruitment 68
4.2.5 Discussion 70
4.3 Equilibrium Analysis of Hive Allocations 71
4.3.1 The n-Hive Game 71
4.3.2 The Multiple Hive IFD is a Strict Nash Equilibrium and ESS 75
4.3.3 Optimality of the Single and Multiple Hive IFD 77
4.3.4 Discussion 80
4.4 Engineering Application: Dynamic Resource Allocation for Multizone Temperature Control 81
4.4.1 Experiment and Honey Bee Social Foraging Algorithm Design 81
4.4.2 Experiment 1: One Hive IFD Achievement 84
4.4.3 Experiment 2: One Hive with Disturbances, IFD, Cross-Inhibition, and Site Truncation 85

4.4.4 Experiment 3: Two Hives and Imperfect Information 89
4.4.5 Discussion 91
4.5 Conclusions 94

5. Conclusion and Future Directions 96

5.1 Summary of Contributions 96
5.2 Future Directions 97

Appendices:

A. Appendix: Proof of Theorems 99

A.1 Proof of Theorem 2.2.1 99
A.2 Proof of Theorem 2.2.2 99
A.3 Proof of Theorem 2.3.1 100
A.4 Proof of Theorem 2.3.2 101
A.5 Proof of Theorem 2.4.1 102
A.6 Proof of Theorem 2.4.3 103
A.7 Proof of Theorem 2.4.4 104
A.8 Proof of Theorem 2.4.5 105
A.9 Proof of Theorem 4.3.1 105
A.10 Proof of Theorem 4.3.2 108
A.11 Proof of Theorem 4.3.3 109

Bibliography 112

LIST OF FIGURES

Figure **Page**

2.1 Temperatures in four zones of the multizone temperature control experiment. The plot represents the temperature in each of the zones (left axis), and the distribution of the x_i (right axis). 33

3.1 Zone layout on a single temperature grid. Each zone contains a lamp and a temperature sensor. 42

3.2 Parameter functions. Panel (a) depicts the determination of task type from encountered error, and panel (b) illustrates the processing times for each task type. 44

3.3 Multizone temperature control tracking performance, desired temperature (dashed), and actual temperature (solid) with plot layout corresponding to spatial zone positions in Figure 3.1. The stem plot at the bottom of each panel indicates the on/off state of the lamp x^i for zone i at a given point in time. 47

3.4 In this figure, we illustrate the task-type encounters of each forager with respect to time. Encounters are downsampled for visualization. . 49

3.5 Multizone temperature control performance when a disturbance is applied. The desired temperature (dashed), the actual temperature (solid), and the lamps that are on (stem) are shown in the plot layout corresponding to spatial zone positions in Figure 3.1. The stem plot at the bottom of each panel indicates the on/off state of the lamp x^i for zone i at a given point in time. 50

3.6 Multizone temperature control performance when there is not perfect information. The desired temperature (dashed), the actual temperature (solid), and the lamps that are on (stem) are shown with plot layout corresponding to spatial zone positions in Figure 3.1. The stem plot at the bottom of each panel indicates the on/off state of the lamp x^i for zone i at a given point in time. 52

3.7 Corresponding zones for each of the four foragers. 53

4.1 Dance strength function. 66

4.2 Layout for the multizone temperature control grid experiment. 82

4.3 Temperature and number of bees per zone when there is one hive and no disturbances. The top plots show the temperature in each zone, and the average of the last 100 seconds (solid constant line). The stems in the bottom plots represent the number of bees that were allocated to each zone. 85

4.4 Number of employed foragers B_f and the average of the last 100 seconds (top plot). The bottom plot shows the number of explorers B_e and the average of the last 100 seconds. 86

4.5 Temperature and number of bees per zone for the second experiment. In the top plot the solid constant line represents the average of the last 100 seconds in each zone. The numbers 1, 2, and 3 correspond to the disturbances. The stems in the bottom plot represent the number of bees that were allocated to each zone. 88

4.6 Temperature and number of bees per zone for the last experiment. In the top plot the solid constant line represents the average of the last 100 seconds in each zone. In the bottom plot, "o" corresponds to the bees that were allocated by the first hive, while "x" corresponds to the bees that were allocated by the second hive. 90

4.7 The top plot shows the final temperature, while the bottom plot shows the final value for the number of bees in each zone for each experiment. This final value corresponds to the average for the last 100 seconds of data. In each experiment, zone 1 corresponds to the left bar, and zone 4 to the right bar for each of the 3 groups of four bars. 91

CHAPTER 1

INTRODUCTION

1.1 Problem Statement

The concept of ideal free distribution (IFD) was originally introduced in [1]. For many years, this concept has been used to analyze how animals distribute themselves across different habitats. These habitats have different characteristics (e.g., one habitat might have a higher nutrient input rate than another), but animals tend to reach an equilibrium point where each has the same correlate of fitness (e.g., consumption rate). The term "ideal" means that the animals can perfectly sense the quality of all habitats and seek to maximize the suitability of the habitat they are in, and the term "free" means that the animals can go to any habitat. In [2, 3] the authors survey the various extensions to the IFD (e.g., the interference model [4] and standing crop idea [5]), and overview the experimental biological evidence that supports these models. In this dissertation we study three different cases where the IFD is achieved, and we provide analytical methods to study this important concept from theoretical ecology as well as some engineering applications.

1.2 Thesis Summary

The dissertation is divided in three main parts. In Chapter 2 we extend the theory of the IFD by providing methods to analytically find the distribution for a relatively general class of "suitability" functions. We show that the resulting IFD is a Nash equilibrium and an evolutionarily stable strategy (ESS). Moreover, we show that for a certain cost function it is a global optimum point. We introduce the "replicator dynamics" for the IFD and show that they provide an allocation strategy that is guaranteed to achieve the IFD. Finally, we show how this allocation strategy can achieve an IFD for a multizone temperature control problem that corresponds to achieving the maximum uniform temperature on a grid under a multivariable saturation constraint.

Models from behavioral ecology, specifically foraging theory, are used to describe the decisions an animal forager must make in order to maximize its rate of energy gain and thereby improve its survival probability. Using a bioinspired methodology, in Chapter 3 we view an animal as a software agent, the foraging landscape as a spatial layout of temperature zones, and nutrients as errors between the desired and actual temperatures in the zones. Then, using foraging theory, we define a decision strategy for the agent that has an objective of reducing the temperature errors in order to track a desired temperature. We describe an implementation of a multizone temperature experiment, and show that the use of multiple agents defines a distributed controller that can equilibrate the temperatures in the zones in spite of interzone, ambient, and network effects. We discuss relations to ideas from theoretical ecology, and identify a number of promising research directions.

Finally, in Chapter 4, a model of honey bee social foraging is introduced to create an algorithm that solves a class of optimal resource allocation problems. We prove that if several such algorithms ("hives") compete in the same problem domain, the strategy they use is a Nash equilibirium and an evolutionarily stable strategy. Moreover, for a single or multiple hives we prove that the allocation strategy is globally optimal. To illustrate the practical utility of the theoretical results and algorithm we show how it can solve a dynamic voltage allocation problem to achieve a maximum uniformly elevated temperature in an interconnected grid of temperature zones.

CHAPTER 2

OPTIMALITY, STABILITY, AND ALLOCATION STRATEGIES FOR THE IDEAL FREE DISTRIBUTION

2.1 Introduction

We start our dissertation by studying the IFD for a general class of correlates of fitness called suitability functions. This general class of suitability functions covers the ones studied in [6, 7] for the "continuous-input" model, and also includes the case of "interference" [4, 7, 8]. We also study a suitability function studied in [1]. For these suitability functions, we prove the equivalence of the habitat [6, 7] and input matching rules [4, 9], an equivalence only previously recognized to hold for one special class of suitability functions [4, 2]. We introduce the concept of an individual animal with a fitness and explain the type of equivalences that hold between habitat suitability and individual animal fitness equalization. Then we show that the treatment of a more general class of suitability functions allows us to characterize and analyze the "ideal dominance distribution" [1], something that has not been done in the literature to date [3]. Next, we explain how the IFD is a Nash equilibrium and an evolutionarily stable strategy (ESS) [10] for the case of a "game against the field" [11] for our expanded set of suitability functions. This means that in a large population of animals,

whose mean population strategy is an IFD, no mutant animal strategy can invade the population. While this means that the IFD is locally optimal in a game-theoretic sense (i.e., unilateral strategy deviations by a single animal are not profitable for that animal), here we show that the IFD possesses much stronger optimality properties. We show how to model a group of animals all simultaneously seeking to maximize their fitness as a "minimax" optimization problem. For this problem, we prove that the IFD is a global optimum point. This means that even if an arbitrary number of animals deviate so that the distribution is not an IFD, then there can be an arbitrary number of animals who need to change strategies to maximize their fitness. Moreover, it means that there is no other animal distribution where all the animals can simultaneously maximize their fitness. Our results bear some relationships to the work in [12] but here we consider a different (and more generic) class of suitability functions, and a "nonlinear" game against the field. Finally, we study how evolutionary dynamics can represent the animal allocation process over long time periods. In particular, we introduce the "replicator dynamics" [13] for the animal distribution "population game" [14, 15] and show how it relates to a steepest descent allocation strategy. For this model, natural selection according to differential fitness is the mechanism underlying the animal allocation and animal strategy mutations are represented by perturbations in the population "strategy mix" [14]. We show that the IFD is an equilibrium of the replicator dynamics, and via Lyapunov stability analysis show that the IFD is asymptotically stable for our general class of suitability functions (thereby extending earlier such analysis [13, 14, 15]). This means that the population will recover from perturbations (mutations) off the IFD equilibrium and the population's strategy mix dynamics eliminate mutants that are different from the

IFD so that evolution leads to the maintenance of an IFD strategy. We show one case where the IFD is exponentially stable so that mutant rejection is fast, and relate the size of the population to the rate of rejection of mutant strategies.

In the last section of this chapter we use the theory to solve a challenging engineering problem that involves achieving temperature control for multiple zones of a planar temperature grid, in spite of limited current available to drive the heaters and significant ambient and inter-zone effects. This problem can be seen as a distributed multivariable "dynamic resource allocation" problem because we want to split some quantity (current or voltage) that we have a limited amount of, and dedicate appropriate proportions of it to optimize some quantity of interest (quality of regulation). The allocations are inputs to a dynamical system and its response determines the quality of the allocation. The control goal could be a standard regulation or tracking objective (e.g., making all zones have the same given temperature), or a nontraditional objective like reaching the maximum uniform temperature across the entire grid. Control goals like these arise in the context of a variety of commercial applications (e.g., building temperature control) industrial systems. For instance, in semiconductor processing, one challenge is to achieve a uniform temperature on a plate [16]. Others [17] study distributed control of wafer temperature via multizone rapid thermal processing systems. In related work, the authors of [18] describe a multizone space heating system that maintains a desired temperature in different zones. Another application where the type of multizone temperature control that we study is very important is in personal computers. In [19], the author describes several current strategies used to solve this problem. In addition to such strategies, several other methods are currently available for distributed control design when set-point

regulation or tracking is the objective objective. For instance, in [20] the authors show how systems with a spatial interconnection topology can be controlled using conditions that can be expressed as linear matrix inequalities.

Unlike the work outlined above, we seek to confront the problem of the allocation of a limited amount of current (a multivariable saturation nonlinearity) in order to achieve a *maximum* uniform temperature on a planar grid, which is a true dynamic resource allocation problem. Dynamic resource allocation problems are found in a variety of applications beyond temperature control and are currently one of the most important challenges in the control systems area [21]. Current work on allocation for dynamical systems has its roots in the extensive literature that focuses on solving "static" resource allocation problems in optimization theory [22]. Unfortunately such methods do not directly apply to a dynamic resource allocation problem like the one we are confronting since they neither consider feedback-based allocation nor simultaneous constraints involving differential equations, equalities, and inequalities. An excellent example of innovative work in resource allocation for dynamical systems is found in [23] where the authors define a model for an air-jet system that describes the relationship between macro and micro-level forces, and derive dynamic allocations that can be mapped to, and configured for, different levels in a control hierarchy. Three other examples of dynamic resource allocation challenges are provided in [24], one for scheduling, one for temperature control, and the other for levitating balls in tubes (a university educational experiment). Here, we show how to apply the IFD strategy described in Section 2.5 to simultaneously satisfy current limitations and try to minimize energy use for a version of the planar temperature control problem

in [24]. We provide data from an experimental testbed to demonstrate the dynamical behavior and effectiveness of the method, particularly for achieving disturbance rejection. In this way, we show one case where the IFD theoretical framework we establish in this chapter can be used to provide a methodology to design strategies for dynamic resource allocation. Due to the generic nature of the theory we developed in this chapter it is likely that other applications can follow (e.g., for other applications in dynamic resource allocation see [24], or for potential uses of the IFD in other engineering applications see [25, 26]).

2.2 The Ideal Free Distribution

Suppose that there is a set $H = \{1, 2, \ldots, N\}$ of N disjoint habitats in an environment that are indexed by $i = 1, 2, \ldots, N$. Let the continuous variable $x_i(t) \in \mathbb{R}_+$ be the amount of animals in the i^{th} habitat at time $t \geq 0$, where $\mathbb{R}_+ = [0, \infty)$. Let $x = [x_1, x_2, \ldots, x_N]^\top \in \mathbb{R}_+^N$. Suppose that $\sum_{j=1}^N x_j = P$, where $P > 0$ is a constant for all time t, i.e., the amount of animals in the environment is constant. We say that a habitat i is truncated if $x_i = 0$, and is inhabited if $x_i > 0$ for some $i = 1, 2, \ldots, N$.

2.2.1 A General Class of Suitability Functions

Suppose that $b_i \geq 0$, is a constant that we sometimes interpret as a fixed number of resident animals in the i^{th} habitat, and $c_i > 0$ is a constant associated with the i^{th} habitat. Assume that $\sum_{j=1}^N a_j > 0$ and $a_i \geq 0$ for all $i = 1, 2, \ldots, N$. Let $H^* = \{i \in H : a_i > 0\}$ so $j \in H - H^*$ have $a_j = 0$. Let $m > 0$ be a constant. Let s_i be the suitability function for the i^{th} habitat, and in this case it is defined as

$$s_i = \frac{a_i}{(c_i x_i + b_i)^m} \tag{2.1}$$

In the literature, the most common function that has been used to describe the "continuous-input model" [2, 3] is a function that assumes that $b_i = 0$, and $c_i = m = 1$, so

$$s_i = \frac{a_i}{x_i} \tag{2.2}$$

Then, if a_i is in nutrients per second, $\frac{a_i}{x_i}$ is each animal's consumption rate at habitat i. This suitability is typically assumed to be a correlate of Darwinian fitness so sometimes it is called the fitness of an animal at habitat i. In this case, it is said that animals distribute in a way that they all achieve equal fitness. Below, in Section 2.2.4 we will derive an explicit relationship between habitat suitability and individual animal fitness for the general case since strictly speaking these two are different. In any case, the IFD is achieved via a sequential allocation process that places more (fewer) animals in higher (lower, respectively) suitability habitats until the suitability functions and fitnesses equalize at the IFD. That is, the IFD is achieved via a process where each animal simultaneously maximizes its own fitness.

Another popular suitability function found in the literature is the one that describes the "interference model" [4, 7, 8]. For it, in (2.1) let $c_i = 1$ and $b_i = 0$, so

$$s_i = \frac{a_i}{x_i^m} \tag{2.3}$$

Notice that in the case of (2.3), if we use the fact that at the IFD all the habitats will end up with the same suitability, then we can transform the interference model into a suitability function that looks like the standard one in (2.2) by taking the m^{th} root on the right-hand-side of (2.3). In this case, we will end up with a suitability

function of the form $s_i = \frac{a_i^{\frac{1}{m}}}{x_i}$. The animals will achieve an IFD, but they will not be able to determine precisely the quality of each habitat if they do not know m.

Since Equation (2.1) is more general than the ones in (2.2) and (2.3), our analysis is based on (2.1). The analysis starts by studying the habitat and input matching rules [6, 7, 9, 4]. Then, we define the ideal dominance distribution (IDD), and finally we define the idea of individual animal fitness equalization that will be useful for the game-theoretic and optimality analysis of the IFD.

2.2.2 Habitat and Input Matching Rules

The "habitat matching rule" [6, 7] says that at the IFD, the animals will distribute so that for each $i, j \in H^*$,

$$a_i(c_j x_j + b_j)^m = a_j(c_i x_i + b_i)^m \tag{2.4}$$

Since all the terms in (2.4) are positive, we can write this equation as

$$a_i^{\frac{1}{m}}(c_j x_j + b_j) = a_j^{\frac{1}{m}}(c_i x_i + b_i)$$

which is equivalent to

$$\frac{c_i x_i + b_i}{c_j x_j + b_j} = \frac{a_i^{\frac{1}{m}}}{a_j^{\frac{1}{m}}}$$

If we assume that c_i is a scaling factor, and that b_i is the number of fixed animals in the i^{th} habitat, we can say that what we have is the relative proportion of animals between two different habitats should be equal to some scaled relative proportion of the quality between the same habitats. Equation (2.4) can also be written as

$$\frac{a_j^{\frac{1}{m}}}{c_j x_j + b_j} = \frac{a_i^{\frac{1}{m}}}{c_i x_i + b_i}$$

So for the rest of our analysis, we assume that the suitability function in (2.1) is written as

$$s_i = \frac{a_i^{\frac{1}{m}}}{c_i x_i + b_i} \tag{2.5}$$

For (2.2), the habitat matching rule simply says that nutrient consumption rates are equal at all habitats.

Another common approach to characterize the IFD is to use the "input matching rule" [4, 9] which says the animals distribute so that for all $i \in H^*$,

$$\frac{c_i x_i + b_i}{\sum_{j=1}^{N} c_j x_j + b_j} = \frac{a_i^{\frac{1}{m}}}{\sum_{j=1}^{N} a_j^{\frac{1}{m}}} \tag{2.6}$$

This equation can be written as

$$\frac{a_i^{\frac{1}{m}}}{c_i x_i + b_i} = \frac{\sum_{j=1}^{N} a_j^{\frac{1}{m}}}{\sum_{j=1}^{N} c_j x_j + b_j}$$

Notice that for (2.2) what we obtain is that the overall consumption rate in the environment, characterized by the right-hand-side of this equation (with $c_i = m = 1$, and $b_i = 0$) has to be equal to the consumption rate in any single habitat. The IFD is achieved via a sequential allocation process that places more animals in habitats that have $s_i > \frac{\sum_{j=1}^{N} a_j}{\sum_{j=1}^{N} x_j}$ which lowers the suitability of habitat i for each animal there and raises the suitability of other habitats for animals there. Note that (2.2) is also equivalent to

$$s_i^{-1} = \frac{x_i}{a_i} = \frac{\sum_{j=1}^{N} x_j}{\sum_{j=1}^{N} a_j}$$

for $i \in H^*$. The right-hand-side of this equation is the total number of animals in the environment divided by the total number of nutrients arriving per second. At the IFD, the animals are distributed so that no matter which habitat they are at,

they get the same amount of nutrients. In this case, we can view the IFD as being achieved via the sequential allocation of animals to habitats with $s_i^{-1} < \frac{\sum_{j=1}^{N} x_j}{\sum_{j=1}^{N} a_j}$.

Since both Equations (2.4) and (2.6) are going to be used extensively in our analysis, we provide a proof of their equivalence in the next theorem[1].

Theorem 2.2.1 *Assume that* $\sum_{i=1}^{N} x_i = P > 0$, $\sum_{i=1}^{N} a_i^{\frac{1}{m}} > 0$, $c_i, m > 0$, *and* $a_i, b_i \geq 0$ *for* $i = 1, 2, \ldots, N$. *The habitat and input matching rules are equivalent characterizations of the IFD in that for a given set of* a_i, b_i, c_i, m, *the* x_i, $i = 1, 2, \ldots, N$ *are the same for either rule.*

Remark: There is another type of suitability function, that is similar to the one in [1]. Let b_i be the basic suitability of the i^{th} habitat, and let $\psi(x_i)$ be a function such that as x_i increases, $\psi(x_i)$ also increases, but the suitability decreases. We can write then the suitability as

$$s_i = b_i - \psi(x_i) \tag{2.7}$$

One possible $\psi(x_i)$ function is

$$\psi(x_i) = c_i x_i$$

where $c_i > 0$. In this case, the habitat matching rule is satisfied when the suitabilities for two different habitats i, j are equal, so

$$b_i - c_i x_i = b_j - c_j x_j \tag{2.8}$$

The input matching rule is in this case

$$\frac{\frac{b_i}{c_i} - x_i}{\sum_{j=1}^{N} \left(\frac{b_j}{c_j} - x_j \right)} = \frac{\frac{1}{c_i}}{\sum_{j=1}^{N} \frac{1}{c_j}} \tag{2.9}$$

[1]Proofs of all theorems are in the Appendix.

As before, the equivalence between Equations (2.8) and (2.9) can be proved using the same ideas as in Theorem 2.2.1.

2.2.3 Ideal Free and Dominance Distributions

The ideal dominance distribution (IDD) concept introduced in [1] comes from a type of relaxation of the "free" assumption of the IFD. The basic idea is that, assuming that all individuals are not equally aggressive, if there are new individuals arriving, then it will be more difficult for these "unsettled" individuals to access any habitat dominated by current residents. Thus, the unsettled individuals will end up in habitats that might not optimize their fitness compared to the case where they were the first arrivals.

The IDD can be interpreted via sequential settling of species of animals at IFDs. Suppose that we have $\bar{N}$ species who are arriving sequentially into the environment. We assume that the index $k = 1, 2, \ldots, \bar{N}$, represents the arrival and settling at the IFD for each of these species. Let $i = 1, 2, \ldots, N$, be each of the N habitats that can be chosen for the distribution of each species. Let a_i^k be the input rate for habitat i when the species k is settling. Let x_i^k be the number of animals of species k at habitat i. Then, x_i^{k-1} is the fixed number of individuals that settled down in habitat i, where $x_i^0 = 0$ (i.e., only the first species will distribute in such a way that there is no interference with animals that are already settled in a particular habitat). Let $c_i^k > 0$ and $m^k > 0$ be constants associated with the k^{th} species. Let P^k be the total number of animals associated with the k^{th} species. For each species arrival the individuals want to settle down in the best available habitat by maximizing fitness. The suitability function that each species uses to determine which is the best habitat,

is defined as

$$s_i^k = \frac{(a_i^k)^{\frac{1}{m^k}}}{c_i^k x_i^k + x_i^{k-1}} \tag{2.10}$$

with the constraint $\sum_{j=1}^{N} x_j^k = P^k$ for all k. Equation (2.10) defines a nonlinear difference equation for the distribution of subsequent species. If $P^k > 0$ is such that $P = \sum_{k=1}^{\bar{N}} P^k \to \infty$ as $\bar{N}$ and $k \to \infty$ then for some finite $k' \geq 0$ no habitat will be truncated. Since the parameter m skews the distribution it will change the k' such that truncation first disappears in an IDD.

The question that arises is: can we know the final value for each species in any habitat? Notice that (2.10) is similar to (2.5), with a slight change in the variables. Thus, the distribution of the individuals will be given by the IFD for this specific case. The next theorem shows how to find the distribution representing the IFD for the suitability functions as defined in (2.5) (or (2.10)). It gives a solution for the IFD for a general class of suitability functions (not available in the literature) and a solution to (2.10) (when for each species k we have that $x_i^{k-1} = b_i$) so that the IDD can be found for any number of species $\bar{N}$ that sequentially arrive at the environment.

Theorem 2.2.2 *For $i = 1, 2, \ldots, N$, the point*

$$x_i^* = \frac{\frac{a_i^{\frac{1}{m}}}{c_i} P + \frac{a_i^{\frac{1}{m}}}{c_i} \sum_{j=1}^{N} \frac{b_j}{c_j} - \frac{b_i}{c_i} \sum_{j=1}^{N} \frac{a_j^{\frac{1}{m}}}{c_j}}{\sum_{j=1}^{N} \frac{a_j^{\frac{1}{m}}}{c_j}} \tag{2.11}$$

is the IFD for the suitability function defined in (2.5), whenever P satisfies

$$P \geq \max_{i=1,2,\ldots,N} \left\{ \frac{b_i}{a_i^{\frac{1}{m}}} \sum_{j=1}^{N} \frac{a_j^{\frac{1}{m}}}{c_j} - \sum_{j=1}^{N} \frac{b_j}{c_j} \right\} \tag{2.12}$$

If (2.12) is not satisfied, and without (significant) loss of generality we assume that $\frac{a_1^{\frac{1}{m}}}{b_1} > \frac{a_2^{\frac{1}{m}}}{b_2} > \ldots > \frac{a_N^{\frac{1}{m}}}{b_N}$*, the IFD is given by*

$$x_i^* = \begin{cases} \frac{\frac{a_i^{\frac{1}{m}}}{c_i} P + \frac{a_i^{\frac{1}{m}}}{c_i} \sum_{j=1}^{k^*} \frac{b_j}{c_j} - \frac{b_i}{c_i} \sum_{j=1}^{k^*} \frac{a_j^{\frac{1}{m}}}{c_j}}{\sum_{j=1}^{k^*} \frac{a_j^{\frac{1}{m}}}{c_j}} & i = 1, 2 \ldots, k^* \\ 0 & i = k^* + 1, k^* + 2, \ldots, N \end{cases} \tag{2.13}$$

where

$$k^* = \arg\max \left\{ k : \frac{a_k^{\frac{1}{m}}}{b_k} > \frac{\sum_{j=1}^{N} \frac{a_j^{\frac{1}{m}}}{c_j}}{P + \sum_{j=1}^{N} \frac{b_j}{c_j}} \right\} \tag{2.14}$$

Notice that whenever (2.12) is satisfied with strict inequality, $x_i^* > 0$, which implies that all the habitats end up inhabited. Also, notice that k^* is given by analyzing the values of the suitability functions when $x_i = 0$. It is clear that if P is big enough, then the right-hand-side of the inequality in (2.14) becomes almost 0, and hence all habitats will end up inhabited.

2.2.4 Individual Animal Fitness Equalization

Normally, the number of habitats N, the a_i, b_i, c_i, m, $i = 1, 2, \ldots, N$, and $P > 0$ are given. Then, the x_i, $i = 1, 2, \ldots, N$, must be found that achieve the IFD via (2.6). Problems with existence of the IFD can arise, however, if x_i is the number of animals since in that case it is natural to assume that x_i is discrete. For example, assume that $x_i \in \{0, 1, 2, \ldots\}$. In this case, the IFD may not exist (e.g., if $P = 7$, $N = 2$, $m = 1$, $a_1 = 0.1$, $b_1 = b_2 = 0$, $c_1 = c_2 = 1$ and $a_2 = 0.2$, then (2.6) cannot be satisfied). But, if the P, a_i, b_i, c_i, m, and N have appropriate values, Equation (2.6) can be satisfied. The standard approach to cope with this problem is to assume that there is a large enough number of animals so that it is a good approximation to consider x_i to vary continuously. We will take this same approach so we are assured that an IFD

exists. But, with x_i continuous we lose the ability to distinguish between individual animals. In this framework it is, however, still possible to introduce a limited notion of an individual. This will allow us to assign each individual a fitness and then clearly relate equalization of habitat suitabilities to equalization of individual animal fitnesses. Moreover, our concept of an individual is critical to modeling the IFD as a game between many individuals in Section 2.3.1, showing how individuals' fitness maximization objective leads to an IFD, and relating this to optimality formulations for the IFD.

To introduce the concept of an individual, assume that each animal is identical and represented by some arbitrarily small $\epsilon_x > 0$ so that there is an arbitrarily large (integer) number $n > 0$ of animals in the environment, where

$$n\epsilon_x = P$$

and

$$b_i = \bar{b}_i \epsilon_x$$

with $\bar{b}_i \geq 0$ being the integer fixed number of resident animals in the i^{th} habitat. Then, if $n_i \geq 0$ is the (integer) number of animals at habitat i, $\sum_{j=1}^{N} n_j = n$, $x_i = n_i \epsilon_x$, and the IFD in (2.6) is achieved when for all $i = 1, 2, \ldots, N$,

$$\frac{\epsilon_x(c_i n_i + \bar{b}_i)}{\sum_{j=1}^{N} \epsilon_x(c_j n_j + \bar{b}_j)} = \frac{(c_i n_i + \bar{b}_i)}{\sum_{j=1}^{N}(c_j n_j + \bar{b}_j)} = \frac{a_i^{\frac{1}{m}}}{\sum_{j=1}^{N} a_j^{\frac{1}{m}}} \tag{2.15}$$

which has been another interpretation of the IFD in the literature (e.g., in [1, 3]) for the case $b_i = 0$, $c_i = m = 1$. Notice that for an arbitrary P and b_i, in order to ensure the existence of the IFD we need to have an arbitrarily small positive value ϵ_x.

Given the concept of an individual animal $\epsilon_x > 0$ at habitat i, $i = 1, 2, \ldots, N$, we define this animal's fitness as $f(i) = \frac{a_i^{\frac{1}{m}}}{c_i n_i + \bar{b}_i}$. In the case when $b_i = 0$, $c_i = m = 1$, if

a_i is nutrients per second, $f(i)$ is the number of nutrients per second that an animal gets at habitat i. This choice is consistent with the results in [7], which show other ways to relate fitness and suitability. Notice that

$$f(i) = \frac{a_i^{\frac{1}{m}}}{c_i n_i + \bar{b}_i} = \epsilon_x \frac{a_i^{\frac{1}{m}}}{\epsilon_x (c_i n_i + \bar{b}_i)} = \epsilon_x \frac{a_i^{\frac{1}{m}}}{c_i x_i + b_i} \tag{2.16}$$

Notice that if we use the suitability function in (2.2) we have

$$f(i) = \frac{a_i}{n_i} = \epsilon_x \frac{a_i}{\epsilon_x n_i} = \epsilon_x \frac{a_i}{x_i} = \epsilon_x s_i$$

so that individual animal fitness is indeed a correlate of habitat suitability. Clearly, however, even though they are linearly related, habitat suitability is not the same as individual animal fitness. Moreover, if $a_i, b_i, c_i > 0$ and $x_i > 0$, $i = 1, 2, \ldots, N$, then equalization of habitat suitability (i.e., $s_i = s_j$, $i, j = 1, 2, \ldots, N$) is equivalent to equalization of animal fitness (i.e., $f(i) = f(j)$, $i, j = 1, 2, \ldots, N$). The equivalence characterized by Theorem 2.2.1 holds for the fitness of all individuals at any habitat $j \in H^*$.

Remark: For the suitability function defined in (2.7), if we let $\bar{b}_i$ be the integer number of fixed resident animals that we have in the i^{th} habitat. Let also $\bar{\epsilon}_x$ be some arbitrarily small positive value, such that

$$b_i = \bar{\epsilon}_x \bar{b}_i$$

$$x_i = \bar{\epsilon}_x n_i$$

where n_i is an arbitrarily large integer number of animals in the i^{th} habitat. Then, we can define the animal fitness as

$$f(i) = \bar{b}_i - c_i n_i = \frac{1}{\bar{\epsilon}_x}(b_i - c_i x_i) \tag{2.17}$$

2.3 Game-Theoretic and Optimality Properties of the IFD

In this section, first we define the basic concepts of evolutionary game-theory in order to prove that the IFD is indeed an evolutionarily stable strategy (ESS). Then, in order to extend this result, we model the IFD achievement as solving an optimization problem, and we prove that the IFD is a global optimum point.

2.3.1 Nash Equilibria and Evolutionarily Stable Strategies

In this and the next section, to use a game-theoretic perspective we view each "player" as an individual animal that makes strategy choices to maximize its payoff, which is fitness. A Nash equilibrium is a set of animal strategy choices such that any unilateral deviation by any animal from its strategy choice will not be better for that animal [27]. The standard definition for an evolutionarily stable strategy (ESS) is a strategy such that no "mutant" can invade a population of members ("incumbents") who use this strategy [10]. The classical ESS idea is based on a two-player game where incumbents either play other incumbents or mutants (and vice versa). These players are drawn from an infinite population. There is an extension of this ESS concept that is called a "game against the field" where the success of each individual does not depend on a single opponent, but instead depends on the strategies of all other members of the population (see [11], page 23).

Let $f(\bar{x}, P_{\bar{y}})$ be the fitness of a single $\bar{x}$-strategist in a population (set) of $\bar{y}$-strategists that we denote by $P_{\bar{y}}$. We will say that $\bar{x}$ is an ESS if both of the following two conditions hold [11]:

1. For all $\bar{y} \neq \bar{x}$

$$f(\bar{y}, P_{\bar{x}}) \leq f(\bar{x}, P_{\bar{x}}) \tag{2.18}$$

and

2. For any $\bar{y} \neq \bar{x}$, if $f(\bar{y}, P_{\bar{x}}) = f(\bar{x}, P_{\bar{x}})$, then for a small $q > 0$,

$$f(\bar{y}, P_{\bar{y}_q}) < f(\bar{x}, P_{\bar{y}_q}) \tag{2.19}$$

where $f(\bar{y}, P_{\bar{y}_q})$ is defined as the fitness of a $\bar{y}$-strategist in a population consisting of individuals playing the strategy $\bar{y}_q = q\bar{y} + (1-q)\bar{x}$.

The first condition means that $\bar{x}$ is a Nash equilibrium, since no mutant strategy $\bar{y}$ does better than the incumbent strategy $\bar{x}$, and usually this condition is called the "equilibrium condition" [14]. The second condition states that if the mutant strategy $\bar{y}$ does as well as the incumbent strategy $\bar{x}$, then the mutant strategy does not do as well than the incumbent strategy when they play against a population formed from both the incumbent and the mutant strategies. This is a variation of what is known as the "stability condition" [14].

2.3.2 Game-Theoretic Characteristics of the IFD

In this section we characterize the relationships between equilibria in games and the IFD. In a game-theoretic interpretation of the animal distribution problem each animal has N pure strategies [27] corresponding to choosing habitat i, $i = 1, 2, \ldots, N$. Each animal can only reside in one and only one habitat. Hence, each animal ϵ_x has a strategy of the form

$$\bar{x} = [0, \ldots, \epsilon_x, \ldots, 0]^\top$$

where ϵ_x is in the i^{th} position, $i = 1, 2, \ldots, N$. These strategies can be interpreted as pure strategies of a polymorphic population [14]. The meaning of "$\bar{y} \neq \bar{x}$" for Equations (2.18) and (2.19) is that $\bar{y}$ can correspond to placement of ϵ_x in any habitat $j \neq i$. In the next theorem $P_{\bar{x}}$ for Equation (2.18) is any population such that all individuals play a strategy so that the IFD defined by (2.6) is satisfied. Clearly, in this case, the strategies of individuals in $P_{\bar{x}}$ are not the same since the animals must play different strategies to achieve the IFD.

Theorem 2.3.1 *If x_i is a continuous variable with $\epsilon_x > 0$ representing an animal, then the x_i, $i = 1, 2, \ldots, N$, given by the IFD in (2.6) are the result of animals using a (unique, strict) Nash equilibrium strategy and hence an evolutionarily stable strategy.*

The game-theoretic model is developed from the perspective of the individual animals. Theorem 2.3.1 shows that if each individual uses a strategy that maximizes its own fitness, they will achieve an IFD which is an ESS and hence a Nash strategy. Due to the equivalence of individual fitness equalization and habitat suitability equalization, Theorem 2.3.1 implies that choices at the individual level lead to habitat suitability equalization across the entire environment. The Nash equilibrium is often called an "optimal" strategy since no animal can do better by deviating from the strategy. The *only* allowed deviations from the IFD in the game-theoretic model of animal distribution problem correspond to shifting ϵ_x from one habitat to another and this is consistent with the assumption that animals can adopt one of N pure strategies. This fits with the ESS concept above since this corresponds to a single "rare" mutation in a population. Clearly if there are certain types of simultaneous deviations of animals (e.g., by swapping habitats via simultaneous mutations), the

strict Nash can also be maintained; however, such deviations would require coordination and this is not possible since we are inherently considering a competitive game-theoretic framework via the Nash concept, and hence also the ESS. In the next section we will, however, reconsider this assumption.

Finally, we note that while in [11] and other papers it has been pointed out that the IFD is an ESS, this is to our knowledge the first formal proof of this fact. The value of the formal proof lies in the treatment of fitness, and it clearly connects individual fitness maximization to habitat-level suitability equalization. The proof shows that the IFD is a *strict* Nash equilibrium so some would consider the animal distribution game to be unique since most games do not have strict Nash equilibria [15]. Moreover, the proof shows that the IFD of the animal distribution population game is what is called a "local ESS" in [14].

2.3.3 Optimality of the IFD

In this section we show how optimization models can represent the animal distribution game and how the IFD is a global optimum point for such a model. Recall that the animal distribution game assumes that all animals in the population seek to simultaneously maximize their fitness. Assume that $a_i, b_i, c_i > 0$ and $x_i \geq 0$, $i = 1, 2, \ldots, N$. An optimization model for the animal distribution game is one where the minimum fitness is maximized. In other words,

$$\begin{array}{ll} \max\min & \left\{ \epsilon_x \frac{a_1^{\frac{1}{m}}}{(c_1 x_1 + b_1)}, \epsilon_x \frac{a_2^{\frac{1}{m}}}{(c_2 x_2 + b_2)}, \ldots, \epsilon_x \frac{a_N^{\frac{1}{m}}}{(c_N x_N + b_N)} \right\} \\ \text{subject to} & \sum_{j=1}^{N} x_j = P \\ & x_i \geq 0,\ i = 1, 2, \ldots, N \end{array} \tag{2.20}$$

The constraints demand that the population size stays constant and that the number of animals at each habitat is non-negative. The terms $\epsilon_x \frac{a_i^{\frac{1}{m}}}{(c_i x_i + b_i)}$ are the fitnesses

for *any* animal that chooses habitat i, $i = 1, 2, \ldots, N$. Consider a single individual $\epsilon_x > 0$. If this animal is at habitat i and $\epsilon_x \frac{a_i^{\frac{1}{m}}}{(c_i x_i + b_i)} < \epsilon_x \frac{a_j^{\frac{1}{m}}}{(c_j x_j + b_j)}$, $j \neq i$, then it can move to habitat j (i.e., change strategies). The "max min" represents that multiple animals simultaneously shift strategies to improve their fitness since at least some animals with lowest fitness shift habitats (and if $\epsilon_x \frac{a_i^{\frac{1}{m}}}{(c_i x_i + b_i)} = \epsilon_x \frac{a_j^{\frac{1}{m}}}{(c_j x_j + b_j)}$ for some i and j the min can be achieved at multiple habitats).

The following theorem shows that the animals choose the IFD in order to maximize their fitness when everybody else is trying to do the same.

Theorem 2.3.2 *The point $x^* = [x_1^*, \ldots, x_N^*]^\top$, such that for all $i = 1, 2, \ldots, N$, (with x_i^* defined in Equations (2.13) and (2.14)) is a unique global maximum point that solves the optimization problem in (2.20) that represents that each animal simultaneously chooses a habitat to maximize its own fitness.*

The value of Theorem 2.3.2 is that it shows that the IFD is a *global* optimum point for the animal distribution problem. The game-theoretic setting of Section 2.3.2 only illustrated *local* optimality in the Nash sense. Theorem 2.3.2 shows that *any* number of simultaneous perturbations from the IFD result in possibly many animals incurring a degradation in fitness. Hence, an arbitrary number of mutants cannot invade the population. This idea will be studied further in Section 2.4.

Remark: For the case in (2.7) with $\psi(x_i) = c_i x_i$, the idea is again try to maximize the minimum fitness in the environment. The fitness function in this case is defined as $f(i) = \frac{1}{\epsilon_x}(b_i - c_i x_i)$. Without (significant) loss of generality, we assume that all habitats are ranked in such a way that $b_1 > b_2 > \ldots > b_N$. Using an approach like in

Theorem 2.3.2, the optimum point for this case is

$$x_i^* = \begin{cases} \frac{b_i \sum_{j=1}^{k^*} \frac{1}{c_j} + P - \sum_{j=1}^{k^*} \frac{b_j}{c_j}}{c_i \sum_{j=1}^{k^*} \frac{1}{c_j}} & i = 1, 2, \ldots, k^* \\ 0 & i = k^* + 1, k^* + 2, \ldots, N \end{cases} \tag{2.21}$$

with

$$k^* = \arg\max \left\{ k : b_k > \frac{\sum_{j=1}^{N} \frac{b_j}{c_j} - P}{\sum_{j=1}^{N} \frac{1}{c_j}} \right\}$$

2.4 Evolutionary Allocation Dynamics for IFD Achievement

In this section we consider animal allocation dynamics from evolutionary and decision-making perspectives. We focus on defining allocation dynamics that guarantee the achievement of an IFD.

2.4.1 The Replicator Dynamics Model

The replicator dynamics are a simple model of how selection via differential fitness affects the proportions of animals using different strategies [14, 15, 28]. Here, building on the game-theoretic formulation in Section 2.3 we show how equilibria of one class of replicator dynamics are related to the IFD. These are not the standard replicator dynamics that are developed based on random pairings of two individuals in what is called a "linear game." Here, we extend such standard formulations in [13, 14] to represent our game against the field which is classified as a nonlinear game.

Recall that each animal has N pure strategies, which correspond to choosing which habitat to live in for its entire life, and that the number of animals is constant and $\sum_{j=1}^{N} x_j = P$ for some $P > 0$ and all $t \geq 0$. Let

$$p_i = \frac{x_i}{\sum_{j=1}^{N} x_j}$$

represent the fraction of individuals in a population of animals playing pure strategy i, $i = 1, 2, \ldots, N$. Clearly $p_i(t) \geq 0$ for $i = 1, 2, \ldots, N$, and $\sum_{j=1}^{N} p_j = 1$ for all $t \geq 0$. The vector $p = [p_1, p_2, \ldots, p_N]^\top$ is the "population state" which represents the strategy mix of the population [14]. Clearly, $p(t) \in \Delta$ for all $t \geq 0$, where

$$\Delta = \left\{ p(t) \in \mathbb{R}_+^N : \sum_{i=1}^{N} p_i(t) = 1 \right\}$$

is the "constraint set" (simplex) that defines a subset of the state space. The vector $x(t) = [x_1, x_2, \ldots, x_N]^\top$ lies in the simplex Δ_x, where $\Delta_x = \{x(t) \in \mathbb{R}_+^N : \sum_{i=1}^{N} x_i = P\}$.

The replicator dynamics assume continuously mixed generations and are given by

$$\frac{\dot{p}_i}{p_i} = \beta_i \left[\{\text{fitness of animals that play } i \in H\} - \{\text{average fitness in population}\} \right] \tag{2.22}$$

where $\beta_i > 0$ are proportionality constants, $i = 1, 2, \ldots, N$. The left-hand-side of (2.22) is the normalized rate of increase in the population share playing strategy i. The right-hand-side of (2.22) indicates that if i-strategists are more successful (less successful) than the average, their population share will increase (decrease, respectively).

The replicator dynamics generally describe the evolution of the state of the population p. Note, however, in the case where the players only have pure strategies $i \in H$, the *mean population strategy* is

$$\sum_{i=1}^{N} p_i e_i = p$$

where $e_i = [0, \ldots, 1, \ldots, 0]^\top$, a vector with a 1 in the i^{th} position, represents the pure strategy $i \in H$. This means that the population state is the mean population

strategy. Hence, we can think of the replicator dynamics as representing the evolution of the IFD strategy by the process of natural selection.

In this specific case, we have defined the fitness of animals that play $i \in H$ in (2.22) at time t as (2.16), i.e.,

$$f(i) = \epsilon_x \frac{a_i^{\frac{1}{m}}}{c_i P p_i + b_i}$$

where $\epsilon_x > 0$ and the average fitness (of a randomly selected individual from the population) is

$$\bar{f} = \sum_{j=1}^{N} p_j f(j) = \sum_{j=1}^{N} \epsilon_x \frac{p_j a_j^{\frac{1}{m}}}{c_j P p_j + b_j}$$

Hence, the replicator dynamics are

$$\dot{p}_i = \beta_i p_i \left(f(i) - \bar{f} \right) \tag{2.23}$$

or

$$\dot{p}_i = \beta_i \epsilon_x p_i \left(\frac{a_i^{\frac{1}{m}}}{c_i P p_i + b_i} - \sum_{j=1}^{N} \frac{p_j a_j^{\frac{1}{m}}}{c_j P p_j + b_j} \right) \tag{2.24}$$

with $\beta_i > 0$ for all $i = 1, 2, \ldots, N$, when $p(0) \in \Delta$. Notice that $f(i) - \bar{f}$ measures the deviation from the IFD as quantified by the habitat matching rule (after some mathematical manipulation). The replicator dynamics for our population game are in the form of "monotone selection dynamics" [14]. The monotone selection dynamics in [14], p. 88, show what is essential to set up a replicator dynamics so that Δ is invariant. Notice that when s_i is defined as in (2.2), the average payoff $\bar{f}$ is constant.

2.4.2 Constraint Set Invariance for the Replicator Dynamics

First, we specify conditions under which (2.24) can be satisfied at the same time that the constraints $\sum_{j=1}^{N} p_j = 1$ and $p_i \geq 0$, $i = 1, 2, \ldots, N$ are satisfied. This is

essential since we are only interested in solutions to (2.24) that satisfy the appropriate constraints.

Theorem 2.4.1 *The system in (2.24) satisfies the constraint $p(t) \in \Delta$, for all $t \geq 0$ if and only if $\beta_i = \beta_j$, $i, j = 1, 2, \ldots, N$, and $p(0) \in \Delta$.*

This shows that the rate of increase or decrease in proportions of the strategies must be the same in order for the ordinary differential equation describing the replicator dynamics to satisfy the constraints of $\sum_{j=1}^{N} p_j = 1$, $p_i \geq 0$, $i = 1, 2, \ldots, N$. A special case of this result is the following theorem which is from [14].

Theorem 2.4.2 *If $\beta_i = \beta_j = \beta$ for all $i, j = 1, 2, \ldots, N$, and $p(0) \in \Delta$, then $p \in \Delta$ for all $t \geq 0$ (i.e., Δ is invariant with respect to (2.23)).*

To ensure that the constraint set Δ is satisfied in all that follows we assume that $\beta_i = \beta_j$, $i, j = 1, 2, \ldots, N$.

2.4.3 Stability Analysis of the IFD

First, we need to find the equilibrium point in (2.24). We assume in the following analysis that $p_i(t) \in \Delta - \partial\Delta$ for all $t \geq 0$, i.e., we are working strictly inside the simplex. If we set $\dot{p}_i = 0$, we get

$$0 = \beta \epsilon_x p_i^* \left(\frac{a_i^{\frac{1}{m}}}{c_i P p_i^* + b_i} - \sum_{j=1}^{N} \frac{p_j^* a_j^{\frac{1}{m}}}{c_j P p_j^* + b_j} \right)$$

where p_i^* is the equilibrium point. Since we are working inside the simplex $p_i^* \neq 0$, so we have

$$\frac{a_i^{\frac{1}{m}}}{c_i P p_i^* + b_i} = \sum_{j=1}^{N} \frac{p_j^* a_j^{\frac{1}{m}}}{c_j P p_j^* + b_j}$$

This equation has to be valid for all $i = 1, 2, \ldots, N$, hence for any i, j we obtain

$$\frac{a_i^{\frac{1}{m}}}{c_i P p_i^* + b_i} = \frac{a_j^{\frac{1}{m}}}{c_j P p_j^* + b_j}$$

which is the habitat matching rule in (2.4) but in p-coordinates. In Theorem 2.2.2 we have shown that this equilibrium point is given by (2.11) in x-coordinates, whenever P satisfies (2.12) with strict inequality.

Note that, for (2.2), when we try to find this equilibrium point, if $p_i \neq 0$ the solution would be $f(i) = \bar{f}$, which means that the consumption rate in each habitat i has to be equal to the overall consumption rate (in this case this one is described by $\bar{f}$) at the IFD equilibrium. Otherwise, the strategy mix of the population will continue to change.

Theorem 2.4.3 *For the replicator dynamics in (2.24), the IFD equilibrium given by* $p^* = \frac{x^*}{P}$ *(where* x^* *is defined in (2.11)) is asymptotically stable, with region of asymptotic stability* $\Delta - \partial\Delta$.

Theorem 2.4.3 is a "semiglobal" result which means that if the population state perturbs from the IFD to a point within some set, then the population state will return to the IFD. Note that under the game-theoretic interpretation, only a special type of perturbation is allowed: perturbations correspond to a single animal $\epsilon_x > 0$ switching to another strategy where ϵ_x is arbitrarily small. Theorem 2.4.3 includes this strategy perturbation as a special case so it applies to the game-theoretic setting. What does it mean for the population state to "return" to the IFD? If any animal switches habitats, then the mechanisms of reproduction via differential fitness will always shift the animal distribution back to the IFD. The shift of animal ϵ_x will result

in more deaths in its new habitat and correspondingly more births in the habitat it shifted from.

In [13, 14] it was shown that any ESS for a two-player game must be an asymptotically stable equilibrium in the replicator dynamics defined for that type of game, but that there could exist asymptotically stable equilibria that are not ESS. For our replicator dynamics for the game against the field, the above results show that there is one unique equilibrium strictly inside the simplex, that this equilibrium is the IFD (which we showed was an ESS in Section 2.3), and that the IFD is asymptotically stable (or exponentially stable for the standard suitability function in (2.2)).

Remark: For the case of (2.7) with $\psi(x_i) = c_i x_i$, we can define the replicator dynamics as before. Since the fitness function for this case is defined as $f(i) = \frac{1}{\bar{\epsilon}_x}(b_i - c_i x_i)$, we have the following ODE that represents the replicator dynamics.

$$\dot{p}_i = p_i \frac{1}{\bar{\epsilon}_x} \left((b_i - P c_i p_i) - \sum_{j=1}^{N} p_j (b_j - P c_j p_j) \right) \tag{2.25}$$

The stability proof for this case is similar to the one for (2.24).

2.4.4 Allocation Dynamics: Gradient Optimization Perspective

Related work has been done via the study of the Shahshahani gradient [14] and for linear games in [12].

Consider the cost function

$$J = \frac{1}{2} \sum_{i=1}^{N} \left(\frac{x_i}{P} - \frac{x_i^*}{P} \right)^2 \tag{2.26}$$

where x_i^* is defined in (2.11), and $\sum_{j=1}^N x_j = P$. Note that (2.26) measures the deviation off the IFD defined by (2.6). The following theorem shows that minimization of J, results in an IFD.

Theorem 2.4.4 *The point x_i^* in (2.11) is a global minimizer for the constrained optimization problem defined as*

$$\begin{array}{ll} \text{minimize} & J = \frac{1}{2}\sum_{i=1}^N \left(\frac{x_i}{P} - \frac{x_i^*}{P}\right)^2 \\ \text{subject to} & \sum_{j=1}^N x_j = P \\ & x_i > 0, \quad i = 1, 2, \ldots, N \end{array} \tag{2.27}$$

where x_i^* is defined in (2.11), when P is satisfied with strict inequality in (2.12).

Next, suppose that a steepest descent method is used in animal reallocation so that

$$\dot{x}_i = -\lambda P \frac{\partial J}{\partial x_i} \tag{2.28}$$

where $\lambda > 0$ is a "step-size" parameter. Note that if we let $b_i = 0$, and choose $\lambda = \beta\epsilon_x \sum_{j=1}^N \frac{a_j^{\frac{1}{m}}}{c_j}$, Equation (2.28) is

$$\dot{x}_i = -\left(\beta\epsilon_x \sum_{j=1}^N \frac{a_j^{\frac{1}{m}}}{c_j}\right)\left(\frac{x_i}{P} - \frac{\frac{a_i^{\frac{1}{m}}}{c_i}}{\sum_{j=1}^N \frac{a_j^{\frac{1}{m}}}{c_j}}\right) \tag{2.29}$$

These allocation dynamics are *equivalent* to the replicator dynamics in (2.24). If in (2.23) we take $f(i) = \epsilon_x \frac{a_i^{\frac{1}{m}}}{c_i x_i}$, then the replicator dynamics in (2.24) are the same as in (2.29). Hence, we know that the constraint $\sum_{j=1}^N x_j = P$ is met for all $t \geq 0$. Moreover, for the optimal allocation dynamics the following result holds.

Theorem 2.4.5 *The optimal allocation dynamics in (2.29) have the IFD as an equilibrium and it has a region of exponential stability given by $\Delta_x - \partial\Delta_x$.*

Hence, the allocation strategy will not get "stuck" and will result in a distribution of effort that converges to the IFD. Convergence is achieved independent of where the effort distribution starts. Equation (2.28) and the proof illustrate that if P is small (big) we will have a faster (slower) convergence rate. Also, notice that there is a critical difference compared to the strict Nash equilibrium and replicator dynamics viewpoint. Perturbations for the game-theoretic formulation are due to a single animal $\epsilon_x > 0$ switching habitats, and the replicator dynamics are built upon that perspective. With the optimal allocation perspective, any perturbation is allowed (i.e., any initial condition corresponding to the initial animal effort distribution must be possible), even ones that are not small perturbations $\epsilon_x > 0$.

2.5 Multizone Temperature Control Application

Here, to illustrate the theoretical results shown in the previous sections, we consider a multizone temperature control problem that has a voltage saturation constraint [24]. The experiment consists of $N = 4$ zones, where each zone consists of one lamp with voltage input $v_i(t)$ and one sensor that provides the temperature $T_i(t)$, $t \geq 0$. The idea of this experiment is to use the replicator dynamics in (2.24) to reach a *maximum* uniform temperature in each of the zones (it is important to note that this is not a standard tracking problem since the maximum achievable temperature is not known). For that, we assume that $\epsilon_x = c_i = m = b_i = \beta = 1$.

Equation (2.24) has two main variables: the proportion of the number of animals in habitat i, p_i, and the arrival rate a_i for the i^{th} habitat. In the previous analysis, the a_i values were positive constants, however, these arrival rates could vary with time. Suppose we define each arrival rate to be the inverse of the temperature sensed

in each zone, so that for $i = 1, 2, \ldots, N$, $a_i(t) = \frac{1}{T_i(t)}$. Since $T_i(t) > 0$, $a_i(t) > 0$ for all $i = 1, 2, \ldots, N$. Next, let $x_i(t) = p_i(t)P = v_i(t)$, where $\sum_{j=1}^{N} v_j(t) = P > 0$ is the total amount of voltage that can be applied to all zones. For our lamps, $v_i(t) \geq 0$, $t \geq 0$, and this fits with the assumptions on $x_i(t)$ in the theory. For a given $v_i(0)$, the replicator dynamics indicate how to redistribute voltage, depending on $a_i(t)$. Here, the temperature will change due to ambient and interzone influences, and the replicator dynamics will persistently and dynamically redistribute the constrained amount of voltage. Will it do this in a way to try to achieve the maximum uniform temperature? The results below seem to illustrate that it will. Why? Because, it will allocate more voltage to the minimum temperature at each time step. It will tend to force the lowest (minimum) temperatures to rise faster than the higher temperatures.

While we expect that the temperature in each of the zones will be the same after some time, there are certain features of the physical experiment that conspire against us achieving this goal. One problem is the physical location of the lamps and the sensors. Since we are working with breadboards, it is difficult to have the same sensor-lamp, inter-lamp, and inter-sensor distances for all the zones, and hence the interzone effects are different for each zone. The second problem is the sensors. We calibrate one sensor and then we pick three others that provide temperatures close to it *before* construction. Next, there is sensor noise. If all the sensors were the same, and there was no noise, after a period of time the same temperature would be achieved in each of the zones.

The results are shown in Fig. 2.1. This figure shows the first 50 minutes of the experiment. At the beginning, the experiment was at 22 degrees Celsius, and as we can see, practically all the zones were around this temperature. The temperature in each

of the zones starts to increase according to the voltage that we allocate to each of the lamps. The idea is to distribute 3.5 volts across the zones. We assume that these 3.5 volts are equivalent to P. For this case, we assume that $P = 20$. The initial conditions are $x_1(0) = 0.44$, $x_2(0) = 0.57$, $x_3(0) = 0.51$, and $x_4(0) = 1.98$. All the units are in volts. After 15 minutes, the experiment almost reaches a uniform temperature, around 29 degrees Celsius. At 18 minutes, we add a disturbance to the grid. This disturbance consists of turning on a lamp that is close to the first temperature zone, and leaving it on for 2 minutes. As we can see in Fig. 2.1 the first zone drastically increases its temperature, but at the same time there is a reallocation of the resource (voltage) across the four zones. We can see then that at 18 minutes, all the zones but the first one start to have more voltage, and that occurs until the disturbance finishes. The final temperature in the grid is practically the same, ± 1 degree Celsius. In this case, it is clear that we do not reach a unique equilibrium point described by the input matching rule due to ambient and interzone influences. However, as we can see in Fig. 2.1 the final values allocated are $x_1(3000) = 0.88$, $x_2(3000) = 0.88$, $x_3(3000) = 0.86$, and $x_4(3000) = 0.88$. However, using our previous analysis the final values should be $x_1^* = 0.88$, $x_2^* = 0.87$, $x_3^* = 0.86$, and $x_4^* = 0.89$, which as we can see are relatively close to what we have in the experiment. Notice that the only computations needed to implement the control are those for the computation of (2.24), using $a_i = \frac{1}{T_i}$, and with $\epsilon_x = c_i = m = b_i = \beta = 1$. Clearly, the computational complexity is not a concern for this application.

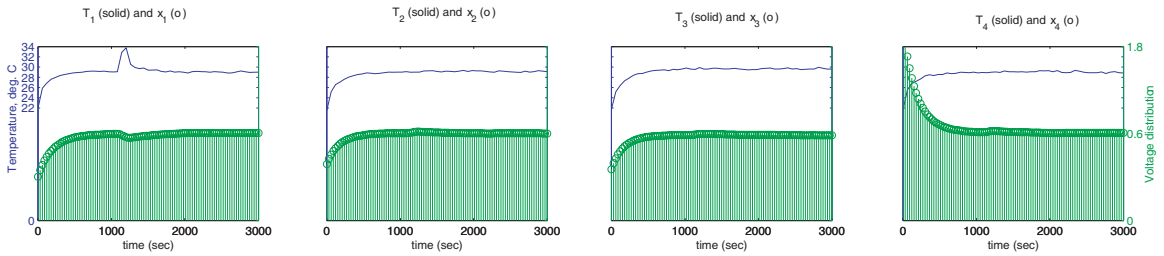

Figure 2.1: Temperatures in four zones of the multizone temperature control experiment. The plot represents the temperature in each of the zones (left axis), and the distribution of the x_i (right axis).

2.6 Conclusions

We have analyzed the ideal free distribution (IFD) for a general class of suitability functions. We have proven that the habitat and input matching rules are equivalent for this general case. We also proved that the IFD is indeed an evolutionarily stable strategy (ESS) for the general case. Since this last concept only provides local results, we state a constrained optimization problem where we prove that the IFD is a global optimum point. Finally, from an evolutionary time perspective, we set up the replicator dynamics and show that the IFD is an asymptotically stable equilibrium point. An interesting characteristic for this case is that under some constraints, a gradient optimization perspective leads us to the same replicator dynamics. Finally, in order to provide more insight on why these allocation dynamics are useful from an engineering perspective, we applied the approach to a multizone temperature control problem. Using the replicator dynamics ideas, we showed how in spite of limiting the input voltage, we can manage to have a uniform temperature in each of four temperature zones.

CHAPTER 3

FORAGING THEORY FOR MULTIZONE TEMPERATURE CONTROL

3.1 Introduction

Foraging theory is an area of behavioral ecology that mathematically describes a foraging animal searching for nutrients and choosing which ones to consume [29, 30]. One of the classical foraging models is the prey model. This model describes a forager searching for prey items individually dispersed throughout its environment and predicts which types of prey the forager should exploit in order to maximize its rate of energy gain. The analogy established in [31, 32] between a biological forager and an "agent" (autonomous vehicle or software module) allows for application of foraging models to engineering problems involving agents (i) searching for tasks dispersed throughout a domain, and (ii) deciding which task types to process and how long to process tasks or sets (patches) of tasks.

Here, we use the conceptual framework in [31, 32], along with the idea of "foraging for error" from [33, 34] to develop a controller for a multizone temperature control problem. The goal is to achieve a uniform desired temperature across a grid of eight temperature zones, where a zone comprises a temperature sensor and a lamp. The

controller (agent) moves around the grid searching for regions of temperature error (the task). The prey model approach to the problem relies on the definition of a "task type" as a zone with a particular error with respect to the desired temperature. Given this definition, an encounter with a task of type i occurs when the controller comes across a zone with a temperature error corresponding to task type i. The controller then uses the prey model algorithm [29] to decide whether to process the task, that is, whether to heat the zone associated with the error. We implement the experiment and controller in our laboratory [35] and provide data to illustrate the performance of the foraging algorithm.

The temperature control problem we are addressing is essentially that of a distributed feedback control problem. Recent relevant work in this area includes spatially distributed control [36, 23], modeling and estimation of distributed processes [37], distributed control of thermal processes [38, 18, 39, 40], spatially interconnected systems [41], and semiconductor processing [42, 43, 44]. In [23], the authors implement various decentralized and hierarchical control ideas for the actuation allocation problem of an air-jet system. Distributed temperature control of thermal processes is addressed in [39], and the authors focus on multivariable distributed control in order to maintain a uniform temperature across a wafer during ramp-up. In [42, 44] the authors present methods where resources are allocated using geometric and adaptive techniques in order to utilize a heat source in designing a model-based control signal. In [45], the authors describe a lithographical system that is heated by 49 independently controlled zones. Distributed temperature control methods have been used

to improve the performance of some devices in personal computers [19]. More recently, in [24] the authors studied dynamic resource allocation strategies for different processes (e.g., a multizone temperature control with 16 zones).

Our approach is novel with respect to what is found in the literature. Broadly speaking, we demonstrate for the first time the utility of merging the fields of engineering and behavioral ecology by using models from foraging theory to address an important class of distributed temperature control problems. Specifically, we show how a bioinspired distributed decision-making system (i.e., multiagent system) that communicates over a network can be used to control a complex dynamical system. The communication network consists of two "clients," which obtain data from each of the temperature zones, connected to a central "supervisor" that controls agent actions across the grids. Network delays from this topology as well as disturbances, such as interzone effects, ambient temperature changes, and wind, introduce additional challenges that, when overcome, highlight the robust nature of the agent-based controller. Restrictions on the number of agents and the amount of lamp voltage they can apply give our control strategy characteristics of dynamic resource allocation problems such as those mentioned above. Overall, while applications of foraging theory to autonomous vehicles are studied in [31, 32, 46], this is to our knowledge the only other existing control engineering application of foraging theory. This chapter should, thus, be viewed as early work, but with results that show clear paths to further exploit concepts from mathematical behavioral ecology in engineering.

We begin by discussing the theory of the prey model, and how this theory can be used in a multizone temperature control experiment. Then, we show implementation results for tracking and regulation problems where we specify a desired temperature

that must be reached by each zone in the temperature grid. In order to test the controller's performance, we add a disturbance and we limit the number of zones that a forager can search. Finally, to explain a key feature of the emergent behavior of the temperatures in our experiment, we discuss connections between our foraging algorithm approach and the "ideal free distribution" (IFD) [1], an idea from theoretical ecology that has recently been found to have potential uses in engineering applications [47, 25, 26].

3.2 Foraging Model

From a biological perspective, the environment of a foraging animal comprises prey or food items that are spatially dispersed. Each forager's primary "goal" is to obtain energy, and the only way in which to do so is by searching for, attacking, and consuming prey. The forager must make decisions about how to interact with its environment to maximize some correlate of Darwinian fitness. If there are different types of prey, which types should be attacked? Why not specialize on particular types to avoid wasting time on substandard prey? On the other hand, why not generalize and take advantage of all opportunities? This optimal diet problem is studied using the so-called prey model from foraging theory [29]. The work in [31, 32] discusses the applicability of this theory to many engineering problems by viewing a forager as an agent and sources of energy or prey as tasks that must be processed. Here, using this general agent-based terminology, we provide an overview of the prey model following the treatment in [29].

The prey model describes an agent searching for tasks of different types in a particular environment. Each task holds a certain "point value" corresponding to

the increment in the success level of an agent if it successfully processes the task. Processing is the equivalent of a biological forager handling prey. Point values quantify reward. The agent must search for tasks, recognize a task once it is encountered, and then decide whether to process the task based upon this recognition. The prey model, in its original form, assumes that a task is recognized correctly, that no time is required for recognition, and that the goal of the agent is to maximize its average rate of point gain.

Let there be n different types of tasks in the environment described by: e_i, the expected time required to process a task of type i; v_i, the expected number of points obtained from processing a task of type i; λ_i, the average rate of encounter with tasks of type i while searching; and p_i, the probability of processing a task of type i if it is found and recognized. Encounters with type i are assumed to be sequential and to follow a Poisson process. While we have assumed no explicit cost for time spent searching, one may be accounted for by redefining v_i [29]. The average rate of point gain J for the agent is the expected number of points obtained divided by the expected total amount of time spent foraging, which includes both search time and time spent processing tasks. If an agent spends on average T_s time units searching, then we have

$$J = \frac{\sum_{i=1}^{n} p_i \lambda_i T_s v_i}{T_s + \sum_{i=1}^{n} p_i \lambda_i T_s e_i} = \frac{\sum_{i=1}^{n} p_i \lambda_i v_i}{1 + \sum_{i=1}^{n} p_i \lambda_i e_i}.$$

The probability of processing each task type is the decision variable for the agent. Thus, the goal of the agent is to choose the p_i that maximizes J. We first rewrite J as

$$J = \frac{p_i \lambda_i v_i + k_i}{c_i + p_i \lambda_i e_i},$$

where k_i is the summation of all terms in the numerator not involving task type i and c_i is a similar variable for the denominator. Differentiating with respect to p_i,

$$\frac{\partial J}{\partial p_i} = \frac{\lambda_i v_i (c_i + p_i \lambda_i e_i) - \lambda_i e_i (p_i \lambda_i v_i + k_i)}{(c_i + p_i \lambda_i e_i)^2} = \frac{\lambda_i v_i c_i - \lambda_i e_i k_i}{(c_i + p_i \lambda_i e_i)^2}. \tag{3.1}$$

Note that if the numerator of Equation (3.1) is negative, then J is maximized by choosing the lowest possible p_i. Correspondingly, if the numerator is positive, then J is maximized by choosing the highest possible p_i. Therefore, because $0 \leq p_i \leq 1$, the p_i that maximizes J is either $p_i = 1$ or $p_i = 0$ for each i depending on the sign of $v_i c_i - e_i k_i$. This concept is known as the *zero-one rule*: to maximize its rate of point gain, an agent must either process a task of type i every time it encounters it or never process a task of type i. The question then is which tasks the agent should process and which tasks it should ignore. The answer must account for missed opportunity. If the rate of point gain that results from processing task type i is larger than that of searching for and processing tasks of other types, then the agent should process the task of type i. On the other hand, if the agent would gain more points by searching for other tasks and processing those, then the task of type i should not be processed. Summarizing, this results in the rule

$$\text{set} \quad p_i = 0 \quad \text{if} \quad v_i/e_i < k_i/c_i$$

$$\text{set} \quad p_i = 1 \quad \text{if} \quad v_i/e_i > k_i/c_i,$$

where v_i/e_i is the rate of gain that results from processing task type i and k_i/c_i is the alternative rate of gain resulting from searching for and processing other task types.

We now describe the prey model algorithm in light of the above discussion. Denote the rate of point gain that results from processing type i (v_i/e_i) as the profitability

of task type i, and rank the tasks in the environment according to their profitability such that $v_1/e_1 > v_2/e_2 > \cdots > v_n/e_n$. If type j is included in the agent's "task pool," those types that the agent will process once encountered, then all types with profitabilities greater than that of type j will be included in the task pool as well. Thus, the prey algorithm states that, after ranking the task types by profitability, include types in the task pool starting with the most profitable type until

$$\frac{\sum_{i=1}^{j} \lambda_i v_i}{1 + \sum_{i=1}^{j} \lambda_i e_i} > \frac{v_{j+1}}{e_{j+1}}. \tag{3.2}$$

The highest j that satisfies this equation is the least profitable task type in the task pool. In other words, if task types in the environment are ranked according to profitability with $i = 1$ being the most profitable, and if type $j + 1$ is the most profitable type such that the agent will benefit more from searching for and processing types with profitability higher than that of $j + 1$, then tasks of types 1 through j should be processed when encountered and all other tasks should not. If the equation does not hold for any j, then all task types should be processed when encountered. A derivation of (3.2) is given in [29].

The exclusion of type $j + 1$ does not depend on the rate of encounter with type $j+1$. This exclusion implies that if the expected missed opportunity gains exceed the immediate gains of processing a particular type, then it does not benefit the agent to process the type, no matter how often the agent encounters it. Equivalently, if a type's rate of encounter exceeds a critical threshold, then less profitable types should be ignored regardless of how common they are in the environment.

It is important to note that the prey model assumes the agent has knowledge of all parameters. In many engineering applications, it is reasonable to imagine the expected processing time e_i and the expected points obtained v_i to be parameters that are known or approximated. However, knowledge of the rate of encounter with tasks λ_i often may be an unrealistic assumption, and online estimation techniques may need to be used [31]. An additional assumption of the prey model is that the agent has infinite life; for example, infinite fuel for an autonomous vehicle. Also, since the rate of encounter is constant, an infinite number of tasks are assumed to exist. This idea might imply the ability of tasks to arrive within the environment, an infinite number of spatial task arrangements, or an infinite number of ways that the agent can move through the environment. More realistic, time-constrained situations are accounted for in a risk-sensitive version of the prey model [29, 30, 31].

3.3 Temperature System and Application of the Prey Model

The temperature system under consideration comprises a temperature grid divided into eight "zones" as shown in Figure 3.1. A zone contains a lamp and a National Semiconductors LM35CAZ temperature sensor. Two computers (clients) are each connected to four different zones via four analog inputs and four analog outputs on a DS1104 dSPACE card. The digital outputs transmit on/off signals from the client to the lamps, and the analog inputs transmit temperature data from the sensors on the grid to the client. The DS1104 card has eight analog inputs: four with 16 bit resolution and four with 12 bit resolution. Because of this, the use of two computers (and correspondingly two dSPACE cards) allows for all eight zones to have a 16 bit resolution input connection. Communication between each client and

the supervisor takes place over a TCP/IP connection via Matlab. Data collected via dSPACE and the Real-Time Workshop is acquired with MLIB/MTRACE. In general, MLIB/MTRACE captures the data from the board and transfers the information to Matlab. This provides access to all variables from the application running on the dSPACE card, and allows the use of various Matlab commands. Using these capabilities, data is acquired and sent over the network connection to the supervisor. The supervisor gathers data from the clients, implements the appropriate control algorithm, and then sends information back to the clients as to which lamps should be turned on.

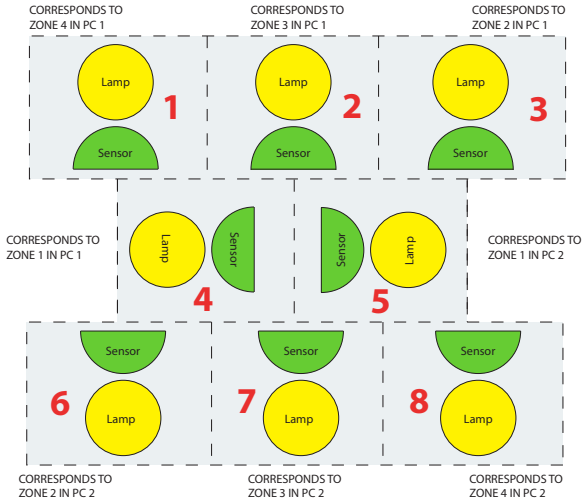

Figure 3.1: Zone layout on a single temperature grid. Each zone contains a lamp and a temperature sensor.

To apply the prey model to the temperature control experiment, we view a controller as an agent (animal) and a task (prey) as a zone with a specific error relative to the overall desired temperature. Hence, the number of task types n is free to be

chosen as any reasonable number of discretized error quantities. In the specific application that follows, we choose $n = 100$ so that the agent may encounter any of 100 types of error. We choose these 100 types to span a range of error of 0°C (type 100) to 5°C (type 1) with the type distribution defined by the function

$$i = \text{ceil}(100e^{-1.2(T_d - T^k)}) \tag{3.3}$$

where $k = 1, 2, \ldots, 8$ is the zone number and "ceil" is the standard ceiling function for converting to an integer. Equation (3.3) is shown in Figure 3.2(a), where i is the task type and $(T_d - T^k) \in [0, 5]$ is the error of the k^{th} zone with respect to the desired temperature T_d. This nonlinear function is chosen since it defines a larger number of types for errors with small magnitude, thus providing better accuracy near the desired temperature. The ceiling function discretizes the type, and a saturation function is used to assure that the error lies within the required domain. In other words, errors that correspond to T^k being above T_d are equivalent to 0°C errors and are considered to be of type 100.

The controller "moves" around the temperature grid by being randomly placed on one of the eight zones and detecting the temperature associated with that zone. Since the temperature of each zone constantly changes, placement of the controller on a specific zone does not imply an encounter with a particular task type. The type that the controller encounters depends on the temperature of the zone. The random zone selection adds to the stochastic nature of search and prevents oscillatory behavior that may result from systematic movement over the zones.

Processing times for each task type are determined by the function

$$e_i = 100 + 1000e^{-0.05(i-30)}$$

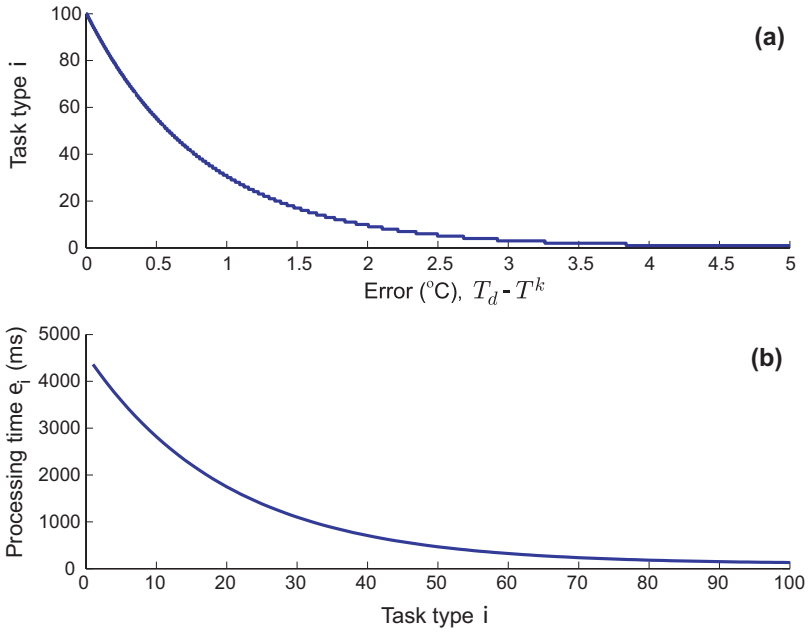

Figure 3.2: Parameter functions. Panel (a) depicts the determination of task type from encountered error, and panel (b) illustrates the processing times for each task type.

shown in Figure 3.2(b) where i is the task type. This function assigns longer processing times to task types that correspond to larger $T_d - T^k$ temperature errors since larger errors require a longer length of heating time by a lamp. The exponential characteristic of this function matches the distribution of processing times to the distribution of task types. Note that the processing times span a range of more than 4 seconds to 0.1 seconds. Although we examine one specific illustrative e_i, other processing-time functions may be chosen and will potentially result in different performance.

Task type point values are additional parameters that can be chosen freely and will affect the performance of the controller. Generally, task types corresponding to

larger errors should have larger point values than task types corresponding to smaller errors. We choose point values according to the function

$$v_i = 101 - i$$

for $i \in \{1, \ldots, n-1\}$. This point gain function assigns point values ranging from 100 points for a type-1 task to two points for a type-99 task. For a type-100 task, we assign a negative point value since tasks corresponding to zero or negative error do not need to be actuated with the lamp.

Rates of encounter λ_i with different task types are estimated in real time as the experiment runs. The controller of an agent has a memory and is able to keep track of its number of encounters with a specific error. At any given time instant, an estimate $\hat{\lambda}_i$ of the rate of encounter with type i for that particular agent is calculated as the number of times type i has been encountered by the agent divided by the time that the agent has spent searching for tasks. Once the relationship between error and type, the processing time function e_i, and the point value function v_i are determined, the prey model algorithm described by (3.2) is implemented at each simulation time step using the rate of encounter estimates in order to determine which task types should be processed when encountered.

Summarizing, the controller agent is randomly placed on a zone (implying an encounter with, for example, task type i), $\hat{\lambda}_i$ is updated, and the prey model algorithm is calculated using the new rate of encounter estimate in order to determine whether the controller should stop searching for tasks momentarily and heat (with the lamp) the zone corresponding to the encountered task for the amount of time specified by e_i.

3.4 Experiments and Results

To illustrate the ideas described in the theory, we performed three different experiments. The first is a tracking problem where the desired temperature is altered over time. The second experiment illustrates how the foragers reallocate when a disturbance is applied after the desired temperature is reached in the temperature grid. Finally, we limit the number of zones that each forager can search to see whether a desired temperature is achieved. In all of these cases we use four foragers, each of which use the prey algorithm described in the previous section. Our results show that the desired temperature is achieved despite sensor inaccuracy, noise, and network delays. We also highlight an interesting connection with the "ideal free distribution" (IFD) concept from theoretical ecology [1, 3].

3.4.1 Tracking

To evaluate controller tracking abilities, we alter the desired temperature over time. Initially, the desired temperature is set to $T_d = 23°\text{C}$. We then change T_d at 340 and 680 seconds to $T_d = 24°\text{C}$ and $T_d = 22°\text{C}$, respectively. The ambient room temperature is $T_a = 21.3°\text{C}$. Typical results are shown in Figure 3.3. We ran the experiment many times and found similar performances for other T_d values and ambient conditions.

The prey model algorithm achieves the desired result: the temperature of each zone tracks the desired temperature changes. Note that data is acquired from the sensors at a sampling rate of 1 ms. This value was chosen to obtain accurate estimates of the rate of encounter with tasks for a particular agent. Although the sensors are very accurate ($\pm 0.2°\text{C}$ typical accuracy, and $\pm 0.5°\text{C}$ guaranteed), their thermal

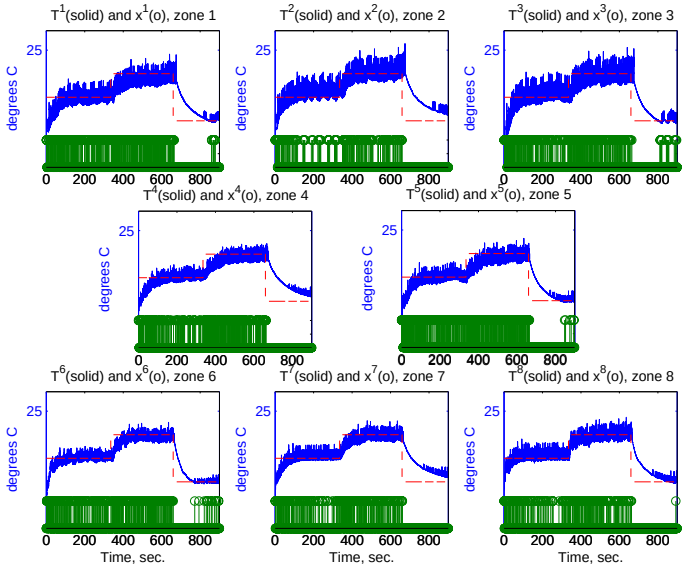

Figure 3.3: Multizone temperature control tracking performance, desired temperature (dashed), and actual temperature (solid) with plot layout corresponding to spatial zone positions in Figure 3.1. The stem plot at the bottom of each panel indicates the on/off state of the lamp x^i for zone i at a given point in time.

constants are slow relative to the chosen sampling rate, yielding the noisy responses observed in Figure 3.3. Nevertheless, Figure 3.3 shows that on average good tracking performance is achieved.

The processing of tasks in each zone over time is indicated by the overlaying stem plot in Figure 3.3, which shows whether the lamp for a given zone is on or off at a particular point in time. It is clear from this plot that the decrease in desired temperature at 680 seconds results in no tasks being processed for a short period. This is because the temperature error of all zones during this time is negative (the actual temperature is above the desired temperature) implying encounters with only type 100 tasks, which have negative point value and are not worth processing. Also

note that when the zones' temperatures are essentially at the desired temperature, some task types are still ignored. This is evident from the existence of gaps in the stem plot around steady state and is due to the exponential nature of the e_i curve. When all of the errors are small, the processing times of the encountered types do not differ much from one another (since they occur on the flatter part of the e_i curve). The controller then is not willing to waste time processing very tiny errors when it can search for and spend the same amount of time processing small (but not tiny) errors and receive a larger number of points.

The task types that each forager encounters over time are shown in Figure 3.4. Each forager encounters lower task types at the beginning due to the initial presence of large positive errors that correspond to low task types (Figure 3.2(a)). This characteristic is also seen when the desired temperature is increased at 340 seconds. As mentioned above, however, the second T_d change at 680 seconds causes encounters with only type-100 tasks because of a negative temperature error.

3.4.2 Disturbance Effects

The tracking experiment showed that the prey model controller achieves good tracking performance. Here, we introduce a disturbance by means of an extra lamp located next to the sensor in zone 3. The idea is to regulate the temperature of the grid to a desired temperature $T_d = 20°\text{C}$, and once a steady-state value is achieved, the new lamp in zone 3 is turned on.

The experiment was begun with an ambient room temperature of $T_a = 18.5°\text{C}$. Figure 3.5 illustrates the temperatures and the lamps that were on for the first 10 minutes of the experiment. The controller was initially run in the absence of any

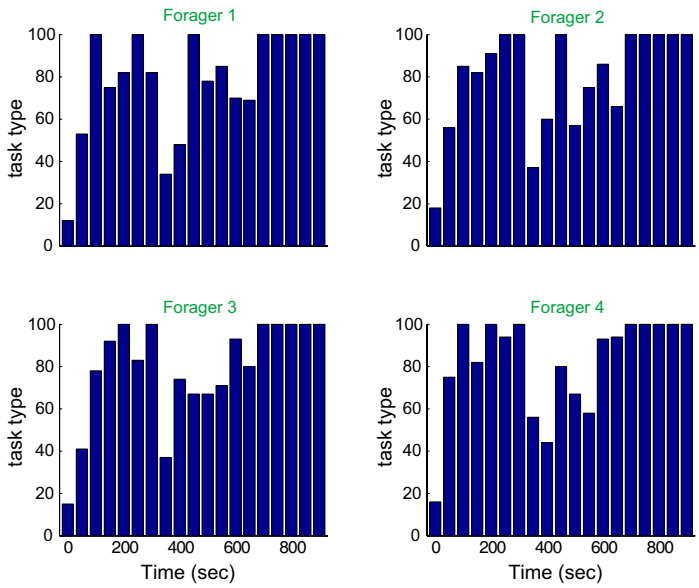

Figure 3.4: In this figure, we illustrate the task-type encounters of each forager with respect to time. Encounters are downsampled for visualization.

disturbance, and the extra lamp in zone 3 was turned on after approximately 60 seconds. As seen in Figure 3.5, the temperature in zone 3 starts to increase, but the temperature in the other zones remains close to the desired temperature T_d. The disturbance is turned off around 110 seconds, and the temperature drops until it again reaches T_d. Figure 3.5 also shows the lamps that are on at a given time. We see that, during the time the disturbance was on, no foragers heated zone 3, even though the zone could have been selected by the algorithm. This behavior is expected considering the negative error in zone 3 after the disturbance. Foragers that randomly select zone 3 encounter a type-100 task and do not process it because it is not profitable enough to be included in the task pool. However, once the disturbance is turned off, and the

temperature returns close to T_d, the foragers visit that zone in order to keep the grid at the desired temperature.

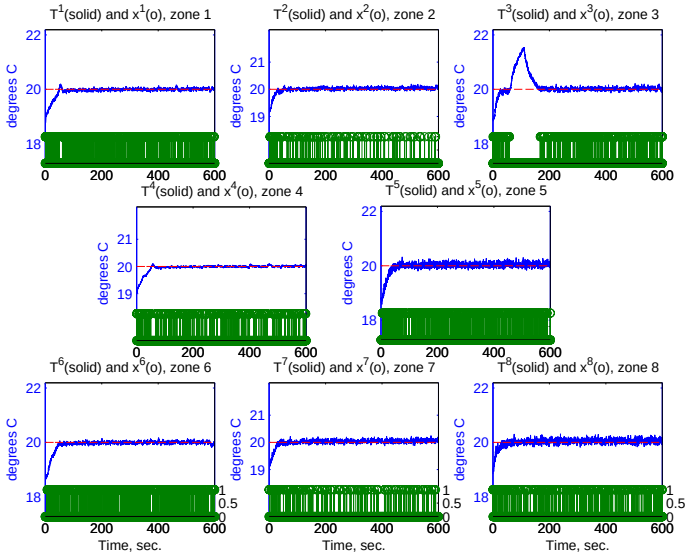

Figure 3.5: Multizone temperature control performance when a disturbance is applied. The desired temperature (dashed), the actual temperature (solid), and the lamps that are on (stem) are shown in the plot layout corresponding to spatial zone positions in Figure 3.1. The stem plot at the bottom of each panel indicates the on/off state of the lamp x^i for zone i at a given point in time.

3.4.3 Search Limitations

The previous two experiments were based on the assumption that all foragers could sense the temperature in every zone of the multizone temperature grid. However, an interesting case arises when the foragers do not have access to all zones' temperatures. To investigate this issue, we divide the four foragers into two sets of two. The first set contains foragers 1 and 2, which are limited to search zones 1 through 5. The second set, comprising foragers 3 and 4, is limited to search only zones 4 through 8.

Zones 4 and 5 are common to both sets. The prey model is still applied; however, the number of zones the forager can randomly encounter is limited.

The goal of this experiment is to regulate the temperature grid to a desired temperature $T_d = 20°\text{C}$ when the ambient room temperature is $T_a = 18.9°\text{C}$. Figure 3.6 shows the results for 600 seconds. After 10 minutes, the temperature across the multizone temperature grid is essentially constant at the desired temperature. Some expected oscillations exist around the desired temperature due to the number of foragers, network delays, and sensing limitations. The search limitation is evident in Figure 3.7: only two foragers search zones 1 through 5, while the other two search zones 4 through 8. These limitations, however, do not affect tracking performance. The desired temperature is reached even in the absence of perfect information.

3.4.4 Discussion

Our results show that the temperature of each zone reaches each desired temperature that is applied despite several performance-limiting effects, namely resource allocation constraints, network delays, disturbances, and imperfect information. Resources are limited owing to the fact that only four foragers are allocated around the grid. Thus, the maximum number of lamps on at any given time is four. The result is at least four unattended zones that must experience a decrease in temperature and then later receive attention again due to the temperature error that has developed. This pattern yields slight oscillatory behavior in Figure 3.3 that is most evident in the zones where the desired temperature is reached the fastest. Network and communication delays also affect controller performance. The clients sample temperature

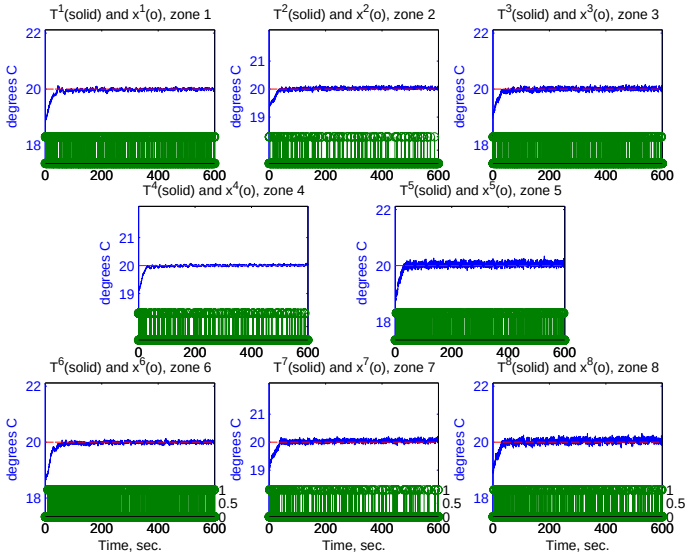

Figure 3.6: Multizone temperature control performance when there is not perfect information. The desired temperature (dashed), the actual temperature (solid), and the lamps that are on (stem) are shown with plot layout corresponding to spatial zone positions in Figure 3.1. The stem plot at the bottom of each panel indicates the on/off state of the lamp x^i for zone i at a given point in time.

data every 1 ms via the sensors and transmit this data back to the supervisor. Because these connections are implemented over a TCP/IP connection, internet delays exist. However, the controller performs quite well in the presence of such constraints. Additionally, good performance was achieved after the introduction of disturbances and information limitations.

It should be noted that the experiments were performed at different times of the day and year, leading to different ambient conditions. In addition to temperature fluctuations from experiment to experiment, wind current due to, for example, air conditioning systems and window drafts also exists. Although such adverse experimental conditions can significantly affect experiment results (e.g., making achieved

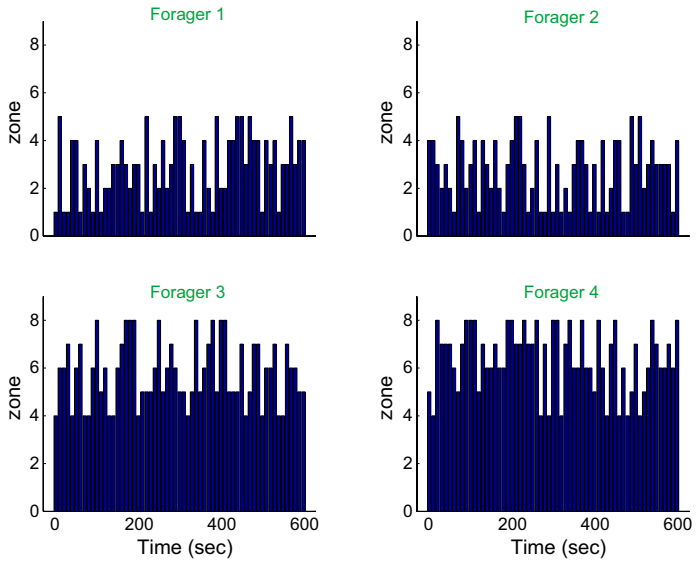

Figure 3.7: Corresponding zones for each of the four foragers.

steady-state behavior different, compare Figure 3.3 to Figures 3.5 and 3.6), the performance of the controller is quite good. Furthermore, parameter value and function tuning may lead to improved results. For example, the type function in (3.3), the processing-time function e_i, and the point-value function v_i were chosen in our experiments to simply demonstrate the utility of a foraging theory approach to control; however, different functions may be used and, with proper tuning, may result in improved performance.

An important characteristic of the experimental results given above is the connection to the IFD. In the temperature control experiment, the group of foragers tends to reach an IFD. Why? If we think of temperature error in a given zone as a nutrient, the foragers will allocate themselves in the zones where the temperature is below the desired one, and they tend to choose those zones where the reward is higher (i.e.,

where they are getting a high number of points v_i). In this way, they persistently move around the grid and maintain the same consumption rate for each of them that corresponds to the equilibration of the zone temperatures in Figures 3.3, 3.5, and 3.6.

3.5 Conclusions

The utility of foraging theory for decision-making system design was established in [31, 32] for autonomous vehicles via simulations. Here we examine an application of the theory to an actual physical experiment, namely temperature control of a grid of eight zones. A controller is thought of as an agent searching for error across the grid, and it uses the prey model algorithm to decide which types of error to actuate with a lamp to achieve a uniform desired temperature across the grid. The algorithm causes the controller to ignore certain types of error when the missed opportunity of more profitable types is too great to forgo. Results show that the controller does very well in tracking desired temperatures, even in the presence of disturbances and sensing limitations. The results also illustrate a connection between the prey model and the ideal free distribution. The desired temperature is reached in all three experiments by the foragers allocating themselves in the zones where the error is higher.

Future directions include applications of extended foraging theory concepts such as the patch model to determine how long to process certain error types and risk-sensitive foraging theory to decide which types to process when time is limited. Moreover, there is a need to mathematically analyze the stability of the controller; however, this is quite challenging due to the need to consider sensor noise, disturbances, lack of perfect information (i.e., decentralized control), asynchronous operation, and the fact

that the control input is of the on-off type that is constrained so that only a limited number of zones can be heated at one time.

CHAPTER 4

HONEY BEE SOCIAL FORAGING ALGORITHMS FOR RESOURCE ALLOCATION: THEORY AND APPLICATION

4.1 Introduction

Evolution by natural selection has shaped biosystem optimization and control processes to enhance the probability of species survival [48]. The "bioinspired" design approach [34] seeks to exploit the evolved "tricks" of nature to construct robust high performance technological solutions. For instance, the ant colony optimization (ACO) algorithms introduced by M. Dorigo and colleagues (e.g., see [49, 50, 51, 52]) mimic ant foraging behavior and have been used in the solution to classical optimization problems (e.g., discrete combinatorial optimization problems [53]) and in engineering applications (e.g., [54, 55]). The primary goal of this chapter is to show that honey bee social foraging techniques can be exploited in a bioinspired design approach to (i) solve a continuous optimization problem underlying resource allocation [22], and (ii) provide novel strategies for multizone temperature control, an important industrial engineering application.

Our model of honey bee social foraging relies on experimental studies [56] and some ideas from other mathematical models of the process. A differential equation model of functional aspects of dynamic labor force allocation of honey bees is developed and validated for one set of experimental conditions in [57, 48]. The work in [58] extends this model (e.g., by adding details on energetics and currency) and [59] introduced a generic nonlinear differential equation model that can represent social foraging processes in both bees and ants. Like in [59, 58], our model of recruitment uses the idea from [57, 48] that dance strength proportioning on the dance floor shares some characteristics with the evolutionary process (e.g., with fitness corresponding to forage site profitability and reproduction to recruitment as discussed in [56]). Here we make such connections more concrete by modeling the bee recruitment process in an analogous manner to how survival of the fittest and natural selection are modeled in genetic algorithms using a stochastic process of fitness proportionate selection [60]. The authors in [61] introduce an "individual-oriented" model of social foraging and validate it against one set of experimental conditions as was done in [57, 48]. More recently, in [62] the authors expanded and improved the model in [61] (e.g., taking into account the findings in [63] and by studying an equal harvest rate forager allocation distribution). The work in [64] studies the pattern of forager allocation and the optimality of it. The authors in [65] study the spatial distribution of solitary and social food provisioners under different currency assumptions. The work in [64, 65, 62] identifies connections to the concept of the "ideal free distribution" (IFD) [1]. Here, we do not use a detailed characterization of bee and nectar energetics and currency since there is not enough experimental evidence to justify whether or when a gathering rate or efficiency-based currency is used [56]; instead, we develop a *generic* measure

of forage site profitability. This general profitability measure approach is the same one used in [66] to represent the nest-site quality landscape for the honey bee nest-site selection process. Our general measure has the advantage of allowing us to easily represent a wide range of density-dependent foraging currencies via the classical "suitability function" approach to IFD studies [1]. Also, it eases the transition to the multizone temperature control problem since the temperature control objective can be easily characterized with our general profitability measure.

In this chapter, the IFD is a central unifying concept. The IFD will emerge for one hive as the foragers are *cooperatively* allocated across sites. Moreover, if n hives *compete* in the same environment for a resource the IFD will also emerge. Here, we create a mathematical representation of the n-hive game where each hive's strategy choice entails picking the distribution of its foragers across the environment. Our analytical study starts by showing that the IFD is a strict Nash equilibrium [27] in terms of the payoffs to each hive and a special type of evolutionarily stable strategy (ESS). The original definition of an ESS is based on one important assumption: the population size has to be infinite. In [67, 68] the authors define the conditions that must be satisfied in order to prove that a strategy is evolutionarily stable for a finite-population size. Using the ideas in [67] we state the conditions for what we call a *one-stable* ESS, and show that the IFD satisfies those conditions. This means that in an n-hive game, if a single hive's strategy (forager allocation) mutates from the IFD it cannot survive when competing against a field of $n-1$ hives that use the IFD strategy. While this means that the IFD is locally optimal in a game-theoretic sense (i.e., unilateral forager allocation deviations by a hive are not profitable), here we show that the achieved IFD is a global optimum point for both single hive and n-hive

allocations. For the n-hive case, this means that if the forager allocation of all hives but one is at the IFD, then the remaining hive has to distribute its effort according to the IFD if it is to maximize its return.

The utility of these theoretical concepts and the honey bee social foraging algorithm are illustrated by means of an engineering application. One possible engineering application is the dynamical allocation of servers on the Internet [69]. However, the technological challenge we confront is multizone temperature control. Achievement of high performance multizone temperature control is very important in a range of commercial and industrial applications. For instance, recent work in this area includes distributed control of thermal processes [38, 18, 39, 40, 19], and semiconductor processing [42, 43, 44]. Particularly relevant to our work is the study in [39], where the authors use multivariable distributed control in order to maintain a uniform temperature across a wafer during ramp-up (similar to the control objective we study here). In [45] the authors describe a lithographical system that is heated by 49 independently controlled zones. Here, we use a multizone experimental setup that is similar to the one in [24] where dynamic resource allocation methods are studied. Our experiments demonstrate how one hive can achieve an IFD that corresponds to maximum uniform temperatures on the temperature grid. We illustrate the dynamics of the foraging algorithm by showing how it can successfully eliminate the effects of ambient temperature disturbances. Moreover, we show that even if two hives have *imperfect information* they can be used as a feedback control that will still achieve an IFD.

The chapter is organized as follows. First, in Section 4.2 we introduce the honey bee social foraging algorithm. In Section 4.3 we perform a theoretical analysis of

the hives' achieved IFD equilibrium. In Section 4.4 we apply the honey bee social foraging algorithm to a multizone temperature control experiment and show how the IFD emerges under a variety of conditions.

4.2 Honey Bee Social Foraging Algorithm

Modeling social foraging for nectar involves representing the environment, activities during bee expeditions (exploration and foraging), unloading nectar, dance strength decisions, explorer allocation, recruitment on the dance floor, and accounting for interactions with other hive functions. The experimental studies we rely on are summarized in [56]. Our primary sources for constructing components of our model are as follows: dance strength determination, dance threshold, and unloading area [70, 71, 63]; dance floor and recruitment rates [57]; and explorer allocation and its relation to recruitment [72, 73].

4.2.1 Foraging Profitability Landscape

We assume that there are a fixed number of B bees involved in foraging. For $i = 1, 2, ..., B$ bee i is represented by $\theta^i \in \Re^2$ which is its position in two-dimensional space. During foraging, bees sample a "foraging profitability landscape" which we think of as a spatial distribution of forage sites with encoded information on foraging profitability that quantifies distance from hive, nectar sugar content, nectar abundance, and any other relevant site variables. The foraging profitability landscape is denoted by $J_f(\theta)$. It has a value $J_f(\theta) \in [0, 1]$ that is proportional to the profitability of nectar at a location specified by $\theta \in \Re^2$. Hence, $J_f(\theta) = 1$ represents a location with the highest possible profitability, $J_f(\theta) = 0$ represents a location with no profitability,

and $0 < J_f(\theta) < 1$ represents locations of intermediate profitability. For $\theta = [\theta_1, \theta_2]^\top$, the θ_1 and θ_2 directions for our example foraging area are for convenience scaled to $[-1, 1]$ since the distance from the hive is assumed to be represented in the landscape. We assume the hive is at $[0, 0]^\top$.

As an example of the type of foraging profitability landscape we could have four forage sites centered at various positions that are initially unknown to the bees (e.g., site 1 could be at $[1.5, 2.0]^\top$). The "spread" of each site characterizes the size of the forage site, and the height is proportional to the nectar profitability. For example, we could use cylinders with heights $N_f^j \in [0, 1]$ that are proportional to nectar profitability, and the spread of each site can be defined by the radius of the cylinders ϵ_f. Below, we will say that bee i, $\theta^i = [\theta_1^i, \theta_2^i]^\top$, is "at forage site 1" if $\sqrt{(\theta^i - [1.5, 2]^\top)^\top (\theta^i - [1.5, 2]^\top)} < \epsilon_f$. We use a similar approach for other sites.

4.2.2 Bee Roles and Expeditions

Let k be the index of the foraging expedition and assume that bees go out at one time and return with their foraging profitability assessments at one time (an asynchronous model with randomly spaced arrivals and departures will behave in a qualitatively similar manner). Our convention is that at time $k = 0$ no expeditions have occurred (e.g., start of a foraging day), at time $k = 1$ one has occurred, and so on. All bees, $i = 1, 2, ..., B$, have $\theta^i(0) = [0, 0]^\top$ so that initially they are at the hive.

Let $x_j(k)$ be the number of bees at site j at k. We assume that the profitability of being at site j, which we denote by s_j for a bee at a location in site j, decreases as the number of bees visiting that site increases. A typical choice [1, 2] is to represent

this by letting, for each j,

$$s_j(k) = \frac{a_j}{x_j(k)}$$

In this case, we could assume that a_j is the number of nutrients per second at the j^{th} site. With this representation we think of a site as a choice for the hive, with the site degrading in profitability via the visit of each additional bee, a common assumption in theoretical ecology. In IFD theory s_j is called the "suitability function" [1].

Of the B bees involved in the foraging process, we assume that there are $B_f(k)$ "employed foragers" (ones actively bringing nectar back from some site and that will not follow dances). Initially, $B_f(0) = 0$ since no foraging sites have been found. We assume that there are $B_u(k) = B_o(k) + B_r(k)$ "unemployed foragers" with $B_o(k)$ that *seek to* observe the dances of employed foragers on the dance floor and $B_r(k)$ that rest (or are involved in some other activity). Initially, $B_u(0) = B$, which with the rules for resting and observing given below will set the number of resters and observers. We assume that there are $B_e(k)$ "forage explorers" that go to random positions in the environment, bring their nectar back if they find any, and dance accordingly, but were not dedicated to the site (of course they may become dedicated if they find a relatively good site).

We ignore the specific path used by the foragers on expeditions and what specific activities they perform. We assume that a bee simply samples the foraging profitability landscape once on its expedition and hence this sample represents its combined overall assessment of foraging profitability for location $\theta^i(k)$. It is this value that it holds when it returns to the hive. It also brings back knowledge of the forage location which is represented with $\theta^i(k)$ for the k^{th} foraging expedition. Let the foraging

profitability assessment by employed forager (or forage explorer) i be

$$F^i(k) = \begin{cases} 1 & \text{if } J_f(\theta^i(k)) + w_f^i(k) \geq 1 \\ J_f(\theta^i(k)) + w_f^i(k) & \text{if } 1 > J_f(\theta^i(k)) + w_f^i(k) > \epsilon_n \\ 0 & \text{if } J_f(\theta^i(k)) + w_f^i(k) \leq \epsilon_n \end{cases}$$

where $w_f^i(k)$ is profitability assessment noise. Here, we let $w_f^i(k)$ be uniformly distributed on $(-w_f, w_f)$ with $w_f = 0.1$ (to represent up to a $\pm 10\%$ error in profitability assessment). The value $\epsilon_n > 0$ sets a lower threshold on site profitability. Here, $\epsilon_n = 0.1$. For mid-range above-threshold profitabilities the bees will on average have an accurate profitability assessment since the expected value with respect to k of $w_f^i(k)$, $E[w_f^i(k)] = 0$. Let $F^i(k) = 0$ for all unemployed foragers.

4.2.3 Dance Strength Determination

Let $L_f^i(k)$ be the number of waggle runs of bee i at step k, what is called "dance strength." The $B_u(k)$ unemployed foragers have $L_f^i(k) = 0$. All employed foragers and forage explorers that have $F^i(k) = 0$ will have $L_f^i(k) = 0$ since they did not find a location above the profitability threshold ϵ_n so they will not seek to be unloaded and will not dance; these bees will become unemployed foragers.

Unload Wait Time

Next, we will explain dance strength decisions for the employed foragers and forage explorers with $F^i(k) > \epsilon_n$. To do this, we first model wait times to get unloaded and how they influence the "dance threshold." Define $F_t(k) = \sum_{i=1}^{B} F^i(k)$ as the total nectar profitability assessment at step k for the hive. Foragers at profitable sites tend to gather a greater quantity of nectar than at low profitability sites. Let $F_q^i(k)$ be the quantity of nectar (load size) gathered for a profitability assessment $F^i(k)$. We assume that $F_q^i(k) = \alpha F^i(k)$ where $\alpha > 0$ is a proportionality constant. We choose

$\alpha = 1$ so that $F_q^i(k) \in [0,1]$, with $F_q^i(k) = 1$ representing the largest nectar load size. Notice that if we let $F_{tq}(k)$ be the total quantity of nectar influx to the hive at step k,

$$F_{tq}(k) = \sum_{i=1}^{B} F_q^i(k) = \alpha \sum_{i=1}^{B} F^i(k) = \alpha F_t(k)$$

so the total hive nectar influx is proportional to the total nectar profitability assessment. Also, $F_{tq}(k) \in [0, \alpha B]$ since each successful forager contributes to the total nectar influx.

The average wait time to be unloaded for each bee with with $F^i(k) > \epsilon_n$ is proportional to the total nectar influx. Suppose that the number of food-storer bees is sufficiently large so the wait time $W^i(k)$ that bee i experiences is given by

$$W^i(k) = \psi \max\left\{F_{tq}(k) + w_w^i(k), 0\right\} = \psi \max\left\{\alpha F_t(k) + w_w^i(k), 0\right\} \tag{4.1}$$

where $\psi > 0$ is a scale factor and $w_w^i(k)$ is a random variable that represents variations in the wait time a bee experiences. We assume that $w_w^i(k)$ is uniformly distributed on $(-w_w, w_w)$. Since $F_{tq}(k) \in [0, \alpha B]$, $\psi(\alpha B + w_w)$ is the maximum value of the wait time which is achieved when total nectar influx is maximum. For the experiments in [63] (July 12 and 14 data) the maximum wait time is about 30 sec. (and we know that it must be under this value or bees will tend to perform a tremble dance rather than a waggle dance to recruit unloaders [56]); hence, we choose $\psi(\alpha B + w_w) = 30$. Note that $\pm\psi w_w$ seconds is the variation in the number of seconds in wait time due to the noise and w_w should be set accordingly. We let $\psi w_w = 5$ to get a variation of ± 5 seconds. If $B = 200$ is known, we have two equations and two unknowns, so combining these we have $\psi B + \psi w_w = 30$, which gives $\psi = 25/200$ and $w_w = 40$.

That there is a linear relationship between wait times and total nectar influx *for sufficiently high nectar influxes* is justified via experiments described in [63] and [56] p. 112. Deviations from linearity come from two sources, the $w_w^i(k)$ noise and the "max" in Equation (4.1). Each successful forager has a *different* and inaccurate individual assessment of the total nectar influx since each individual bee experiences different wait times in the unloading area. The noise $w_w^i(k)$ in Equation (4.1) represents this. Some foragers can get lucky and get unloaded quickly and this will give them the impression that nectar influx is low. Other foragers may be unlucky and slow to get unloaded and this will result in an impression that there is a very high nectar influx.

The Dance Decision Function

Next, we assume that the i^{th} successful forager converts the wait time it experienced into a *scaled* version of an estimate of the total nectar influx that we define as

$$\hat{F}_{tq}^i(k) = \delta W^i(k) \tag{4.2}$$

So, we are assuming that each bee has an internal mechanism for relating the wait time it experiences to its guess at how well all the other foragers are doing [56]. The proportionality constant for this is $\delta > 0$ and since $W^i(k) \in [0, \psi(\alpha B + w_w)] = [0, 30]$ sec. we have $\hat{F}_{tq}^i(k) \in [0, 30\delta]$.

So, how does total nectar influx influence the dance strength decision, and in particular the dance threshold? This is explained in on p. 118 in [56]. Here we build on this by defining a "decision function" for each bee that shows how the dance threshold for each individual bee shifts based on the i^{th} bee's estimate of total nectar

influx. The decision function is

$$L_f^i(k) = \max\left\{\beta\left(F^i(k) - \hat{F}_{tq}^i(k)\right), 0\right\} \tag{4.3}$$

which is shown in Figure 4.1. The parameter $\beta > 0$ affects the number of dances produced for an above-threshold profitability.

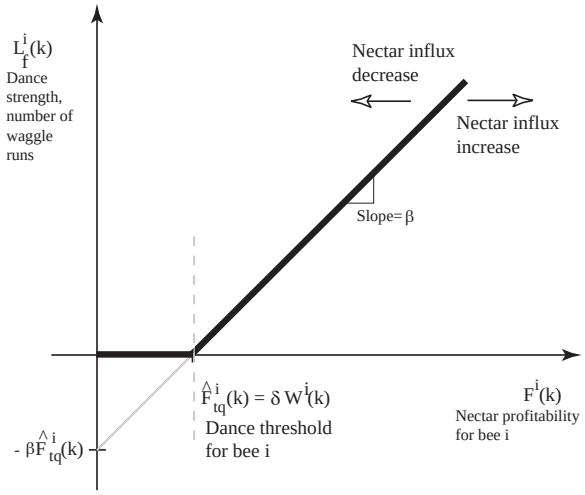

Figure 4.1: Dance strength function.

In Figure 4.1, $-\beta\hat{F}_{tq}^i(k)$ is the intercept on the dance strength axis. The diagonal bold line in Figure 4.1 shifts based on the bee's estimation of total nectar influx since this is proportional to $\hat{F}_{tq}^i(k)$. Notice that since the line's slope is β, and since we take the maximum with zero in Equation (4.3), the lowest value of nectar profitability $F^i(k)$ that the i^{th} bee will decide to still dance for is the "dance threshold" $\hat{F}_{tq}^i(k)$ and from Equation (4.2), the bee's scaled estimate of the total nectar influx. Note that changing β does *not* shift the dance threshold. The parameter β will, however, have the effect of a gain on the rate of recruitment for sites above the dance threshold. In

the case where $F_{tq}(k) = \hat{F}^i_{tq}(k) = 0$ there is no nectar influx to the hive and it has been found experimentally [56] that in such cases, if a bee finds a highly profitable site, she can dance with 100 or more waggle runs. Hence, we choose $\beta = 100$ so $L^i_f(k) = 100$ waggle runs in this case. Then, $L^i_f(k) \in [0, \beta] = [0, 100]$ waggle runs for all i and k.

The dance threshold in Equation (4.2) is defined using the parameter δ. What value would we expect a bee to hold for δ? Since the nectar profitability $F^i(k) \in [0, 1]$, δ needs to be defined so that $\hat{F}^i_{tq}(k) \in [0, 1]$ so that the dance threshold is within the range of possible nectar profitabilities. This means that we need

$$0 < \delta \leq \frac{1}{30} \tag{4.4}$$

To gain insight into how to pick δ in this range notice that δ is proportional to the site abandonment rate: (i) if $\delta \approx 0$, then the dance threshold $\hat{F}^i_{tq}(k) \approx 0$ independent of wait times and so sites of significantly inferior relative profitability will never be abandoned, something that does not occur in nature; and (ii) if $\delta \approx \frac{1}{30} = 0.0333$, then almost all sites are not danced for since the dance threshold is so high and the foraging process fails completely, something that does not occur in nature. Hence, δ must be somewhere in the middle of the range in Equation (4.4); in simulations we tuned the value of δ to match experiments and found $\delta = 0.02$.

Dance/No-Dance Choice

The set of bees that, after dance strength determination as outlined in the previous section, have $L^i_f(k) > 0$ are ones that *consider* dancing for their forage site. Here, we let $p_r(i, k) \in [0, 1]$ denote the probability that bee i with $L^i_f(k) > 0$ will dance for the

site it is dedicated to. We assume that

$$p_r(i,k) = \frac{\phi}{\beta} L_f^i(k)$$

where $\phi \in [0,1]$ (which ensures that $p_r(i,k) \in [0,1]$). We choose $\phi = 1$ since it resulted in matching the qualitative behavior of what is found in experiments. Hence, a bee with an above-threshold profitability is more likely to dance the further its profitability is above the threshold as seen in experiments [56]. In this way, relatively high quality new discoveries will typically be danced for, but as more bees are recruited for that site and hive nectar influx increases, it will become less likely that bees (e.g., the recruits) will dance for it and this will limit the number of dancers for all sites. Relatively low quality sites are not as likely to be danced for; however, bees that decide not to dance will still go back to the site and remain an employed forager for it. If bee i dances, then it uses a dance strength of $L_f^i(k)$. If it does not dance, we force $L_f^i(k) = 0$ and the bee simply remains an employed forager for its last site. We let $B_{fd}(k)$ denote the number of employed foragers with above-threshold profitability that dance.

4.2.4 Explorer Allocation and Forager Recruitment

Resters and Observers

The bees that either were not successful on an expedition, or were successful enough to get unloaded but judged that the profitability of their site was below the dance threshold, become unemployed foragers. Some of these bees will start to rest and other dance "observers" will actively pursue getting involved in the foraging process by seeking a dancing bee to get recruited. Here, at each k we let $p_o \in [0,1]$ denote the probability that an unemployed forager or currently resting bee will become

an observer bee; hence $1 - p_o$ is the probability that an unemployed forager will rest or a currently resting bee will continue to rest. It has been seen experimentally [56] that in times where there are no forage sites being harvested there can be about 35% of the bees performing as forage explorers, but when there are many sites being harvested there can be as few as 5%. Hence, we choose $p_o = 0.35$ so that when all bees are unemployed, 35% will seek dances.

Explorers and Recruits

Here, we assume that an observer bee on the dance floor searches for dances to follow and if it does not find one after some length of time, it gives up and goes exploring. To model explorer allocation based on wait-time cues, we assume that wait-time is assumed to be proportional to the total number of waggle runs on the dance floor. Let

$$L_t(k) = \sum_{i=1}^{B_f(k)} L_f^i(k)$$

be the total number of waggle runs on the dance floor at step k. We take the $B_o(k)$ observer bees and for each one, with probability $p_e(k)$ we make it an explorer. We choose

$$p_e(k) = \exp\left(-\frac{1}{2}\frac{L_t^2(k)}{\sigma^2}\right) \tag{4.5}$$

Notice that if $L_t(k) = 0$, there is no dancing on the cluster so that $p_e(k) = 1$ and all the observer bees will explore (e.g., $L_t(0) = 0$ so initially all observer bees will choose to explore). If $L_t(k)$ is low, the observer bees are less likely to find a dancer and hence will not get recruited to a forage site. They will, in a sense, be "recruited to explore" by the lack of the presence of any dance. As $L_t(k)$ increases, they become less likely to explore and, as discussed below, will be more likely to find a dancer and

get recruited to a forage site. Here, we choose $\sigma = 1000$ since it produces patterns of foraging behavior in simulations that correspond to experiments.

The explorer allocation process is concurrent with the recruitment of observer bees to forage sites. Observer bees are recruited to forage sites with probability $1 - p_e(k)$ by taking any observer bee that did not go explore and have it be recruited. To model the actual forager recruitment process we view $L_f^i(k)$ as the "fitness" of the forage site that the i^{th} bee visited during expedition k. Then, the probability that an observer bee will follow the dance of bee i is defined to be

$$p_i(k) = \frac{L_f^i(k)}{\sum_{i=1}^{B_f(k)} L_f^i(k)} \tag{4.6}$$

In this manner, bees that dance stronger will tend to recruit more foragers to their site.

4.2.5 Discussion

We have conducted extensive simulations to validate the qualitative characteristics of our model of social foraging by honey bees. In particular, we have shown that the model represents achievement of the IFD of foragers per relative site profitabilities [56] for a range of suitability functions, "cross-inhibition" seen in [57, 48] (the main experiments used in model validation for all other bee foraging models discussed earlier), reallocation when new forage sites suddenly appear or disappear, or when site qualities change [56, 57, 48]. In the interest of brevity we do not include these simulations here since: (i) our focus is *not* on model validation (i.e., accurate representation of numerical data from experiments on honey bee social foraging) but on bioinspired design based on the main algorithm features; and (ii) the key qualitative

features of the allocation dynamics are all illustrated in our implementation of the bee algorithm for multizone temperature control in the next section.

4.3 Equilibrium Analysis of Hive Allocations

In Section 4.2 we explained how the honey bee social foraging algorithm achieves the ideal free distribution (IFD). In this section we prove that the hives' IFD is a global optimum point. For that, some assumptions have to be made. In the previous section we saw how bees in different roles were allocated to different forage sites by their behavior in the hive. In the following analysis we assume that there exists a fixed number of hives n in an environment, that each hive contains a fixed amount of employed forager bees B_f^i, $i = 1, 2, \ldots, n$, and that *all* bees are allocated to N different sites (i.e., we ignore the components of the process associated with searching for forage sites).

4.3.1 The n-Hive Game

Nash Equilibrium

Let $x_j^i > 0$ denote the number of bees that the i^{th} hive allocates to the j^{th} (forage) site choice, where $i = 1, 2, \ldots, n$, and $j = 1, 2, \ldots, N$. We assume for simplicity that $\sum_{j=1}^{N} x_j^i = B_f$, for all i, is the total amount of bees the i^{th} hive can allocate. Also, assume that $a_j > 0$ is the constant quality of site j (e.g., in the classical IFD it is the input rate of nutrients to the j^{th} site, in applications, this constant could be proportional to site profitability). Hence, in an n-hive game each hive has N pure strategies corresponding to choosing the sites $j = 1, 2, \ldots, N$. But the strategy is the

number of bees it allocates to each site, or for hive i, the strategy is

$$x^i = \left[x_1^i, x_2^i, \ldots, x_N^i\right]^\top$$

where $\sum_{j=1}^{N} x_j^i = B_f$, for each $i = 1, 2, \ldots, n$. Notice that x^i is an element of the simplex

$$\Delta_x = \left\{ x = [x_1, \ldots, x_N] : \sum_{j=1}^{N} x_j = B_f,\ x_j \geq 0,\ j = 1, 2, \ldots, N \right\}$$

The strategy $x = [x^1, x^2, \ldots, x^n]^\top$ is a Nash equilibrium if the following is valid for all $y^i \neq x^i$, $i = 1, 2, \ldots, n$,

$$f\left(y^i | x^{-i}\right) \leq f\left(x^i | x^{-i}\right) \tag{4.7}$$

where x^{-i} denotes the vector of all other strategies except strategy x^i, and $f(\cdot, \cdot)$ is the fitness payoff. Equation (4.7) means that the hive must allocate the bees using the optimum strategy x so that its gain is maximum in terms of fitness payoff. Notice that if the inequality in Equation (4.7) is strict, we have what is called a strict Nash equilibrium.

Evolutionarily Stable Strategies (ESS) for a Finite Population of Hives

The original formulation of an evolutionarily stable strategy (ESS) introduced in [10, 11] assumes that the population size (number of hives) is infinite and hence does not apply here. There have been a number of studies that treat the ESS concept for a large and finite population sizes (e.g., [74, 75, 76]). However, the seminal work is contained in [68, 67] where the authors state the equilibrium and stability conditions similar to the ones defined in [14]. The n-hive game that we set up in this case can be seen as a game "against the field" [11] i.e., the population size is equal to the contest size. We can define the ESS for finite populations as follows.

Definition 4.3.1 *Let y be a mutant strategy, and $P_{x,y}$ a population set made up of $n-2$ x-strategists and only one y-strategist. Let $f(y, P_x)$ be the fitness of a single y-strategist in a population set P_x of $n-1$ x-strategists. The mixed incumbent strategy $x = [x^1, x^2, \ldots, x^n]^\top$ is one-stable ESS if the following condition holds:*

$$f(y, P_x) < f(x, P_{x,y}) \tag{4.8}$$

for all $y \neq x$.

This is what is known as the equilibrium condition for the game against the field for a finite population size [67]. It is clear that this condition only tests if the population of hives cannot be invaded by *only* one mutant. If we have more than one mutant, we have to check another condition. This condition is usually known as the stability condition, and it says that a strategy is *Y-stable* if the incumbent strategy cannot be invaded by a total of up to Y identical mutant strategists [67]. It is said that the ESS is globally stable whenever $Y = n-1$. Here, we assume that there is *only* one mutant since mutants are rare; hence, we do not need to check the stability condition.

Hive/Bee Fitness Definitions

Before we show that the IFD is a strict Nash equilibrium, we need to define the payoff of hive i. First, let us define the contribution to the fitness of hive i at site j as

$$f^i(j) = a_j \frac{x_j^i}{\sum_{k=1}^n x_j^k} = a_j \frac{x_j^i}{x_j^i + \sum_{k=1, k\neq i}^n x_j^k} \tag{4.9}$$

Equation (4.9) can be divided in two parts. First, we have the proportion of bees allocated by the i^{th} hive to site j, with respect to the total number of bees allocated to that site by all hives. Then, there is the a_j term that can be seen as a constant

that is proportional to the profitability of the site. If a_j is in nutrients per second, then this quantity is the amount of nutrients per second hive i gets for investing x_j^i bees at site j, while the other $n-1$ hives invest $\sum_{k=1,k\neq i}^{n} x_j^k$ bees at the same site. Hence, the fitness (payoff) of hive i, $i = 1, 2, \ldots, n$, is

$$f^i = \sum_{j=1}^{N} f^i(j) = \sum_{j=1}^{N} x_j^i \frac{a_j}{\sum_{k=1}^{n} x_j^k} \tag{4.10}$$

The IFD is achieved when the fitness of hives i and i' are equal, for all $i \neq i'$, as in

$$f^i = \sum_{j=1}^{N} f^i(j) = \sum_{j=1}^{N} f^{i'}(j) = f^{i'} \tag{4.11}$$

Using Equation (4.10), Equation (4.11) can be satisfied if the hive allocate bees equally in every site so that

$$x_j^i = x_j^{i'} \tag{4.12}$$

for all $i, i' = 1, 2, \ldots, n$. If each hive chooses the IFD, then for each $i = 1, 2, \ldots, n$, for $j = 1, 2, \ldots, N$,

$$\frac{x_j^i}{\sum_{k=1}^{N} x_k^i} = \frac{a_j}{\sum_{k=1}^{N} a_k} \tag{4.13}$$

Notice that since $\sum_{k=1}^{N} x_k^i = B_f$ for all $i = 1, 2, \ldots, n$, Equation (4.12) holds. Equation (4.13) is a generalization of the input matching rule [4, 9] to the n-hive game. In Chapter 2 the authors have shown the equivalence between the input and the habitat matching rule for a general case of suitability functions. We can use the same ideas as in Chapter 2 to prove that Equation (4.13) can also be written as

$$x_k^i a_j = x_j^i a_k$$

for all $k, j = 1, 2, \ldots, N$, and $i = 1, 2, \ldots, n$.

Equation (4.9) defines the fitness for multiple hives. However, when there is only a single hive, the definition for the payoff changes. For that, we can assume that each

bee is identical and represented by a small $\epsilon_x > 0$ so that there is an arbitrarily large (integer) number $n > 0$ of bees in the hive, where

$$n\epsilon_x = B_f$$

Given the concept of an individual bee $\epsilon_x > 0$ at site j, $j = 1, 2, \ldots, N$, we define this bee's fitness as $f(j) = \frac{a_j}{n_j}$. If a_j is nutrients per second, $f(j)$ is the number of nutrients per second that a bee gets at site j. Notice that

$$f(j) = \frac{a_j}{n_j} = \epsilon_x \frac{a_j}{\epsilon_x n_j} = \epsilon_x \frac{a_j}{x_j} \tag{4.14}$$

These ideas will be helpful in Section 4.3.3.

4.3.2 The Multiple Hive IFD is a Strict Nash Equilibrium and ESS

In the next theorem[2] we show that the IFD in Equation (4.13) is a strict Nash Equilibrium. This implies by Equation (4.8) that the IFD is a *one-stable* ESS, because the IFD is the best strategy whenever *one* mutant hive plays against $n-1$ incumbents in an n-hive game.

Theorem 4.3.1 *For the n-hive game if the x_j^i, $j = 1, 2, \ldots, N$, $i = 1, 2, \ldots, n$, are all given by the IFD in Equation (4.13), then hives are using a strict Nash equilibrium strategy to allocate the bees. Hence, the IFD in Equation (4.13) is a finite population one-stable ESS.*

This result shows that if the IFD is used by all hives, no hive can unilaterally deviate and improve its fitness. While the IFD is often discussed as if it were with respect

[2]Proofs of all theorems are in the Appendix.

to a number of animals (e.g., bees) being allocated (e.g., see [2]), this seems to be the first proof that in an n-hive game the IFD is a strict Nash equilibrium (hence, a *one-stable* ESS). It is interesting to note that if we think of achievement of Equation (4.13) by each hive as "individual-level" IFD achievement, then for all $j = 1, 2, \ldots, N$, and $i = 1, 2, \ldots, n$,

$$x_j^i \sum_{k=1}^{N} a_k = a_j \sum_{k=1}^{N} x_k^i$$

and if we sum over i,

$$\left(\sum_{i=1}^{n} x_j^i \right) \left(\sum_{k=1}^{N} a_k \right) = a_j \left(\sum_{i=1}^{n} \sum_{k=1}^{N} x_k^i \right)$$

or for all $j = 1, 2, \ldots, N$,

$$\frac{\sum_{i=1}^{n} x_j^i}{\sum_{i=1}^{n} \sum_{k=1}^{N} x_k^i} = \frac{a_j}{\sum_{k=1}^{N} a_k} \tag{4.15}$$

Equation (4.15) can be interpreted as a "hive population-level" or "environment-wide" IFD. Clearly, however, Equation (4.13) is only one way to achieve this population-level IFD (as the next example will show). Finally, note that there may be strategies, not all the same and different from the IFD in Equation (4.13), but that the hives could use and (i) still get the same fitness as each other and as the fitness achieved at the IFD in Equation (4.13), and (ii) achieve the population-level IFD in Equation (4.15). For example, if $N = n = 2$, $B_f = 1$, $a_1 = a_2 = 1$, $x_1^1 = x_2^2 = \frac{1}{4}$, and $x_2^1 = x_1^2 = \frac{3}{4}$, $f^1 = f^2 = 1$ and this is the same fitness that results if the $x_j^i = \frac{1}{2}$ $j = 1, 2$, $i = 1, 2$, IFD strategy from Equation (4.13) is used. Also, Equation (4.15) holds for the alternative strategy choice.

4.3.3 Optimality of the Single and Multiple Hive IFD

The results in Section 4.3.2 show that the IFD is a local optimum point in a game-theoretic sense. Here, we show that the IFD is a global optimum point for both a single hive and multiple hives.

Single-Hive Allocation

First, we take the perspective that a single hive wants to allocate some number of bees B_f to N choices (sites) in order to optimize its payoff (fitness). We drop the superscript and use x_j. The percentage of the total number of bees to site j is $\frac{x_j}{B_f}$, $j = 1, 2, \ldots, N$. Using Equation (4.14), the total payoff can be written as,

$$J = \sum_{j=1}^{N} \left(\frac{x_j}{B_f} \right) \left(\frac{a_j}{x_j} \right) = \frac{\sum_{j=1}^{N} a_j}{B_f} \tag{4.16}$$

Due to the cancellation of the x_j in Equation (4.16), J is a constant. Hence, *any* allocation involving all x_j nonzero gives the same total return to the hive. This is a consequence of the "continuous input" assumption for the IFD formulation that says that all nutrients arrive at a constant rate and are immediately consumed [1]. Equation (4.16) also shows that a hive cannot use the strategy of maximizing J in order to determine how to allocate the number of bees. Does there exist a payoff function that the hive can try to optimize that does guide it to maximize its payoff? Next, we show two approaches to answer this question.

First, assume that $a_j > 0$, $x_j > 0$, and note that $\frac{a_j}{x_j}$ is the return per investment of x_j. Suppose that the hive wants to maximize its return from each investment, under the constraint that $\sum_{j=1}^{N} x_j = B_f$ and $x_j > 0$. One approach is to try to maximize the

minimum fitness as defined by Equation (4.14), i.e., solve the optimization problem

$$\begin{array}{ll} \max\min & \left\{\frac{a_1}{x_1}, \frac{a_2}{x_2}, \ldots, \frac{a_N}{x_N}\right\} \\ \text{subject to} & \sum_{j=1}^{N} x_j = B_f \\ & x_j > 0,\ j = 1, 2, \ldots, N \end{array} \tag{4.17}$$

The terms $\epsilon_x \frac{a_j}{x_j}$ are the fitnesses for *any* bee that chooses site j, $j = 1, 2, \ldots, N$. Consider a single individual $\epsilon_x > 0$. If this bee is at site j and $\epsilon_x \frac{a_j}{x_j} < \epsilon_x \frac{a_k}{x_k}$, $j \neq k$, then it can move to site k (i.e., change strategies). The "max min" represents that multiple bees simultaneously shift strategies to improve their fitness since at least some bees with lowest fitness shift sites (and if $\epsilon_x \frac{a_j}{x_j} = \epsilon_x \frac{a_k}{x_k}$ for some j and k the min can be achieved at multiple sites). It has been shown in Chapter 2 that the hive should invest its effort according to an IFD as it is the global maximum for that optimization problem and hence will maximize the hive's payoff.

Second, viewing the hive's effort allocation strategy as being adaptive (i.e., shaped by natural selection) it makes sense that it would be appropriately modeled as the optimization of some payoff (fitness) [29]. However, could other payoff functions be used besides the one in Equation (4.17)? Generally, the answer to this question should be yes. Equation (4.17) relates decision variables x_j to payoff J and other equally valid relationships between these two could lead to optimal effort distributions, possibly even the IFD. To illustrate this point in a concrete way we introduce another candidate payoff function J.

To develop this J suppose that $a_j > 0$ and $x_j > 0$ for $j = 1, 2, \ldots, N$, and note that $\frac{x_j}{a_j}$ is the amount of bees allocated to site j per the return from site j. For instance, if a_j is in units of nutrients per second, and a hive allocated x_j in units of "bees per second" it takes of the nutrients, then $\frac{x_j}{a_j}$ is in units of bees per nutrients. A hive wants to invest as few as possible bees, yet get as much return as possible.

Hence, it wants to allocate bees so that it gets as many nutrients per bee as possible. If $\frac{x_j}{B_f}$ is the percentage of the total number of bees allocated to site j, and if the hive tries to minimize

$$J = \sum_{j=1}^{N} \left(\frac{x_j}{B_f} \right) \left(\frac{x_j}{a_j} \right) = \frac{1}{B_f} \sum_{j=1}^{N} \frac{x_j^2}{a_j} \tag{4.18}$$

then it will maximize its return on investment by minimizing its losses. Or, from another perspective, it minimizes the average number of bees per nutrient across all sites. The next result shows that if a hive seeks to minimize J in Equation (4.18), then it will achieve an IFD.

Theorem 4.3.2 *The point*

$$x_j = \frac{a_j B_f}{\sum_{k=1}^{N} a_k}$$

is the global minimizer for the constrained optimization problem defined as

$$\begin{array}{ll} \textit{minimize} & J = \frac{1}{B_f} \sum_{j=1}^{N} \frac{x_j^2}{a_j} \\ \textit{subject to} & \sum_{j=1}^{N} x_j = B_f \\ & x_j > 0,\ j = 1, 2, \ldots, N \end{array}$$

Multiple Hive Allocations

Theorem 4.3.2 shows that the IFD is achieved for a single-hive allocation. Now, we want to prove that the IFD is also reached for the case when we have multiple hives that want to allocate bees across different sites. From the proof of Theorem 4.3.1 it should be clear that there are an infinite number of points x_j^i, $j = 1, 2, \ldots, N$, $i = 1, 2, \ldots, n$, that result in

$$\frac{\sum_{i=1}^{n} x_j^i}{\sum_{k=1}^{N} \sum_{i=1}^{n} x_k^i} = \frac{a_j}{\sum_{k=1}^{N} a_k} \tag{4.19}$$

which is the achievement of an IFD by the aggregate of the number of bees' allocation. In the next theorem, we show that the optimum payoff value is given by what we call the population-level IFD in Equation (4.19).

Theorem 4.3.3 *If the population IFD is achieved by the distribution of the bees that achieve Equation (4.19) then, if one of the n hives deviates and the others stay the same, the one that deviates cannot improve its payoff.*

The optimization problem can be interpreted as one hive allocating some number of bees at the site where $n-1$ hives have allocated the bees in such a way that they are at the IFD. For each hive, the total number of bees across the N sites is equal to $\sum_{j=1}^{N} x_j^i = B_f$, for all $i = 1, 2, \ldots, n$. Since the $n-1$ are at the IFD, it is clear that if we add an n^{th} hive, it can allocate all its bees across the N sites using a strategy that leads to the population-level IFD. In other words, this last hive that disrupts everybody else's return gets the same payoff that all the other hives get if it plays a strategy such that the population-level IFD is achieved.

4.3.4 Discussion

The previous analysis is based on the hypothesis that we have *full* static information. This means that we did not analyze the cases where there is noise, lack of information when strategies are chosen, or when the fitness functions in (4.9) or (4.14) have dynamics. Analysis for these cases remains a (challenging) research direction. In the next section, we motivate the importance of addressing these theoretical questions by showing that multiple poorly informed socially foraging honey bee hives can achieve an IFD in an application where there is significant noise.

4.4 Engineering Application: Dynamic Resource Allocation for Multizone Temperature Control

In this section we introduce an engineering application that illustrates the basic features of the dynamical operation of the honey bee social foraging algorithm. First, we describe the hardware used and some implementation issues. Next, we provide data from three experiments that demonstrate the achievement of the ideal free distribution and the effects of cross-inhibition and imperfect information flow.

4.4.1 Experiment and Honey Bee Social Foraging Algorithm Design

We implemented the multizone temperature control grid shown in Figure 4.2. A zone contains a lamp and a National Semiconductors LM35CAZ temperature sensor. The temperature is acquired using 4 analog inputs with 16 bits resolution each on a dSPACE DS1104 card. Although we cannot guarantee that the four sensors have the same characteristics, they have ± 0.2°C typical accuracy, and ± 0.5°C guaranteed. The lamps are turned on or off by the controller using four analog outputs of the DS1104 card and a DS2003 Darlington device that drives the amount of current necessary to turn on a lamp. The lamps change their intensities drastically when we apply more than 1.6 Volts. We added by software a DC value of 1.25 Volts, which implies that there is a range where the lamps are off even if we allocate a small amount of energy in a zone.

We assume that there is a fixed total amount of voltage V_{tot} (the resource) that can be split up and applied to the zones. The goal is to allocate this fixed amount of

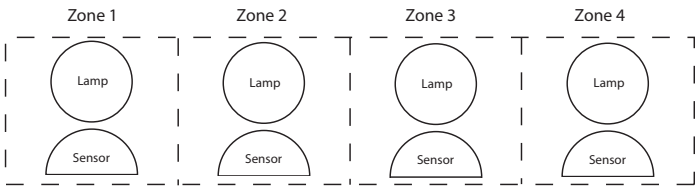

Figure 4.2: Layout for the multizone temperature control grid experiment.

voltage in a way that (i) makes the temperatures in all zones the same, and (ii) maximally elevates the temperature across the grid. In other words, we want a maximum uniform temperature. Achievement of this goal is complicated by interzone effects (e.g., lamps affecting the temperature in neighboring zones), ambient temperature and wind current challenges (from overhead vents), zone component differences, and sensor noise. These effects demand that voltage be dynamically allocated. For example, if there is an ambient temperature increase in zone 4 in Figure 4.2 the voltage applied to the lamp in zone 4 should decrease and that voltage should be allocated across the other three zones.

Given the hardware description and the model, we choose a honey bee social foraging algorithm as follows:

1. We assume that there are a fixed number of bees involved in the foraging process, B. Each bee corresponds to a quanta of energy, which in this case corresponds to a certain amount of volts, of the V_{tot} available volts, that will be specified below.

2. We assume that the foraging landscape is composed of four forage sites, which correspond to the zones j, $j = 1, 2, 3, 4$.

3. Let T_d be a temperature value that *cannot* be achieved in the experiment (here we use $T_d = 29°\text{C}$). Let T_j be the temperature in zone j, and let

$$e_j = T_d - T_j$$

be the temperature error for zone j. We assume that the "best" (most profitable) forage site corresponds to the zone that has the highest error. Bees (quanta of voltage) that are allocated to better sites will raise the temperature there. Repetitive allocation will result in persistently raising the minimum temperature.

4. We assume that the profitability assessment of each site $F^j(k)$ is proportional to e_j and given by

$$F^j(k) = \begin{cases} 1 & \text{if} \quad e_j(k) \geq 1 \\ \gamma e_j(k) & \text{if} \quad \epsilon_n < \gamma e_j(k) < 1 \\ 0 & \text{otherwise} \end{cases} \tag{4.20}$$

We let $\gamma = \frac{1}{8}$ since given T_d the temperature error $e_j < 8°\text{C}$ so $\gamma e_j < 1$ with $\gamma = \frac{1}{8}$. Then we know that $F^j(k) \in [0, 1]$. We let $\epsilon_n = 0.1$ since this means that sensor inaccuracies are not interpreted as profitability differences and, so that with $T_d = 29°\text{C}$ any temperature error is profitable for allocation.

5. The waiting time defined in Equation (4.1) has two tunable parameters, ψ and w_w. In this case, we have tuned these values and we chose $\psi = 0.25$ and $w_w = 20$.

6. We also chose $\alpha = 1$, $\phi = 1$, $p_o = 0.35$, $\sigma = 1000$, $\delta = 0.02$, and $\beta = 100$ to ensure that bees are persistently recruited to achieve the bee (voltage) allocation and persistently explore sites for more temperature error. The particular values

chosen were explained in Section 4.2, and these values did not need to be retuned for the application.

The experimental results shown below were obtained on different days with different ambient room temperatures.

4.4.2 Experiment 1: One Hive IFD Achievement

In this experiment we seek the maximum uniform temperature when we have $V_{tot} = 2.5$ Volts of resource available. We assume that there is one hive that has 200 bees, which are equivalent to V_{tot}. In other words, we assume that each bee is equivalent to 0.0125 Volts. Figure 4.3 shows the experimental results for the temperatures (top plots), and the numbers of bees allocated in each zone (bottom plots), when the room temperature is $T_a = 22°$C.

Figure 4.4 illustrates how the bees are allocated to various roles. The top plot shows how the number of employed foragers B_f increases drastically at the beginning, but then it drops until it arrives to a steady-state. The bottom plot shows the number of explorers B_e, and we can see how it stays high to ensure persistent search for temperature error. From the data obtained, it can also be seen that many bees get recruited. This implies that these bees find a site and they do not abandon it, which provides good temperature regulation.

Figure 4.7, which will be used to compare the results of all the experiments, shows the average temperature (top plot) and the average number of bees (bottom plot) for the last 100 seconds. The data for experiment 1 show how an ideal free distribution is achieved. As we can see, the final temperature reached by all zones is around 27°C. In terms of the average number of bees for the last 100 seconds, we can see that the

voltage allocated is around 1.7 Volts (DC offset included), which is equivalent to 35 bees per zone. However, due to the differences between sensors and lamps, more bees are allocated in the fourth zone (i.e., zone 4 is more difficult to heat). This result is consistent with the experimental results shown below.

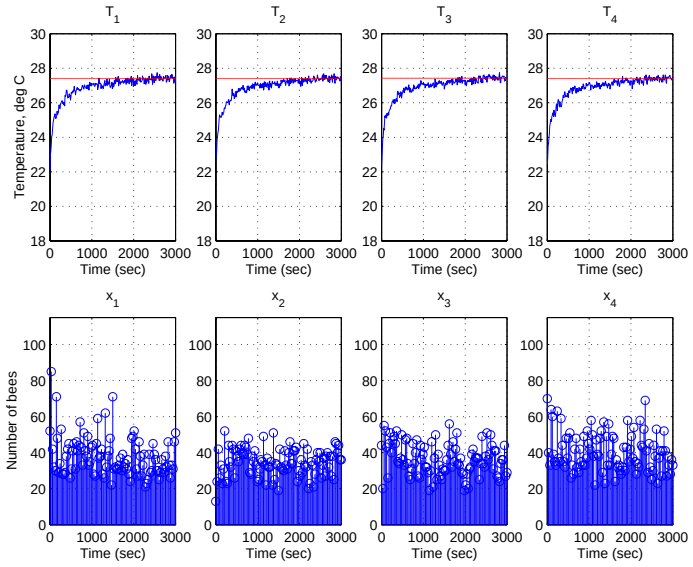

Figure 4.3: Temperature and number of bees per zone when there is one hive and no disturbances. The top plots show the temperature in each zone, and the average of the last 100 seconds (solid constant line). The stems in the bottom plots represent the number of bees that were allocated to each zone.

4.4.3 Experiment 2: One Hive with Disturbances, IFD, Cross-Inhibition, and Site Truncation

The second experiment is similar to the first one, but we add two disturbances to the system. These disturbances are created by two extra lamps, one placed next to zone 1 and another placed next to zone 4. We start the experiment at a room

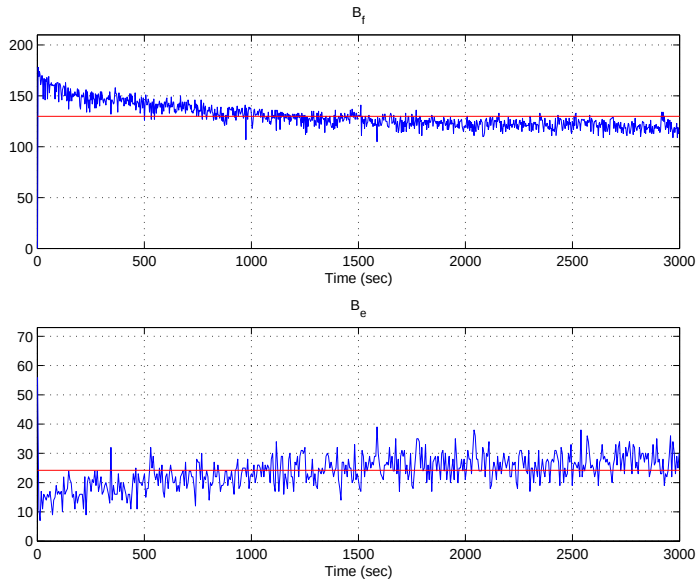

Figure 4.4: Number of employed foragers B_f and the average of the last 100 seconds (top plot). The bottom plot shows the number of explorers B_e and the average of the last 100 seconds.

temperature of $T_a = 20.6°$C. Figure 4.5 shows the results. The numbers in the top left and top right plots represent the *disturbance types* applied to the system:

1. We turn on the disturbance lamp next to zone 4 at $t = 850$ sec, and we turn it off at 1170 sec.

2. We turn on the disturbance lamp next to zone 1 at $t = 2160$ sec, and we turn it off at 2500 sec.

3. We turn on the disturbance lamps next to zones 1 and 4 at $t = 3200$ sec, and we turn them off at 5400 sec.

When we apply disturbance 1, the temperature in zone 4 starts to increase, and the number of bees allocated in that zone decreases drastically. At the same time, the

number of bees in the other three zones increases. This is because site number 4 is the least profitable of all sites, and hence the hive reallocates the bees to the other 3 zones; this is why the temperatures in zones 1, 2, and 3 increase until the disturbance is turned off. At that moment, the temperature in zone 4 drops drastically, and the hive realizes that it must allocate more bees to that site. It does that until all four zones are practically at the same temperature. During the 5 minutes of disturbance, the temperatures in zones 2 and 3 remain close to 25.5°C, while the temperature in zone 1 is around 25.4°C. Therefore, zone 1 becomes the most profitable one, and hence more bees are allocated to that site (around 76 bees were allocated on average to zone 1, while 37, 41, and 10 bees were allocated on average to zones 2, 3, and 4, respectively). The same basic behavior occurs when disturbance 2 is applied to the system. In this case, the temperature at the first site increases to 27°C, while the other temperatures were close to 25.6°C. As in the previous case, the temperature in zone 4 was close to 25.5°C, which implied that more bees were allocated to this site (5, 33, 33, and 93 bees were allocated on average to zones 1 through 4 respectively). We highlight the fact that zone 4 has more bees than the middle zones. As we mentioned in Section 4.4.2 this is due to the differences between sensors and lamps. After disturbance 2 is turned off and the temperatures in all zones was practically the same (i.e., around 25.4°C), we apply disturbance 3 and for it the temperatures equilibrate but with a bee allocation where there are far fewer bees in zones 1 and 4 and more in zones 2 and 3. To see why this is the case, see the experiment 2 data in Figure 4.7. As we can see in the bottom plot, the average number of bees for the last 100 seconds is practically the same for the middle zones (34.8 bees), and there are practically the same number of bees allocated to zones 1 and 4 where there is

a disturbance (10 bees). This leads to a final temperature that is practically the same for zones 1 and 4 (i.e., around 28.6°C) and for the middle zones (i.e., around 28°C). However, as we mentioned before, the fact that there are 10 bees in a zone does not necessarily imply that the lamp is on. In this case, 10 bees corresponds to 0.125 Volts, which implies that the lamp is off (recall that the DC value was 1.25 Volts). Therefore, the bees allocated to zones 1 and 4 do not have any influence on the temperature. Only the disturbances affect these temperatures. Hence the residual number of 10 or so bees simply represents that the hive is continually sampling these sites in case they become profitable.

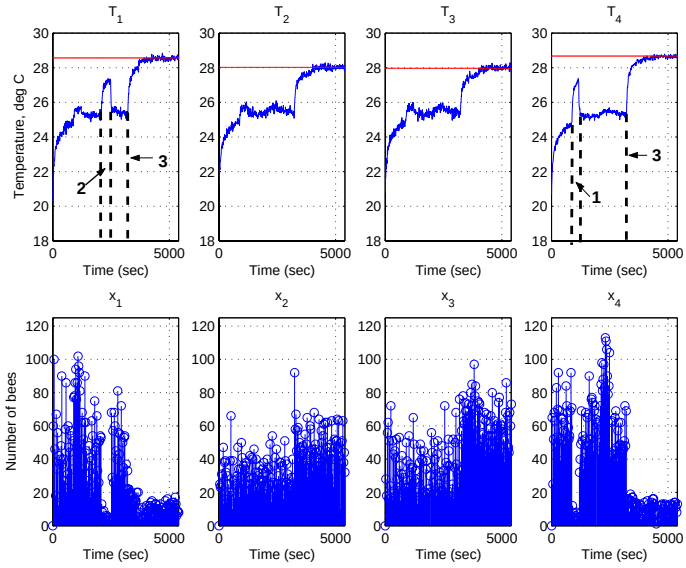

Figure 4.5: Temperature and number of bees per zone for the second experiment. In the top plot the solid constant line represents the average of the last 100 seconds in each zone. The numbers 1, 2, and 3 correspond to the disturbances. The stems in the bottom plot represent the number of bees that were allocated to each zone.

4.4.4 Experiment 3: Two Hives and Imperfect Information

In this final experiment, we change the conditions and instead of using only one hive, we assume that we have two hives each with limited information. The first hive is assumed to only have access to the temperatures in zones 1, 2, and 3, while the second hive has access to the temperatures of zones 2, 3 and 4. This may happen in nature if a hive has not discovered a site. In temperature control applications such sensing restrictions commonly arise due to sensor or other hardware costs.

Each hive is composed of 200 bees, which implies that the 5 Volts that we allocate corresponds to 400 bees (i.e., each bee corresponds again to 0.0125 Volts). Figure 4.6 shows the results for this case when the initial temperature in the room $T_a = 19.6°\text{C}$. The final temperature is practically the same, around 25.4°C. The main difference in this case is that the number of bees in zones 2 and 3 depend on both hives (see the bottom plot of Figure 4.6). Hive 1 allocates on average around 50 bees to zones 2 and 3, while the second hive allocates on average around 20 bees to zones 2 and 3. However, as we can see in the experiment 3 data in the bottom plot of Figure 4.7, the same *total* amount of bees are allocated by the two hives except for zone 4. It is important to notice that the difference between the initial temperature and the final temperature in the first experiment is around 5°C, while in this case is around 6°C. Therefore, as we expect, the maximum temperature reached by the grid is higher than the first one if we compare the temperatures relative to room temperature. This is mainly due to the fact that at the end we are allocating more bees per zone, i.e., more voltage $V_{tot} = 5V$ rather than in experiments 1 and 2 where we had $V_{tot} = 2.5V$. Finally, another important issue that arises in this case is the number of bees that

are allocated to zone 4. Besides the fact that there is a difference between sensors and lamps in zone 4 with respect to the other zones (as it was seen in the previous experiments), there is imperfect information. As we can see, hive 1 allocates more bees to zones 2 and 3 compared to the number allocated by hive 2. This implies that the temperature errors in these zones decrease, while the temperature in zone 4 seems to be lower than the middle zones due to sensor differences. Then, the second hive allocates more bees to the most profitable site (zone 4), and less to zones 2 and 3 (these zones receive more bees from hive 1, and its total value is similar to the number of bees allocated in zone 1). The bottom plot in Figure 4.6 illustrates this point.

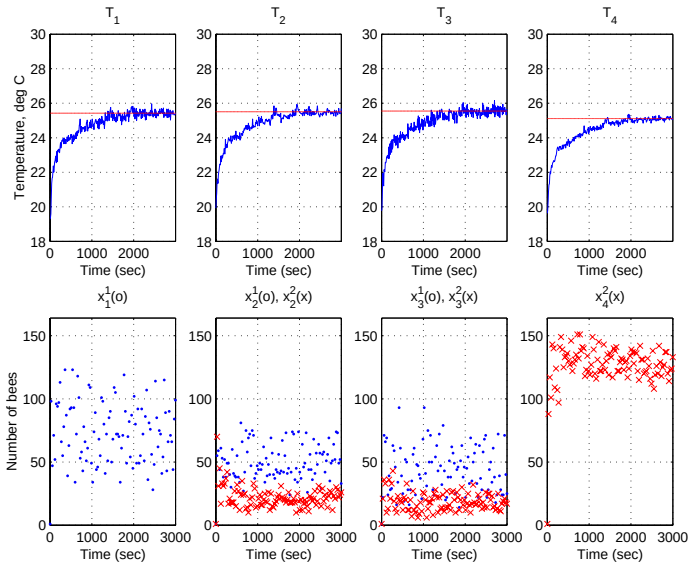

Figure 4.6: Temperature and number of bees per zone for the last experiment. In the top plot the solid constant line represents the average of the last 100 seconds in each zone. In the bottom plot, "o" corresponds to the bees that were allocated by the first hive, while "x" corresponds to the bees that were allocated by the second hive.

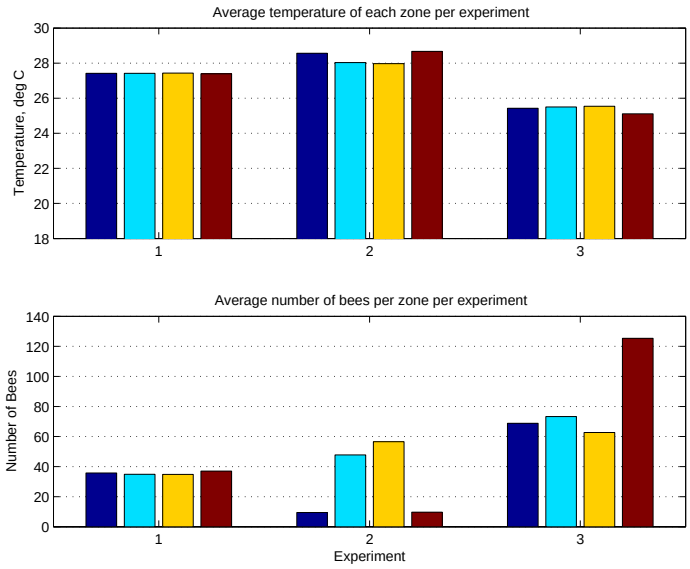

Figure 4.7: The top plot shows the final temperature, while the bottom plot shows the final value for the number of bees in each zone for each experiment. This final value corresponds to the average for the last 100 seconds of data. In each experiment, zone 1 corresponds to the left bar, and zone 4 to the right bar for each of the 3 groups of four bars.

4.4.5 Discussion

Some of the main concepts described in social foraging modeling section (Section 4.2) can be seen in these experiments. In Section 4.4.2 we have seen how an IFD is reached by all zones, and good regulation is obtained even though the search space is limited (Section 4.4.4). As shown in Section 4.4.3, an IFD is also reached when disturbances are applied to the system. The IFD obtained is in terms of the number of bees allocated to each of the zones, depending on whether the disturbance is on or not. In other words, the middle zones that are not significantly affected by any type of disturbance increase their temperature to their maximum possible value. This maximum depends on the amount of energy available. This energy is practically the

same in each zone, which leads to uniformity in these zones. The other two zones have a disturbance associated with each of them, which implies that the number of bees allocated to each of these zones must be lower than for the middle ones. As we expect, the final temperature in this case is higher than in the first experiment because of the disturbances, and the numbers of bees allocated to the middle zones are higher than in the previous case (see Figure 4.7). If we had reduced the magnitude of the disturbances in zones 1 and 4 then we would have gotten results analogous to those for disturbances 1 and 2. We chose the particular disturbance magnitudes in order to illustrate the *elimination* of zones 1 and 4 as possible sites (site "truncation" [1]) and how the hive can then focus most of its attention on only the best sites.

Another important idea that is illustrated in these experiments is the cross-inhibition concept [56], and this can be seen in Figure 4.5. First, all zones were under the same conditions, and practically the same number of bees visited sites 1, 2, and 3 (45, 31, 34 visited on average zones 1 through 3, respectively, while 60 bees where allocated to zone 4 due to sensor differences). When disturbance 1 is applied, more bees start visiting sites 1, 2, and 3, while the number of bees in zone 4 reduces drastically. The same thing happens when disturbances 2 and 3 are applied. It is clear that in any of these cases one or two zones becomes less profitable (the temperature increases due to the disturbance, and hence the error decreases), which implies that the hive has to reduce the number of bees recruited to these poorer sites. This is given in the algorithm by a reduction of the number of dances for those zones where the error is smaller, which leads to a reduction in the number of bees that are recruited to these sites.

Experiment 3 shows how another IFD is achieved over all zones, even though there is not perfect information (see Figure 4.7). As we can see in Figure 4.6, the final temperature in all zones is practically the same (taking into account the sensor differences accuracy). However, as we mentioned before, hive 2 must use more of its bees to raise the temperature in zone 4, and that is why the number of bees allocated by this hive to zones 2 and 3 is small. This problem can be seen also as having a zone with a disturbance. In this case, zone 4 needs more energy, which implies that more bees are allocated by the second hive to it. Thus, the middle zones are not visited as much by the bees since they are less profitable. They are also not as profitable as zone 1, and that is why a smaller amount of bees are allocated to zones 2 and 3 by hive 1 (compared to those that are allocated in zone 1 as it can be seen in the bottom plot in Figure 4.6). However, the total number of bees (those allocated by hives 1 and 2) leads to practically the same numbers of bees in zones 2 and 3, and the grid reaches a maximum uniform temperature.

In all these cases, the temperature grid reached an equilibrium. If we compare the experimental results with the theoretical results (Section 4.3), we can see that the equilibrium point for the first experiment is similar to what is shown in Theorem 4.3.2. In this case, the a_j can be seen as the temperature error, because it is clear that the hive will allocate more bees where the error is higher. For the last experiment a population level type IFD as in (4.19) is achieved, again with a_j proportional to the temperature error. We have proven in Theorem 4.3.3 that the IFD was the optimum point, and the experiments illustrate that this equilibrium was reached for $n = 2$ hives.

4.5 Conclusions

We have developed an engineering application that highlights the main features of a honey bee social foraging algorithm. The application that we have used is a multizone temperature control grid, where the control objective is to seek the maximum uniform temperature. Three experiments illustrate dynamic re-allocation, cross-inhibition, and the ideal free distribution (IFD).

One of the most important concepts in this chapter is the IFD concept from theoretical ecology. We have shown that the IFD is a strict Nash equilibrium for an n-hive game and a one-stable ESS. In other words, in an n-hive game the IFD is reached whenever $n-1$ hives are using it as a strategy and only one hive is not using it. This hive has to choose the IFD strategy to obtain as much as the other hives. Since this is only a local concept, we extend our results to show that the IFD is a global optimum point for both a single hive and multiple hives. In this case we have limited our analysis to an optimality perspective. It is our intent to develop in the future a dynamical model of IFD achievement (e.g., adaptive dynamics such as a replicator dynamics model [14]).

Finally, it is clear that in the implementation we have limited our system and drawn some analogies that might not seem real from a biological perspective. For instance, consider the information structure of the algorithm (i.e., what characteristics are present to provide information to the algorithm and between components of the algorithm). In a honey bee hive, the forage allocation process does not need a centralized entity that makes the decisions and allocates bees to each site, i.e., the hive is a decentralized system [56]. However, if we analyze the honey bee social foraging

algorithm, and more precisely Equations (4.1), (4.5) and (4.6), it is clear that the algorithm is not totally "individual-based" (e.g., Equation (4.5) has to know a noisy version of the total number of waggle runs in order to decide how many observer bees will become an explorer). It is our intent to consider in the future a more fully distributed version that faithfully respects what is known by individuals.

CHAPTER 5

CONCLUSION AND FUTURE DIRECTIONS

5.1 Summary of Contributions

The dissertation starts by analyzing the ideal free distribution (IFD) for a general class of suitability functions. It has been proven that the habitat and input matching rules are equivalent for this general case, and also that the IFD is indeed an evolutionarily stable strategy (ESS). In order to provide global results, a constrained optimization is defined and it is proven that the IFD is a global optimum point. Then, from an evolutionary time perspective, a replicator dynamics model is defined in order to show that the IFD is an asymptotically stable equilibrium point. An interesting characteristic for this case is that under some constraints, a gradient optimization perspective leads to the same replicator dynamics. In order to provide more insight on why these allocation dynamics are useful from an engineering perspective, a multizone temperature control problem is used to show how in spite of limiting the input voltage, a uniform temperature in each of four temperature zones is achieved.

In Chapter 3 another type of multizone temperature control is used to show the utility of foraging theory. A controller is thought of as an agent searching for error across the grid, and it uses the prey model algorithm to decide which types of error

to actuate with a lamp to achieve a uniform desired temperature across the grid. The algorithm causes the controller to ignore certain types of error when the missed opportunity of more profitable types is too great to forgo. Results show that the controller does very well in tracking desired temperatures, even in the presence of disturbances and sensing limitations. The results also illustrate a connection between the prey model and the ideal free distribution. The desired temperature is reached in all three experiments by the foragers allocating themselves in the zones where the error is higher.

Finally, in Chapter 4 an engineering application is developed in order to highlight the main features of a honey bee social foraging algorithm. The application that is used is a multizone temperature control grid, where the control objective is to seek the maximum uniform temperature. The experiments illustrate dynamic re-allocation, cross-inhibition, and the ideal free distribution (IFD). In contrast to Chapter 2, it has been shown that in an n-hive game the IFD is reached whenever $n-1$ hives are using it as a strategy and only one hive is not using it. Therefore, it has been proven that the IFD is a strict Nash equilibrium but for an n-hive game and a one-stable ESS. This hive has to choose the IFD strategy to obtain as much as the other hives. The local concept is extended to show from an optimality perspective that the IFD is a global optimum point for both a single hive and multiple hives.

5.2 Future Directions

The most important future directions that arise in this work can be summarized as follows:

1. Evaluate the relative advantages and disadvantages of other control-theoretic approaches for solving dynamic resource allocation problems such as the multi-zone temperature control problem studied here.

2. Use other foraging theory concepts such as the patch model to determine how long to process certain error types and risk-sensitive foraging theory to decide which types to process when time is limited. Moreover, there is a need to mathematically analyze the stability of the controller; however, this is quite challenging due to the need to consider sensor noise, disturbances, lack of perfect information (i.e., decentralized control), asynchronous operation, and the fact that the control input is of the on-off type that is constrained so that only a limited number of zones can be heated at one time.

3. Consider a more fully distributed version of the honey bee social foraging algorithm that faithfully respects what is known by individuals.

4. Develop a dynamical model of IFD achievement (e.g., adaptive dynamics such as a replicator dynamics model [14]).

APPENDIX A

APPENDIX: PROOF OF THEOREMS

A.1 Proof of Theorem 2.2.1

For (2.4) $\Rightarrow$ (2.6) note that $(c_i x_i + b_i)\sum_{j=1}^{N} a_j^{\frac{1}{m}} = a_i^{\frac{1}{m}} \sum_{j=1}^{N} (c_j x_j + b_j)$, which clearly is (2.6). For (2.6) $\Rightarrow$ (2.4), for all $i = 1, \ldots, N$, $\frac{a_i^{\frac{1}{m}}}{(c_i x_i + b_i)} = \frac{\sum_{j=1}^{N} a_j^{\frac{1}{m}}}{\sum_{j=1}^{N}(c_j x_j + b_j)} = C$, where C is a constant, so for all i, j, (2.4) holds.

A.2 Proof of Theorem 2.2.2

From (2.4), $\frac{a_i^{\frac{1}{m}}}{c_i}\left(x_j^* + \frac{b_j}{c_j}\right) = \frac{a_j^{\frac{1}{m}}}{c_j}\left(x_i^* + \frac{b_i}{c_i}\right)$, so

$$\frac{a_i^{\frac{1}{m}}}{c_i}\sum_{j=1}^{N}\left(x_j^* + \frac{b_j}{c_j}\right) = \left(x_i^* + \frac{b_i}{c_i}\right)\sum_{j=1}^{N}\frac{a_j^{\frac{1}{m}}}{c_j} \tag{A.1}$$

with $\sum_{j=1}^{N} x_j^* = P$, we obtain (2.11). The constraint on P in (2.12) is obtained by using $x_i^* \geq 0$. In the case when $P > 0$, without (2.12) necessarily holding, the analysis changes. Since we need to satisfy the constraint that $x_i \geq 0$, and using the fact that $\frac{a_i^{\frac{1}{m}}}{c_i} > 0$, for some $i = 1, \ldots, N$, for $x_i > 0$,

$$\frac{a_i^{\frac{1}{m}}}{b_i} > \sigma = \frac{\sum_{j=1}^{N}\frac{a_j^{\frac{1}{m}}}{c_j}}{P + \sum_{j=1}^{N}\frac{b_j}{c_j}} \tag{A.2}$$

Since $\frac{a_1^{\frac{1}{m}}}{b_1} > \ldots > \frac{a_N^{\frac{1}{m}}}{b_N}$, if we let k^* be the largest index k for which $\frac{a_k^{\frac{1}{m}}}{b_k} > \sigma$, k^* is given by (2.14). Then, if $i \in \{k^*+1, k^*+2, \ldots, N\}$, (A.2) is not satisfied, and since $c_i > 0$, this equation can be written as $\frac{\frac{a_i^{\frac{1}{m}}}{c_i}P + \frac{a_i^{\frac{1}{m}}}{c_i}\sum_{j=1}^{N}\frac{b_j}{c_j} - \frac{b_i}{c_i}\sum_{j=1}^{N}\frac{a_j^{\frac{1}{m}}}{c_j}}{\sum_{j=1}^{N}\frac{a_j^{\frac{1}{m}}}{c_j}} \leq 0$. The left-hand-side of this inequality is the same x_i^* in (2.11). However, we have assumed that $x_i^* \geq 0$, so $x_i^* = 0$ for $i \in \{k^*+1, \ldots, N\}$. Hence, we will have $N - k^*$ truncated habitats, which implies that $\sum_{j=1}^{N} x_j^* = \sum_{j=1}^{k^*} x_j^* = P$. Therefore, instead of taking the sum over all habitats in (A.1), we need to consider only those habitats that are inhabited, i.e., we need to take the sum over k^* habitats. Then, $\frac{a_i^{\frac{1}{m}}}{c_i}\sum_{j=1}^{k^*}\left(x_j^* + \frac{b_j}{c_j}\right) = \left(x_i^* + \frac{b_i}{c_i}\right)\sum_{j=1}^{k^*}\frac{a_j^{\frac{1}{m}}}{c_j}$. Using the fact that $\sum_{j=1}^{k^*} x_j^* = P$, and the same ideas as before, we obtain that the IFD for the suitability function in (2.5) is given by (2.13) and (2.14).

A.3 Proof of Theorem 2.3.1

Let $\bar{x}$ represent a strategy choice by animal ϵ_x such that all other animals make strategy choices such that the IFD defined by (2.6) holds. From the habitat matching rule we know that for any j such that $a_j = 0$, $x_j = 0$. So $\bar{x}$ will only correspond to strategy (habitat) choices $i \in H^*$ where $a_i > 0$ and $x_i > 0$. Let $P_{\bar{x}}$ represent the population with individuals all playing strategies such that the IFD is achieved. It is impossible to know which habitat $i \in H^*$ player ϵ_x will choose since the IFD can be achieved for any strategy choice $i \in H^*$ provided the other animals adopt the appropriate strategies. In Theorem 2.2.1 we have shown that the habitat matching rule is satisfied and it is given by (2.6), which in terms of fitness is equivalent to

(2.16). Hence, for any $i \in H^*$

$$f(\bar{x}, P_{\bar{x}}) = f(i) = \epsilon_x \frac{a_i^{\frac{1}{m}}}{(c_i x_i + b_i)} = \epsilon_x \frac{a_j^{\frac{1}{m}}}{(c_j x_j + b_j)} = f(j) \tag{A.3}$$

for all $i, j \in H^*$. Suppose that the animal ϵ_x makes a unilateral deviation to strategy $\bar{y} \neq \bar{x}$ that corresponds to choosing habitat $j \neq i$, $j \in H$ (the animal could choose j such that $a_j = 0$). Then, $f(\bar{y}, P_{\bar{x}}) = \epsilon_x \frac{a_j^{\frac{1}{m}}}{(c_j(x_j+\epsilon_x)+b_j)}$, and if $j \in H - H^*$, $a_j = 0$, $f(\bar{y}, P_{\bar{x}}) = 0$. In either case, by monotonicity and from (A.3), $f(\bar{y}, P_{\bar{x}}) < f(\bar{x}, P_{\bar{x}})$. Hence, the IFD is a strict Nash equilibrium and hence an ESS.

A.4 Proof of Theorem 2.3.2

Note that (2.20) is equivalent to the optimization problem

$$\begin{array}{ll} \max & z \\ \text{subject to} & \sum_{j=1}^N x_j = P \\ & x_i \geq 0,\ i = 1, \ldots, N \\ & \epsilon_x \frac{\frac{a_i^{\frac{1}{m}}}{c_i}}{x_i + \frac{b_i}{c_i}} \geq z,\ i = 1, \ldots, N \end{array} \tag{A.4}$$

where we have introduced the new variable $z \in \mathbb{R}$, $z > 0$. If we combine the constraints, we obtain that for each $i = 1, \ldots, N$, $\epsilon_x \frac{\frac{a_i^{\frac{1}{m}}}{c_i}}{z} \geq x_i + \frac{b_i}{c_i} > 0$, since $z > 0$. Adding all the terms across the N habitats we obtain that $z \leq \epsilon_x \frac{\sum_{j=1}^N \frac{a_j^{\frac{1}{m}}}{c_j}}{P + \sum_{j=1}^N \frac{b_j}{c_j}}$. Therefore, (A.4) is equivalent to

$$\begin{array}{ll} \max & z \\ \text{subject to} & z \leq \epsilon_x \frac{\sum_{j=1}^N \frac{a_j^{\frac{1}{m}}}{c_j}}{P + \sum_{j=1}^N \frac{b_j}{c_j}} \end{array}$$

In this case, the maximum is unique and equal to $z^* = \epsilon_x \frac{\sum_{j=1}^N \frac{a_j^{\frac{1}{m}}}{c_j}}{P+\sum_{j=1}^N \frac{b_j}{c_j}}$. Hence, for $i = 1, \ldots, N$, the x_i^* are any values that satisfy the constraints of (A.4) and such that

$$x_i^* \leq \frac{\frac{a_i^{\frac{1}{m}}}{c_i} P + \frac{a_i^{\frac{1}{m}}}{c_i} \sum_{j=1}^N \frac{b_j}{c_j} - \frac{b_i}{c_i} \sum_{j=1}^N \frac{a_j^{\frac{1}{m}}}{c_j}}{\sum_{j=1}^N \frac{a_j^{\frac{1}{m}}}{c_j}} \tag{A.5}$$

We have then two cases. For the "$<$" option, adding all the terms across the N habitats, we obtain a contradiction (i.e., the total population size is less than P). Therefore, the "$=$" option in (A.5) must hold. Using the same ideas as in the proof of Theorem 2.2.2, we can show that the IFD for the suitability function in (2.5) is given by (2.13) and (2.14).

A.5 Proof of Theorem 2.4.1

For ($\Longrightarrow$), since by hypothesis the sum of the p_i is equal to 1 for all $t \geq 0$, and $p_i(0) \geq 0$ for all i, then $p(0) \in \Delta$. For the $N = 2$ case,

$$\begin{aligned}
\dot{p}_1 &= \beta_1 \epsilon_x \left(\frac{a_1^{\frac{1}{m}} p_1(1-p_1)}{(c_1 P p_1 + b_1)} - \frac{a_2^{\frac{1}{m}} p_1(1-p_1)}{(c_2 P p_2 + b_2)} \right) \\
\dot{p}_2 &= \beta_2 \epsilon_x \left(\frac{a_2^{\frac{1}{m}} (1-p_1)(1-(1-p_1))}{(c_2 P p_2 + b_2)} - \frac{a_1^{\frac{1}{m}} p_1(1-p_1)}{(c_1 P p_1 + b_1)} \right)
\end{aligned}$$

Since $\sum_{j=1}^N p_j = 1$, $\sum_{j=1}^N \dot{p}_j = 0$, hence, $\beta_1 = \beta_2$. Next, we assume that $\beta = \beta_i = \beta_j$ for all $i, j = 1, \ldots, N$, and prove that it also holds for $N + 1$. Note that

$$\begin{aligned}
0 &= \sum_{i=1}^N \beta_i p_i \frac{a_i^{\frac{1}{m}}}{(c_i P p_i + b_i)} - \sum_{i=1}^N \beta_i p_i \sum_{j=1}^{N+1} \frac{p_j a_j^{\frac{1}{m}}}{(c_j P p_j + b_j)} \\
&\quad + \beta_{N+1} \frac{a_{N+1}^{\frac{1}{m}} p_{N+1}}{(c_{N+1} P p_{N+1} + b_{N+1})} - \beta_{N+1} p_{N+1} \sum_{j=1}^{N+1} \frac{p_j a_j^{\frac{1}{m}}}{(c_j P p_j + b_j)}
\end{aligned}$$

Using $\sum_{i=1}^{N+1} p_i = 1$, and $\beta_i = \beta$ for all $i = 1, \ldots, N$, by hypothesis, we obtain that $\beta = \beta_{N+1}$. For ($\Longleftarrow$), since $\beta_i = \beta_j$, then $\sum_{i=1}^N \dot{p}_i = \epsilon_x \left(\sum_{i=1}^N \beta_i p_i f(i) - \sum_{i=1}^N \beta_i p_i \bar{f} \right) = 0$.

But, if we take the integral with respect to time, for $t \geq 0$, $\int_0^t \sum_{i=1}^N \dot{p}_i(\tau)d\tau = 0$, or $\sum_{i=1}^N p_i(t) - \sum_{i=1}^N p_i(0) = 0$. But, by hypothesis, the sum of all the initial conditions has to be equal to 1, then we get that for all $t \geq 0$ $\sum_{i=1}^N p_i(t) = 1$. Since by hypothesis $p(0) \in \Delta$, we can conclude that $p \in \Delta$ for all $t \geq 0$.

A.6 Proof of Theorem 2.4.3

Using the Lyapunov function

$$V = -\sum_{i=1}^{N} p_i^* \ln\left(\frac{p_i}{p_i^*}\right) \tag{A.6}$$

In information theory, this function is called the relative entropy function or Kullback-Leibler distance [15]. It has the property that $0 \ln\left(\frac{0}{p_i}\right) = 0 \ln\left(\frac{0}{0}\right) = 0$, and $p_i^* \ln\left(\frac{p_i^*}{0}\right) = +\infty$. It has been proven that V is a valid Lyapunov function candidate (e.g., see [15]). The derivative of V along the trajectories in (2.23), is $\dot{V} = -\sum_{i=1}^N p_i^* \frac{1}{p_i}\left(p_i(f(i) - \bar{f})\right)$. Since $\sum_{j=1}^N p_j^* = 1$

$$\dot{V} = -\sum_{i=1}^{N} p_i^* f(i) + \bar{f}\sum_{i=1}^{N} p_i^* = -\sum_{i=1}^{N} p_i^* f(i) + \sum_{i=1}^{N} p_i f(i) = \sum_{i=1}^{N} f(i)\left(p_i - p_i^*\right) \tag{A.7}$$

In order to show that $\dot{V}$ is non-positive, we will prove that the maximum value of $\dot{V}$ in (A.7) is equal to 0. For that, we let $f(i)$ be as in (2.16) and we solve the optimization problem

$$\begin{array}{ll} \max & J = \dot{V} = \sum_{i=1}^N \epsilon_x \left(\frac{\frac{a_i^{\frac{1}{m}}}{c_i}}{P p_i + \frac{b_i}{c_i}} (p_i - p_i^*) \right) \\ \text{subject to} & \sum_{j=1}^N p_j = 1 \\ & p_i > 0 \ \text{ for all } i = 1, \ldots, N \end{array}$$

Using Lagrange multiplier theory, the Jacobian $\nabla J = \left[\frac{\partial J}{\partial p_1}, \frac{\partial J}{\partial p_2}, \ldots, \frac{\partial J}{\partial p_N}\right]^\top$, where $\frac{\partial J}{\partial p_i} = \epsilon_x \frac{\frac{a_i^{\frac{1}{m}}}{c_i}\left(P p_i^* + \frac{b_i}{c_i}\right)}{(P p_i + \frac{b_i}{c_i})^2}$. Since the inequality constraint $p_i > 0$ is inactive, for $i =$

$1, \ldots, N$,

$$\epsilon_x \frac{\left(\frac{a_i^{\frac{1}{m}}}{c_i}\right)^2 \left(P + \sum_{j=1}^N \frac{b_j}{c_j}\right)}{\left(P\bar{p}_i^* + \frac{b_i}{c_i}\right)^2 \sum_{j=1}^N \frac{a_j^{\frac{1}{m}}}{c_j}} \quad + \quad \lambda^* = 0 \tag{A.8}$$

where $\bar{p}^* = [\bar{p}_1^*, \ldots, \bar{p}_N^*]^\top$ is the regular point for the optimization problem, and λ^* is the Lagrange multiplier. From (A.8), for any $i, j = 1, \ldots, N$, $\frac{a_i^{\frac{1}{m}}}{c_i} \sum_{j=1}^N \left(P\bar{p}_j^* + \frac{b_j}{c_j}\right) = \left(P\bar{p}_i^* + \frac{b_i}{c_i}\right) \sum_{j=1}^N \frac{a_j^{\frac{1}{m}}}{c_j}$. After solving the above equation for $\bar{p}_i^*$, we obtain a scaled version of (2.11), i.e., $\bar{p}_i^* = \frac{x_i^*}{P} = p_i^*$. In order to see if it is a global or a local maximum, we need to check the Hessian $\nabla^2 J$. We have that $\frac{\partial^2 J}{\partial p_i^2} = -\epsilon_x \frac{2P\left(\frac{a_i^{\frac{1}{m}}}{c_i}\right)^2 \left(P + \sum_{j=1}^N \frac{b_j}{c_j}\right)}{\left(Pp_i + \frac{b_i}{c_i}\right)^3 \sum_{j=1}^N \frac{a_j^{\frac{1}{m}}}{c_j}} < 0$, and $\frac{\partial^2 J}{\partial p_i \partial p_j} = 0$. Hence, $\nabla^2 J$ is negative definite, which implies that $\bar{p}^*$ is indeed a global maximum. Therefore, the maximum value of J is $\max J = 0$. Since $\dot{V} < 0$ for all $p_i \neq p_i^*$, and $\dot{V} = 0$ if $p_i = p_i^*$ the IFD is (uniformly) asymptotically stable.

Notice that $\dot{V}$ in (A.7) is negative, except when it is equal to the equilibrium point. The previous analysis showed that whenever we are inside the simplex (i.e., when $p \in \Delta - \partial\Delta$) the Lyapunov function satisfied all the previous conditions. Therefore, the region of asymptotic stability is $\Delta - \partial\Delta$.

A.7 Proof of Theorem 2.4.4

We want to minimize J, subject to $h(x) = \sum_{i=1}^N x_i - P$, and $g_i(x) = x_i$, $i = 1, \ldots, N$ where the g_i constraints are inactive. We have $\frac{\partial J}{\partial x_i} = \frac{1}{P}\left(\frac{x_i}{P} - \frac{x_i^*}{P}\right)$, and $\nabla h(x) = [1, \ldots, 1]^\top$. Also, $\nabla^2 J(x) = \frac{1}{P^2} I_{N\times N}$, where $I_{N\times N}$ is the identity matrix $N \times N$. Since $P > 0$, and satisfies with strict inequality (2.12), $\nabla^2 J(x)$ is positive definite. Using the fact that the constraint is inactive, we have for all $i = 1, \ldots, N$ that $\frac{1}{P}\left(\frac{\bar{x}_i^*}{P} - \frac{x_i^*}{P}\right) + \lambda^* = 0$, where λ^* is the Lagrange multiplier, and $\bar{x}_i^*$ is the optimum

point. Rearranging, we have for any k, w, $\bar{x}_k^* - \bar{x}_w^* = x_k^* - x_w^*$. In terms of k only, we will have $N-1$ of these equations. If we add all these equations, we get that $\bar{x}_k^*(N-1) - \sum_{j=1, j\neq k}^{N} \bar{x}_j^* = x_k^*(N-1) - \sum_{j=1, j\neq k}^{N} x_j^*$, which is equal to (2.11). It is clear that $\bar{x}_i^* > 0$ since P is assumed to satisfy (2.12) with strict inequality. However, J is defined over $\Delta_x - \partial\Delta_x$, and its Hessian is positive definite, which implies that the cost function is convex on $\Delta_x - \partial\Delta_x$. Therefore, the point in (2.11) is a global minimum for the cost function J defined in (2.27), subject to $\sum_{j=1}^{N} x_j = P$, with $x_i > 0$ for all $i = 1, \ldots, N$.

A.8 Proof of Theorem 2.4.5

Since (2.29) is equivalent to (2.24) for the case when $b_i = 0$ for all $i = 1, \ldots, N$. We know that the IFD defined by (2.11) is an equilibrium point whenever $P > 0$ and it is unique, and that $\Delta_x - \partial\Delta_x$ is invariant in x generated by (2.29). Let $e_i = p_i - \frac{\frac{a_i^{\frac{1}{m}}}{c_i}}{\sum_{j=1}^{N} \frac{a_j^{\frac{1}{m}}}{c_j}}$. Since a_i, c_i, and m are positive, we have that $\dot{e}_i = \dot{p}_i = -\left(\frac{\beta\epsilon_x}{P} \sum_{j=1}^{N} \frac{a_j^{\frac{1}{m}}}{c_j}\right) e_i$. Taking the Lyapunov function $V_i = \frac{1}{2} e_i^2$, then $\dot{V}_i = -\left(\frac{\beta\epsilon_x}{P} \sum_{j=1}^{N} \frac{a_j^{\frac{1}{m}}}{c_j}\right) e_i^2(t)$, which implies that the IFD equilibrium is (uniformly) exponentially stable.

A.9 Proof of Theorem 4.3.1

We will show that if $\bar{x}^{i*} = [x_1^{i*}, x_2^{i*}, \ldots, x_N^{i*}]^\top$, where $x_j^{i*} = \frac{B_f a_j}{\sum_{j=1}^{N} a_j}$ for all $j = 1, 2, \ldots, N$, and $i = 1, 2, \ldots, n$, then a single hive mutant $\bar{y}^i \neq \bar{x}^{i*}$ will have a lower fitness for the moment, when $\bar{y}^i \in \Delta_x - \partial\Delta_x$ (i.e., strictly inside the simplex). This is equivalent to show that Equation (4.7) is satisfied for all $i = 1, 2, \ldots, n$. But, it

can also be seen as a constrained optimization problem of the form

$$\begin{array}{lll} \text{maximize} & f^i = \sum_{j=1}^{N} x_j^i \frac{a_j}{\sum_{k=1}^{n} x_j^k} & \\ \text{subject to} & \sum_{j=1}^{N} x_j^i = B_f & i = 1, 2, \ldots, n \\ & x_j^i > 0 & j = 1, 2, \ldots, N \\ & x_j^k = \frac{B_f a_j}{\sum_{m=1}^{N} a_m} & k \neq i,\ k = 1, 2, \ldots, n \end{array} \tag{A.9}$$

This is a nonlinear optimization problem that we will solve using Lagrange multiplier theory (e.g., [77]).

First, since $x_j^i > 0$ the constraint is inactive, so it can be ignored. Second, replace in Equation (4.10) the constraint $x_j^k = \frac{B_f a_j}{\sum_{m=1}^{N} a_m}$, for all $k \neq i$ to get

$$f^i = \sum_{j=1}^{N} x_j^i \frac{a_j}{x_j^i + \phi_j}$$

where

$$\phi_j = \sum_{k=1, k\neq i}^{n} \frac{B_f a_j}{\sum_{m=1}^{N} a_m} = (n-1)\frac{B_f a_j}{\sum_{m=1}^{N} a_m} \tag{A.10}$$

The problem in Equation (A.9) becomes

$$\begin{array}{ll} \text{maximize} & f^i \\ \text{subject to} & \sum_{j=1}^{N} x_j^i = B_f,\ i = 1, 2, \ldots, n \end{array}$$

Now, we define the vector $x = [x_1^i, x_2^i, \ldots, x_N^i]^\top$ which constitutes the points for which we want to find an extremizer point. Let $h(x) = \sum_{j=1}^{N} x_j^i - B_f$. The gradient of f^i with respect to x is equal to

$$\nabla f^i(x) = \left[\frac{\partial f^i}{\partial x_1^i}, \frac{\partial f^i}{\partial x_2^i}, \ldots, \frac{\partial f^i}{\partial x_N^i}\right]^\top$$

$$\nabla f^i(x) = \left[\frac{a_1\phi_1}{(x_1^i + \phi_1)^2}, \frac{a_2\phi_2}{(x_2^i + \phi_2)^2}, \ldots, \frac{a_N\phi_N}{(x_N^i + \phi_N)^2}\right]^\top$$

Also, $\frac{\partial h}{\partial x_j^i} = 1$ for all $j = 1, 2, \ldots, N$. Let λ^* be the Lagrange multiplier for this constrained optimization problem. Then, we have to solve the following set of equations

for $x_j^{i*} > 0$

$$\begin{array}{rcl} \frac{a_1\phi_1}{(x_1^{i*}+\phi_1)^2} + \lambda^* & = & 0 \\ \vdots & & \\ \frac{a_N\phi_N}{(x_N^{i*}+\phi_N)^2} + \lambda^* & = & 0 \\ x_1^{i*} + x_2^{i*} + \ldots x_N^{i*} & = & B_f \end{array}$$

For any $\bar{i}, \bar{j} = 1, 2, \ldots, N$ we have from the previous equations that

$$\frac{a_{\bar{i}}\phi_{\bar{i}}}{(x_{\bar{i}}^{i*} + \phi_{\bar{i}})^2} = \frac{a_{\bar{j}}\phi_{\bar{j}}}{(x_{\bar{j}}^{i*} + \phi_{\bar{j}})^2}$$

Using Equation (A.10),

$$\frac{a_{\bar{i}}^2}{\left(x_{\bar{i}}^{i*}\sum_{m=1}^N a_m + B_f a_{\bar{i}}(n-1)\right)^2} = \frac{a_{\bar{j}}^2}{\left(x_{\bar{j}}^{i*}\sum_{m=1}^N a_m + B_f a_{\bar{j}}(n-1)\right)^2}$$

Since $a_j > 0$ and $x_j^i > 0$, $j = 1, 2, \ldots, N$, $i = 1, 2, \ldots, n$, and $n > 1$,

$$a_{\bar{i}}\left(x_{\bar{j}}^{i*}\sum_{m=1}^N a_m + B_f a_{\bar{j}}(n-1)\right) = a_{\bar{j}}\left(x_{\bar{i}}^{i*}\sum_{m=1}^N a_m + B_f a_{\bar{i}}(n-1)\right)$$

Simplifying, we get that for all $\bar{i}, \bar{j} = 1, 2, \ldots, N$,

$$a_{\bar{i}}x_{\bar{j}}^{i*} = a_{\bar{j}}x_{\bar{i}}^{i*}$$

After some algebraic manipulations, this implies that for all $\bar{i} = 1, 2, \ldots, N$,

$$x_{\bar{i}}^{i*} = \frac{B_f a_{\bar{i}}}{\sum_{m=1}^N a_m} \tag{A.11}$$

In order to see that $x_{\bar{i}}^{i*}$ defined in Equation (A.11) is a local maximum we need to prove the second order sufficiency condition. For that, we need to analyze the Hessian of f^j (because the Hessian of $h(x)$ is 0). In this case,

$$\nabla^2 f^j(x) = \begin{bmatrix} \frac{-2a_1\phi_1}{\left(x_1^i+\phi_1\right)^3} & 0 & \ldots & 0 \\ 0 & \frac{-2a_2\phi_2}{\left(x_2^i+\phi_2\right)^3} & \ldots & 0 \\ \vdots & \vdots & \ddots & \vdots \\ 0 & 0 & \ldots & \frac{-2a_N\phi_N}{\left(x_N^i+\phi_N\right)^3} \end{bmatrix}$$

It is clear that the Hessian of $f^i(x)$ for x_j^{i*}, $j = 1, 2, \ldots, N$, $i = 1, 2, \ldots, n$, in Equation (A.11) is negative definite since $a_j > 0$, $x_j > 0$, $n > 1$ and $\phi_j > 0$, $j = 1, 2, \ldots, N$. Therefore we can conclude that the extremizer points defined in Equation (A.11) are global maximizers (because it is clear that the cost function is convex on the simplex Δ_x). Hence, x_j^{i*} defined by Equation (A.11) (which is equivalent to Equation (4.13)) is a strict Nash equilibrium. Also, since it is a strict Nash equilibrium, Equation (4.8) holds. Therefore, the IFD is a *one-stable* ESS for the finite population in a game against the field.

A.10 Proof of Theorem 4.3.2

As in the case for the proof of Theorem 4.3.1, $x_j > 0$ is an inactive constraint so it can be ignored. Let $h(x) = \sum_{j=1}^{N} x_j - B_f$. For this case, we will have that the gradient of $h(x)$ is equal to

$$\nabla h(x) = [1, 1, \ldots, 1]^\top$$

and the gradient for $J(x)$ is given by

$$\nabla J(x) = \left[\frac{2x_1}{B_f a_1}, \frac{2x_2}{B_f a_2}, \ldots, \frac{2x_N}{B_f a_N}\right]^\top$$

Let λ^* be the Lagrange multiplier for this constrained optimization problem. Then, we have to solve the following set of equations for $x_j^* > 0$

$$\begin{aligned} \tfrac{2x_1^*}{B_f a_1} + \lambda^* &= 0 \\ &\vdots \\ \tfrac{2x_N^*}{B_f a_N} + \lambda^* &= 0 \\ x_1^* + x_2^* + \ldots + x_N^* &= B_f \end{aligned}$$

As in the proof of Theorem 4.3.1 this implies that

$$a_k x_j^* = a_j x_k^*$$

for all $j, k = 1, 2, \ldots, N$, which implies that

$$x_j^* = \frac{B_f a_j}{\sum_{j=1}^{N} a_j} \tag{A.12}$$

In order to see that x_j^* defined in Equation (A.12) is a local minimum we need to prove the second order sufficiency condition. For that, we need to analyze the Hessian of J (because the Hessian of $h(x)$ is 0). In this case,

$$\nabla^2 J(x^*) = \begin{bmatrix} \frac{2}{B_f a_1} & 0 & \ldots & 0 \\ 0 & \frac{2}{B_f a_2} & \ldots & 0 \\ \vdots & \vdots & \ddots & \vdots \\ 0 & 0 & \ldots & \frac{2}{B_f a_N} \end{bmatrix}$$

Since, $B_f > 0$ and $a_j > 0$, $j = 1, 2, \ldots, N$, $\nabla^2 J(x^*)$ is positive definite, which implies by the second-order sufficient condition that x_j^* in Equation (A.12) is a local minimizer. However, we know that the cost function J is defined over a simplex Δ_x, which is nonempty, convex, and a closed subset of $\mathbb{R}^N$. Using this fact, and since the Hessian of $J(x^*)$ is positive definite, we can conclude that the local minimum in Equation (A.12) is also global [77].

A.11 Proof of Theorem 4.3.3

From an optimization point of view, the problem that we want to solve is the same as

$$\begin{array}{lll} \text{maximize} & f^i & \\ \text{subject to} & \sum_{j=1}^{N} x_i^j = B_f & i = 1, 2, \ldots, n \\ & x_j^i > 0 & j = 1, 2, \ldots, N \\ & x_j^{\bar{i}} = \frac{n B_f a_j}{\sum_{j=1}^{N} a_j} - \sum_{k=1, k\neq\bar{i}}^{n} x_j^k & \bar{i} \neq i \end{array} \tag{A.13}$$

Let $h(x) = \sum_{j=1}^{N} x_j^i - B_f$, and since $x_j^i > 0$ that constraint is inactive, so it can be ignored. Using Lagrange multipliers, we need to find first the gradient of the cost

function and the gradient of the constraint. In this case, we have

$$\nabla f^i = \left[\frac{\partial f^i}{\partial x_1^i}, \frac{\partial f^i}{\partial x_2^i}, \ldots, \frac{\partial f^i}{\partial x_N^i}\right]^\top$$

where

$$\frac{\partial f^i}{\partial x_j^i} = \frac{a_j \sum_{k=1,k\neq i}^n x_j^k}{\left(x_j^i + \sum_{k=1,k\neq i}^n x_j^k\right)^2}$$

The gradient of $h(x)$ is $\nabla h(x) = [1, 1, \ldots, 1]^\top$. Therefore, we have to solve the following set of equations for $x_j^{i*} > 0$

$$\begin{array}{rcl} \frac{a_1 \sum_{k=1,k\neq i}^n x_1^{k*}}{(x_1^{i*} + \sum_{k=1,k\neq i}^n x_1^{k*})^2} + \lambda^* & = & 0 \\ \vdots & & \\ \frac{a_N \sum_{k=1,k\neq i}^n x_N^{k*}}{(x_N^{i*} + \sum_{k=1,k\neq i}^n x_N^{k*})^2} + \lambda^* & = & 0 \\ x_1^{i*} + x_2^{i*} + \ldots x_N^{i*} & = & B_f \end{array}$$

Then, for any $\bar{i}, \bar{j} = 1, 2, \ldots, N$,

$$\frac{a_{\bar{i}} \sum_{k=1,k\neq i}^n x_{\bar{i}}^{k*}}{\left(x_{\bar{i}}^{i*} + \sum_{k=1,k\neq i}^n x_{\bar{i}}^{k*}\right)^2} = \frac{a_{\bar{j}} \sum_{k=1,k\neq i}^n x_{\bar{j}}^{k*}}{\left(x_{\bar{j}}^{i*} + \sum_{k=1,k\neq i}^n x_{\bar{j}}^{k*}\right)^2}$$

Replacing the constraint in Equation (A.13),

$$a_{\bar{i}} \left(\frac{nPa_{\bar{i}}}{\sum_{j=1}^N a_j} - x_{\bar{i}}^{i*}\right) \frac{n^2 B_f^2 a_{\bar{j}}^2}{\left(\sum_{j=1}^N a_j\right)^2} = a_{\bar{j}} \left(\frac{nPa_{\bar{j}}}{\sum_{j=1}^N a_j} - x_{\bar{j}}^{i*}\right) \frac{n^2 B_f^2 a_{\bar{i}}^2}{\left(\sum_{j=1}^N a_j\right)^2}$$

which implies that

$$a_{\bar{j}} x_{\bar{i}}^{i*} = a_{\bar{i}} x_{\bar{j}}^{i*}$$

$$x_{\bar{i}}^{i*} = \frac{a_{\bar{i}} B_f}{\sum_{j=1}^N a_j} \tag{A.14}$$

The point in Equation (A.14) is an extremizer for the optimization problem defined in (A.13). Now, let us prove that (A.14) is indeed a global maximizer for this problem.

For that, we need to analyze only the Hessian of our cost function because $\nabla^2 h(x) = 0$. That is,

$$\nabla^2 f^i(x^*) = \begin{bmatrix} \frac{-2a_1 \sum_{k=1,k\neq i}^{n} x_1^{k*}}{\left(x_1^i + \sum_{k=1,k\neq i}^{n} x_1^{k*}\right)^3} & & 0 \\ \vdots & \ddots & \vdots \\ 0 & & \frac{-2a_N \sum_{k=1,k\neq i}^{n} x_N^{k*}}{\left(x_N^i + \sum_{k=1,k\neq i}^{n} x_N^{k*}\right)^3} \end{bmatrix}$$

Clearly, since $a_j > 0$, $B_f > 0$, $x_j^{i*} > 0$, $\sum_{k=1,k\neq i}^{n} x_1^{k*} > 0$, and $n > 1$, the Hessian is negative definite. Therefore we can conclude that the extremizer points defined in Equation (A.14) are global maximizers (because it is clear that the cost function is convex on the simplex Δ_x).

Replacing the optimum point, we can notice that the constraint becomes $x_j^{\bar{i}} = \frac{nB_f a_j}{\sum_{j=1}^{N} a_j} - \sum_{k=1,k\neq\bar{i}}^{n} x_j^k$ that is equivalent to Equation (4.19).

BIBLIOGRAPHY

[1] S. D. Fretwell and H. L. Lucas, "On territorial behavior and other factors influencing habitat distribution in birds," *Acta Biotheoretica*, vol. 19, pp. 16–36, 1970.

[2] L. A. Giraldeau and T. Caraco, *Social Foraging Theory*. Princeton, NJ: Princeton University Press, 2000.

[3] T. Tregenza, "Building on the ideal free distribution," *Advances in Ecological Research*, vol. 26, pp. 253–307, 1995.

[4] G. A. Parker and W. J. Sutherland, "Ideal free distribution when individuals differ in competitive ability: phenotype-limited ideal free models," *Animal Behaviour*, vol. 34, pp. 1222–1242, 1986.

[5] C. M. Lessels, "Putting resource dynamics into continuous input ideal free distribution models," *Animal Behaviour*, vol. 49, pp. 487–494, 1995.

[6] H. R. Pulliam and T. Caraco, "Living in groups: Is there an optimal group size?," in *Behavioural Ecology: An Evolutionary Approach*, pp. 122–147, J. R. Krebs and N. B. Davies, eds, 1984.

[7] R. Fagen, "A generalized habitat matching rule," *Evolutionary Ecology*, vol. 1, pp. 5–10, 1987.

[8] W. J. Sutherland, "Aggregation and the "ideal free" distribution," *Journal of Animal Ecology*, vol. 52, pp. 821–828, 1983.

[9] G. A. Parker, "Searching for mates," in *Behavioural Ecology: An Evolutionary Approach*, pp. 214–244, J. R. Krebs and N. B. Davies, eds, 1978.

[10] J. Maynard Smith and G. R. Price, "The logic of animal conflict," *Nature*, vol. 246, pp. 15–18, 1973.

[11] J. Maynard Smith, *Evolution and the Theory of Games*. Cambridge, UK: Cambridge University Press, 1982.

[12] I. M. Bomze, "Regularity versus degeneracy in dynamics, games, and optimization: A unified approach to different aspects," *SIAM Review*, vol. 44, no. 3, pp. 394–414, 2002.

[13] P. D. Taylor and L. B. Jonker, "Evolutionary stable strategies and game dynamics," *Mathematical Biosciences*, vol. 40, pp. 145–156, 1978.

[14] J. Hofbauer and K. Sigmund, *Evolutionary Games and Population Dynamics*. Cambridge, UK: Cambridge University Press, 1998.

[15] J. W. Weibull, *Evolutionary Game Theory*. London, England: The MIT Press, 1997.

[16] C. D. Schaper, K. El-Awady, and A. Tay, "Spatially-programmable temperature control and measurement for chemically amplified photoresist processing," *SPIE Conference on Process, Equipment, and Materials Control in Integrated Circuit Manufacturing V*, vol. 3882, pp. 74–79, September 1999.

[17] C. D. Schaper, T. Kailath, and Y. J. Lee, "Decentralized control of wafer temperature for multizone rapid thermal processing systems," *IEEE Transactions on Semiconductor Manufacturing*, vol. 12, pp. 193–199, May 1999.

[18] M. Zaheer-uddin, R. V. Patel, and S. A. K. Al-Assadi, "Design of decentralized robust controllers for multizone space heating systems," *IEEE Transactions on Control Systems Technology*, vol. 1, pp. 246–261, December 1993.

[19] P. E. Ross, "Beat the heat," *IEEE Spectrum Magazine*, vol. 41, pp. 38–43, May 2004.

[20] R. D'Andrea and G. E. Dullerud, "Distributed control design for spatially interconnected systems," *IEEE Transactions on Automatic Control*, vol. 48, pp. 1478–1495, September 2003.

[21] R. M. Murray, "Future directions in control, dynamics and systems: Overview, grand challenges and new courses.," *European Journal of Control*, vol. 9, no. 2, pp. 144–158, 2003.

[22] T. Ibaraki and N. Katoh, *Resource Allocation Problems: Algorithmic Approaches*. Cambridge, MA: The MIT Press, 1988.

[23] M. P. J. Fromherz and W. B. Jackson, "Force allocation in a large-scale distributed active surface," *IEEE Transactions on Control Systems Technology*, vol. 11, pp. 641–655, September 2003.

[24] N. Quijano, A. E. Gil, and K. M. Passino, "Experiments for dynamic resource allocation, scheduling, and control," *IEEE Control Systems Magazine*, vol. 25, pp. 63–79, February 2005.

[25] J. Finke and K. M. Passino, "Stable cooperative multiagent spatial distributions," in *Proceedings of the 44th IEEE Conference on Decision and Control and European Control Conference*, (Sevilla, Spain), December 2005.

[26] J. Finke and K. M. Passino, "Stable emergent heterogeneous agent distributions in noisy environments," in *Proceedings of the 2006 American Control Conference*, pp. 2130–2135, 2006.

[27] T. Başar and G. J. Olsder, *Dynamic Noncooperative Game Theory*. Philadelphia, PA: SIAM, 1999.

[28] H. Gintis, *Game Theory Evolving*. Princeton, NJ: Princeton University Press, 2000.

[29] D. Stephens and J. Krebs, *Foraging Theory*. Princeton, NJ: Princeton Univ. Press, 1986.

[30] A. Houston and J. McNamara, *Models of Adaptive Behaviour*. Cambridge: Cambridge University Press, 1999.

[31] B. W. Andrews, K. M. Passino, and T. A. Waite, "Foraging theory for decision-making system design: task-type choice," *Proceedings, 43rd IEEE Conference on Decision and Control*, vol. 5, pp. 4740 – 4745, December 2004.

[32] B. W. Andrews, K. M. Passino, and T. A. Waite, "Social foraging theory for robust multiagent system design," *To appear, IEEE Transactions on Automation Science and Engineering*, 2006.

[33] K. M. Passino, "Biomimicry of bacterial foraging for distributed optimization and control," *IEEE Control Systems Magazine*, vol. 22, no. 3, pp. 52–67, 2002.

[34] K. M. Passino, *Biomimicry for Optimization, Control, and Automation*. London: Springer-Verlag, 2005.

[35] "OSU Distributed Dynamical Systems Laboratory: http://www.ece.osu.edu/~passino/distdynamicsyslab.html.."

[36] G. E. Stewart, D. M. Gorinevsky, and G. A. Dumont, "Feedback controller design for a spatially distributed system: The paper machine problem," *IEEE Transactions on Control Systems Technology*, vol. 11, pp. 612 – 628, July 2003.

[37] M. Boulvin, A. V. Wouwer, R. Lepore, C. Renotte, and M. Remy, "Modeling and control of cement grinding processes," *IEEE Transactions on Control Systems Technology*, vol. 11, pp. 715 – 725, September 2003.

[38] P. D. Jones, S. R. Duncan, T. Rayment, and P. S. Grant, "Control of temperature profile for a spray deposition process," *IEEE Transactions on Control Systems Technology*, vol. 11, pp. 656– 667, September 2003.

[39] A. Emami-Naeini, J. Ebert, D. de Roover, R. Kosut, M. Dettori, L. M. L. Porter, and S. Ghosal, "Modeling and control of distributed thermal systems," *IEEE Transactions on Control Systems Technology*, vol. 11, pp. 668– 683, September 2003.

[40] M. A. Demetriou, A. Paskaleva, O. Vayena, and H. Doumanidis, "Scanning actuator guidance scheme in a 1-d thermal manufacturing process," *IEEE Transactions on Control Systems Technology*, vol. 11, pp. 757 – 764, September 2003.

[41] B. Bamieh, F. Paganini, and M. A. Dahleh, "Distributed control of spatially invariant systems," *IEEE Transactions on Automatic Control*, vol. 47, pp. 1091 – 1107, July 2002.

[42] M. Alaeddine and C. C. Doumanidis, "Distributed parameter thermal controllability: a numerical method for solving the inverse heat conduction problem," *International Journal for Numerical Methods in Engineering*, vol. 59, pp. 945 – 961, February 2004.

[43] C. D. Schaper, T. Kailath, and Y. J. Lee, "Decentralized control of wafer temperature for multizone rapid thermal processing systems," *IEEE Transactions on Semiconductor Manufacturing*, vol. 12, pp. 193–199, May 1999.

[44] M. Alaeddine and C. C. Doumanidis, "Distributed parameter thermal system control and observation by GreenGalerkin methods," *International Journal for Numerical Methods in Engineering*, vol. 61, pp. 1921 – 1937, November 2004.

[45] C. D. Schaper, K. El-Awady, and A. Tay, "Spatially-programmable temperature control and measurement for chemically amplified photoresist processing," *SPIE Conference on Process, Equipment, and Materials Control in Integrated Circuit Manufacturing V*, vol. 3882, pp. 74–79, September 1999.

[46] P. Ulam and T. Balch, "Niche selection for foraging tasks in multi-robot teams using reinforcement learning," in *Proceedings of the 2nd International Workshop on the Mathematics and Algorithms of Social Insects*, (Atlanta, GA), pp. 161–167, December 15-17, 2003.

[47] N. Quijano and K. M. Passino, "Optimality and stability of the ideal free distribution with application to temperature control," in *Proceedings of the 2006 American Control Conference*, pp. 4836–4841, 2006.

[48] S. Camazine and J. Sneyd, "A model of collective nectar source selection by honey bees: self-organization through simple rules," *Journal of Theoretical Biology*, vol. 149, pp. 547–571, 1991.

[49] M. Dorigo and C. Blum, "Ant colony optimization theory: A survey," *Theoretical Computer Science*, vol. 344, no. 2-3, pp. 243–278, 2005.

[50] E. Bonabeau, M. Dorigo, and G. Theraulaz, *Swarm Intelligence: From Natural to Artificial Systems*. New York, NY: Oxford Univ. Press, 1999.

[51] M. Dorigo and T. Stützle, *Ant colony optimization*. Cambridge, MA: MIT Press, 2004.

[52] M. Dorigo, L. Gambardella, M. Middendorf, and T. Stützle, "Guest editorial: special section on ant colony optimization," *IEEE Transactions on Evolutionary Computation*, vol. 6, pp. 317–319, Aug 2002.

[53] M. Dorigo, V. Maniezzo, and A. Colorni, "Ant system: optimization by a colony of cooperating agents," *IEEE Transactions on Systems, Man and Cybernetics, Part B*, vol. 26, pp. 29–41, Feb 1996.

[54] R. Schoonderwoerd, O. E. Holland, J. L. Bruten, and L. J. M. Rothkrantz, "Ant-based load balancing in telecommunications networks," *Adaptive Behavior*, vol. 5, no. 2, pp. 169–207, 1996.

[55] M. Reimann, K. Doerner, and R. Hartl, "D-Ants: Savings based ants divide and conquer the vehicle routing problem," *Computers & Operations Research*, vol. 31, pp. 563–591, April 2004.

[56] T. D. Seeley, *The Wisdom of the Hive*. Cambridge, MA: Harvard University Press, 1995.

[57] T. Seeley, S. Camazine, and J. Sneyd, "Collective decision-making in honey bees: how colonies choose among nectar sources," *Behavioral Ecology and Sociobiology*, vol. 28, pp. 277–290, 1991.

[58] M. Cox and M. Myerscough, "A flexible model of foraging by a honey bee colony: the effects of individual behavior on foraging success," *Journal of Theoretical Biology*, vol. 223, pp. 179–197, 2003.

[59] D. Sumpter and S. Pratt, "A modelling framework for understanding social insect foraging," *Behavioral Ecology and Sociobiology*, vol. 53, pp. 131–144, 2003.

[60] M. Mitchell, *An Introduction to Genetic Algorithms*. Cambridge, MA: MIT Press, 1996.

[61] H. de Vries and J. C. Biesmeijer, "Modeling collective foraging by means of individual behavior rules in honey-bees," *Behavioral Ecology and Sociobiology*, vol. 44, pp. 109–124, 1998.

[62] H. de Vries and J. C. Biesmeijer, "Self-organization in collective honeybee foraging: emergence of symmetry breaking, cross inhibition, and equal harvest-rate distribution," *Behavioral Ecology and Sociobiology*, vol. 51, pp. 557–569, 2002.

[63] T. D. Seeley and C. Tovey, "Why search time to find a food-storer bee accurately indicates the relative rates of nectar collecting and nectar processing in honey bee colonies," *Animal Behaviour*, vol. 47, pp. 311–316, 1994.

[64] J. Bartholdi, T. D. Seeley, C. Tovey, and J. VandeVate, "The pattern and effectiveness of forager allocation among flower patches by honey bee colonies," *Journal of Theoretical Biology*, vol. 160, pp. 23–40, 1993.

[65] R. Dukas and L. Edelstein-Keshet, "The spatial distribution of colonial food provisioners," *Journal of Theoretical Biology*, vol. 190, pp. 121–134, 1998.

[66] K. M. Passino and T. D. Seeley, "Modeling and analysis of nest-site selection by honey bee swarms: The speed and accuracy trade-off," *Behavioral Ecology and Sociobiology*, vol. 59, no. 3, pp. 427–442, 2006.

[67] M. E. Schaffer, "Evolutionary stable strategies for a finite population and a variable contest size," *Journal of Theoretical Biology*, vol. 132, pp. 469–478, 1988.

[68] J. Maynard Smith, "Can a mixed strategy be stable in a finite population?," *Journal of Theoretical Biology*, vol. 130, pp. 247–251, 1988.

[69] S. Nakrani and C. Tovey, "On honey bees and dynamic allocation in an internet server colony," in *Proceedings of 2nd International Workshop on The Mathematics and Algorithms of Social Insects*, 2003.

[70] T. Seeley and W. Towne, "Tactics of dance choice in honeybees: do foragers compare dances?," *Behavioral Ecology and Sociobiology*, vol. 30, pp. 59–69, 1992.

[71] T. D. Seeley, "Honey bee foragers as sensory units of their colonies," *Behavioral Ecology and Sociobiology*, vol. 34, pp. 51–62, 1994.

[72] T. D. Seeley, "Division of labor between scouts and recruits in honeybee foraging," *Behavioral Ecology and Sociobiology*, vol. 12, pp. 253–259, 1983.

[73] T. Seeley and P. Visscher, "Assessing the benefits of cooperation in honey bee foraging: search costs, forage quality, and competitive ability," *Behavioral Ecology and Sociobiology*, vol. 22, pp. 229–237, 1988.

[74] J. G. Riley, "Evolutionary equilibrium strategies," *Journal of Theoretical Biology*, vol. 76, pp. 109–123, 1979.

[75] D. B. Neill, "Evolutionary stability for large populations," *Journal of Theoretical Biology*, vol. 227, pp. 397–401, 2004.

[76] V. P. Crawford, "Nash equilibrium and evolutionary stability in large- and finite-population "Playing the Field Models"," *Journal of Theoretical Biology*, vol. 145, pp. 83–94, 1990.

[77] D. P. Bertsekas, *Nonlinear Programming*. Belmont, MA: Athena Scientific Press, 1995.